1. Report No.	2. Government Accession No.	3. Recipient's Catalog No.
FHWA-AK-RD-88-02		

4. Title and Subtitle
FROST HEAVE FORCES ON H AND PIPE PILES EMBEDDED IN FAIRBANKS SILT

5. Report Date
May 1988

6. Performing Organization Code

7. Author(s)
J.B. JOHNSON AND J.S. BUSKA-

8. Performing Organization Report No.
FHWA-AK-RD-88-02

9. Performing Organization Name and Address
Cold Regions Research & Engineering Laboratroy
U.S. Army Corps of Engineers
USA-CRREL
72 Lyme Road - Hanover NH 03755

10. Work Unit No. (TRAIS)

11. Contract or Grant No.

12. Sponsoring Agency Name and Address
Dept of Transportation & Public Facilities
Statewide Research
2301 Peger Road
Fairbanks, AK 99709

13. Type of Report and Period Covered
Final Report

14. Sponsoring Agency Code

15. Supplementary Notes

16. Abstract

The magnitude and variation of forces and shear stresses, caused by frost heaving of a Fairbanks silt active layer, were determined using computerized data logging of electric strain gauges placed at one foot intervals of depth on both a 12 inch diameter pipe pile, and an H pile. Studies continued for three consecutive winter seasons (1982-1985). The peak frost heaving forces on the H pile during the three winters, were respectively 752, 790, and 802 kN (169, 178, and 180 kips). Peak frost heaving forces on the pipe pile of 1118 and 1115 kN (251 and 2560 kips) were determined only for the second and third winter seasons. Maximum average shear stresses acting on the pipe pile were 627 and 972 kPa (91 and 141 psi) for the second and third winter seasons. Ice collars were placed around the tops of both piles during the first and third winter seasons to measure the adfreeze effects of a surface ice layer. The ice layer may have contributed as much as 20% of the peak forces measured on the piles. A 0.6-m (2.0-ft.) thick gravel layer replaced the soil around the tops of both piles for the second and third winter seasons to measure the adfreeze effects of a gravel backfill. The gravel layer on the H pile may have contributed about 35% of the peak forces measured. The forces for both piles generally increased following a decrease in air temperature and decrease or relaxed following a rise in air temperatures. Changes in forces acting on the piles usually lagged behind corresponding air temperature changes by 1 to 8 days. Maximum heaving forces and shear stresses occurred during periods of maximum cold and maximum soil surface heave. Soil surface have displacement of 2 to 7 cm (0.8 to 2.8 in.) were measured at the experiment site during the study.

17. Key Words		18. Distribution Statement
piling	frost jacking	Unrestricted
frost heave	strain gauge	
field testing	silts	
adfreeze		
bond		

19. Security Classif. (of this report)	20. Security Classif. (of this page)	21. No. of Pages	22. Price

Final Report

FROST HEAVE FORCES ON H AND PIPE PILES EMBEDDED IN FAIRBANKS SILT

J.B. Johnson and J.S. Buska

Cold Regions Research and Engineering Laboratory

May 1988

Prepared for:

State of Alaska
Department of Transportation and Public Facilities
Division of Planning and Programming
Research Section
2301 Peger Road
Fairbanks, Alaska 99701

The contents of this report reflect the views of the authors, who are responsible for the facts and the accuracy of the data presented herein. The contents do not necessarily reflect the official views or policies of the Alaska Department of Transportation and Public Facilities. The report does not constitute a standard, specification or regulation.

IMPLEMENTATION STATEMENT

FROST HEAVE FORCES ON STEEL H AND PIPE PILES

PREPARED BY DAVID C. ESCH
ALASKA TRANSPORTATION & PUBLIC FACILITIES
PROJECT MANAGER

This report summarizes a three year field study of the frost heave stresses and forces induced in both H-Section and Pipe piling, under field conditions of frost heaving of saturated silty soils. The presence of permafrost silt soils at 9 feet beneath this site provided a convenient means of anchoring the bottoms of the piles to prevent their uplifting under the heaving forces. The presence of permafrost is not considered to effect the validity of the adfreeze stress and frost heave force data for use in seasonal frost-heave problems. The generation of maximum heave stresses, after all soils along the piles were frozen, demonstrated a fact previously reported by other researchers: that moisture movement, ice segregation and frost heaving do occur within frozen soils at temperatures near the freezing point.

The data and conclusions from this study were developed in recognition of some uncertainties induced by drift in calibration of the strain gauges over the three year term of the study, along with the failure of numerous gauges. These problems indicate that a confidence level of perhaps $\pm$ 20% should be considered in application of the data. With this precaution, the data from this study should be used in evaluating the frost heave forces on future pile designs.

The simplest design procedure for frost jacking involves the selection of an average "adfreeze bond" or shear stress to represent the bond of the frozen soil zone to the pile surface of pipe piles or to the equivalent "boxed in" section for H-Piles. Yearly maximum full-depth average values for adfreeze stress were measured at 50 psi at an average temperature of $-4^{\circ}C$ for the H-Pile and 90 to 140 psi for the pipe pile. Maximum total jacking forces for the H and Pipe piles were 90 and 125 tons, respectively, and demonstrate that very heavily loaded piles must be used to resist frost jacking in areas of deep frost penetration in saturated silt soils.

The intent of this study to develop adfreeze bond versus temperature data was accomplished and is shown for design consideration purposes by Figure 4 on Page 8. This plot shows peak load adfreeze values which are about twice those reported from other studies where only total heaving forces and averaged values were determined.

The use of a selected adfreeze value based on the average pile temperature in the freezing zone remains the most common design approach. Future field work is needed to verify the incremental frost heave stress-depth-temperature approach before it can be used with confidence in pile design. This method would require the prediction of the temperature distribution along the pile at the time of deepest active soil frost heaving. Additional work is also needed to measure the differences in stresses induced by ice-grip on the piles and by different soil types, before these factors can be analyzed with confidence.

CONTENTS

FIGURES

TABLES

ABSTRACT

The magnitude and variation of forces and shear stresses, caused by frost heaving in Fairbanks silt and the adfreeze effects of a surface ice layer and a gravel layer, were determined using electric strain gauges as a function of depth along the upper 2.75 m (9.0 ft) of a pipe pile, 30.5-cm I.D. x 0.95-cm wall (12 in. x 3/8 in.) and an H pile, 25.4-cm web x 85 kg/lineal m (HP 10 x 57), for three consecutive winter seasons (1982-1985). The peak frost heaving forces on the H pile during each winter were 752, 790 and 802 kN (169, 178 and 180 kips). Peak frost heaving forces on the pipe pile of 1118 and 1115 kN (251 and 251 kips) were determined only for the second and third winter seasons. Maximum average shear stresses acting on the H pile were 256, 348 and 308 kPa (37, 50 and 45 psi) during the three winter seasons. Maximum average shear stresses acting on the pipe pile were 627 and 972 kPa (91 and 141 psi) for the second and third winter seasons. Ice collars were placed around the tops of both piles during the first and third winter seasons to measure the adfreeze effects of a surface ice layer. The ice layer may have contributed 15 to 20% of the peak forces measured on the piles. A 0.6-m (2.0-ft) thick gravel layer replaced the soil around the tops of both piles for the second and third winter seasons to measure the adfreeze effects of a gravel backfill. The gravel layer on the H pile may have contributed about 35% of the peak forces measured. The forces for both piles generally increased after a decrease in air temperature and decreased after an increase in air temperature. Changes in forces acting on the piles usually lagged behind corresponding air temperature changes by 1 to 8 days. Maximum heaving forces and shear stresses occurred

during periods of maximum cold and soil surface heave magnitude. These were not related to the depth of frost penetration for most of the winter since frost was present at all depths extending to the permafrost table. Soil surface displacements of 2 to 7 cm (0.8 to 2.8 in.) were measured at the experiment site during the study. The important mechanisms that determine the magnitude of uplift heave forces are (1) soil heaving as the driving force, and (2) soil temperature, which controls the unfrozen water content, mechanical properties of the soil and the area of influence of heaving pressures.

ACKNOWLEDGMENTS

This report was prepared by Dr. Jerome B. Johnson, Geophysicist, and James S. Buska, Research Civil Engineer, both of the Applied Research Branch, Experimental Engineering Division, U.S. Army Cold Regions Research and Engineering Laboratory. Funding for this research was provided by the Alaska Department of Transportation and Public Facilities and by the Federal Highway Administration.

This project could not have been successfully completed without the help of many individuals. The authors acknowledge the efforts of C. Rohwer, C. Olmstead, S. Perkins, B. Young, R. Briggs, D. Solie, D. Dinwoodie, M. Sturm, W. Zito, L. Kozycki and D. Haynes. The authors also thank Dave Esch for his contributions to the completion of the project.

Dave Esch, Alaska DOT and PF, G.H. Johnston of NRC Canada, and Alan Tice of CRREL technically reviewed the manuscript.

The contents of this report are not to be used for advertising or promotional purposes. Citation of brand names does not constitute an official endorsement or approval of the use of such commercial products.

CONVERSION FACTORS: METRIC (SI) TO U.S. CUSTOMARY UNITS OF MEASUREMENT

These conversion factors include all the significant digits given in the conversion tables in the ASTM Metric Practic Guide (E 380), which has been approved for use by the Department of Defense. Converted values should be rounded to have the same precision as the original (See E 380).

Multiply	By	To obtain
centimeter	0.39371	inch
meter	3.280840	foot
$meter^2$	10.763910	$foot^2$
kilogram	0.453592	pound
kilonewton	0.224809	kip
kilopascal	0.145038	psi

FROST HEAVE FORCES ON H AND PIPE PILES EMBEDDED IN FAIRBANKS SILT

Jerome B. Johnson and James S. Buska

INTRODUCTION

Foundations embedded in frost-susceptible soils can be subjected to large uplift forces resulting from frost heaving of the soils. These forces can cause an upward vertical displacement of foundations which are not embedded below the frost depth or do not have sufficient resistance to counteract heaving forces. In Alaska, H and pipe piles are often used to support buildings, bridges and dock structures. It is important that design engineers know the magnitude of frost heaving forces that can act on foundation piles and how these forces are distributed along the piles. This information is used to determine the depth to which a pile needs to be embedded or how it must be loaded to resist heaving forces and the tensile strength requirements of a pile.

This report presents the results of a three-year study designed to measure and record the magnitude and distribution of axial strains, as a function of depth, time and temperature, for an H pile and a pipe pile penetrating surficial layers of ice and gravel and embedded in Fairbanks silt with an active layer overlying permafrost. The measured strains were used to calculate the uplift forces acting on the piles and the shear stresses at the soil/pile interface. Soil temperatures and surface heave were also measured. These results provided complete force and stress information on the piles as they were subjected to annual cycles of frost

heaving and thaw consolidation. In general, previous studies have provided data on only the total load acting on pipe piles due to frost heaving (Crory and Reed, 1965; Penner and Irwin, 1969; Penner, 1974).

SUMMARY OF PREVIOUS RESEARCH

Studies of the uplift forces induced by frost heaving of foundations date back to early Soviet work in the 1930's reported by Tsytovich (1975). Direct measurements of frost heave forces were made in the U.S.S.R. from 1958 - 1963. Three methods were used to measure frost heave forces: (1) reaction beam and load cell, (2) force balance apparatus, and (3) electric strain gauges. The reaction beam device consisted of a reaction beam held in place with rods anchored into the soil at depth. The test pile was restrained from moving by the reaction beam. The uplift forces acting on the pipe were measured with a load cell placed between the beam and pile. In the force balance scheme, any vertical displacement of the test pile was compensated by an additional load. The load that just stopped the heaving of the pile completely during the freezing of the soil was taken as the maximum total heave force.

Additional frost heave measurements were made using electric strain gauges mounted on the inner surface of a tubular pile. The results of the experiment, reported by Tsytovich (1975), were presented in terms of kgf (kilograms force) per lineal cm of column perimeter. This is equivalent to the shear stress (kgf/cm^2) times a unit depth of 1.0 cm. The pile diameter was not given so the actual shear stress values cannot be determined. The results can, however, be used to examine how the shear stress varies along the depth of the pile. Figure 1 shows the force per lineal centimeter of column perimeter (shear stress times a unit depth of 1.0 cm) acting on the pile with respect to depth. Shear stresses acting on the pile were zero at

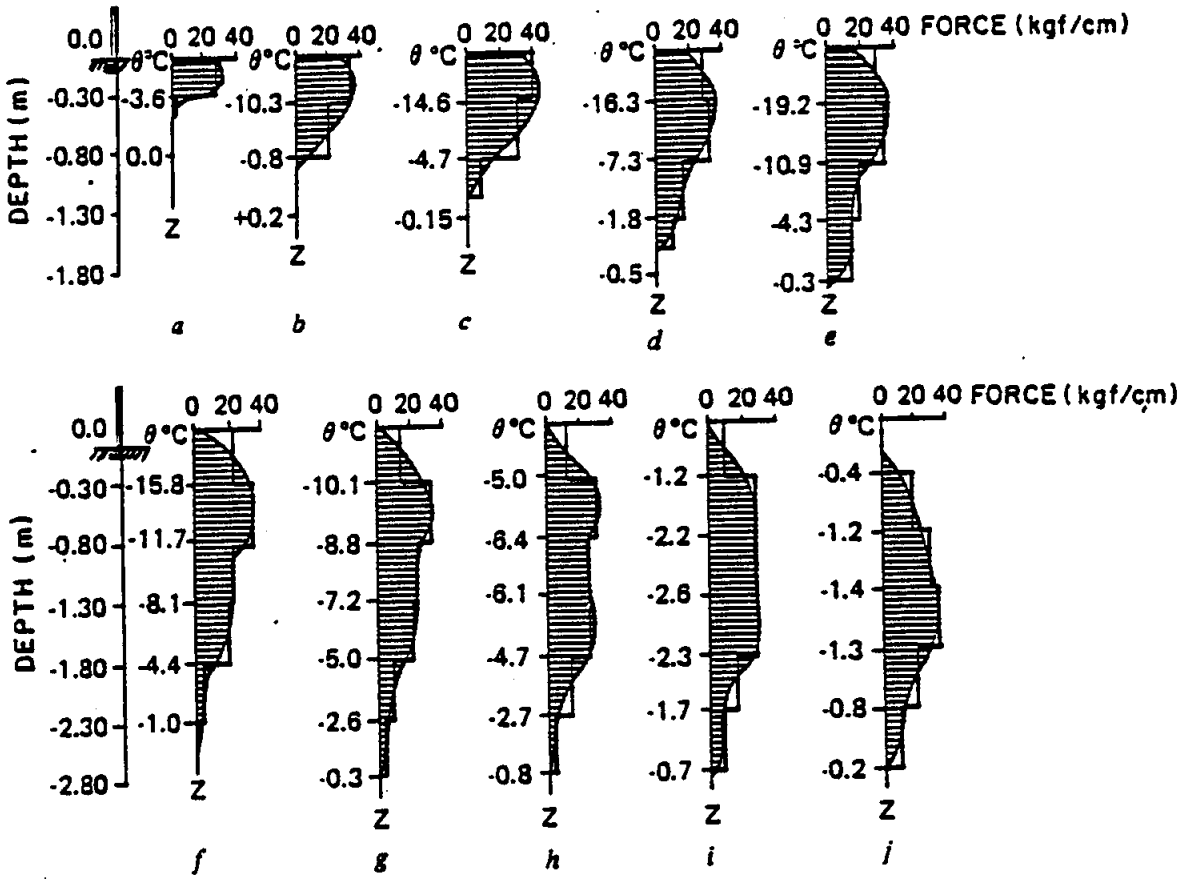

Figure 1. Distribution of relative frost-heaving forces, in kgf per lineal cm of column perimeter, over the lateral surface of the pile (experiments of Yegerev reported by Tsytovich, 1975). (a) 4 Nov 1957; (b) 14 Nov 1957; (c) 25 Nov 1957; (d) 28 Dec 1957; (e) 11 Jan 1958; (f) 11 Mar 1958; (g) 16 Apr 1958; (h) 5 May 1958; (i) 26 May 1958; (j) 11 Jun 1958; z is depth in meters from the surface and θ is the temperature in degrees Celsius.

the soil surface, then reached a maximum at some depth between the soil surface and the 0°C isotherm, and finally decreased to zero near the 0°C isotherm. The maximum of the shear stresses shifted downward toward the freezing boundary as the frost depth increased. Shear stresses acting along the soil/pile interface increased along the pile length with time and decreasing soil temperature (Tsytovich, 1975). The results for the strain-gauged pipe are of interest because of the similarity to the test setup in this study. They indicate that the shear stresses (due to frost heaving) are not uniform along the length of the pile. There is not sufficient information about the

setup or procedures used in the Soviet experiment to allow an accurate comparison to other available experimental results.

Additional field measurements of frost heaving forces on piles have been conducted in Japan, the United States and Canada (Kinosita and Ono, 1963; Crory and Reed, 1965; Penner and Irwin, 1969; Penner and Gold, 1971; Penner, 1974; Domaschuk, 1982). These have consisted of reaction beam and load cell tests. One test was conducted using a strain-gauged pile; however, the results of the test were not published. Crory and Reed (1965) reported the results of frost heaving force measurements conducted from 1956 to 1963 on 203-mm (8-in.) standard steel pipe and 330- to 381-mm (13- to 15-in.) butt diameter creosoted timber piles. The piles were embedded in silty soils overlying permafrost at the USACRREL Fairbanks field station. The site conditions were very similar to those of the current study, which was also located at the field station. Air temperature, soil temperature, heaving of an unrestrained pile, heaving of the test pile and the heave force were measured during the winters of 1956-1957, 1957-1958 and 1962-1963. The forces observed in the first two tests (1956-1957 and 1957-1958) were less than the maximum forces which might have been generated. The adfreeze bond between the reaction beam support piles and permafrost was not sufficient to resist heaving during the 1956-1957 test and the soil was exceptionally dry during the 1957-1958 test. Distinct fluctuations in the heave force measurements were observed for both steel and timber piles. The maximums and minimums of the fluctuations occurred a few days after a respective decrease or increase in air and soil temperatures (Crory and Reed, 1965).

Canadian experiments measured heaving forces of wood, steel and concrete columns, from 76 mm (3 in.) to 305 mm (12 in.) in diameter, embedded

in Leda clay (Penner and Irwin, 1969; Penner and Gold, 1971; Penner, 1974). The shear stresses due to heaving were highest for steel, followed by concrete and wood. This was mostly attributed to the influence of temperature on the adfreeze strength of frozen soil acting on the columns. The steel columns were normally colder than the concrete or wood columns. Domaschuk (1982) conducted controlled heaving tests of steel structural units. Tests were conducted on embedded vertical steel members and steel members inclined to the soil surface. The test results indicated a decrease in vertical stress on the member as the angle of inclination of the member with respect to the frost plane increased. Kinosita and Ono (1963) conducted frost heave force measurement tests on steel, concrete, resin-coated concrete and vinyl columns. These tests indicated that adfreeze strength was the greatest for steel and was less for vinyl and wood. The Canadian and Japanese experiments both showed the fluctuations in heave force associated with changes in the air temperature that had been observed by Crory and Reed (1965). These were attributed to changes in ground temperature and ground temperature gradients caused by air temperature fluctuations. Table 1 summarizes the measurements of maximum averaged uplift shear stress acting along the soil/pile interface. The uplift shear stress is induced by frost heaving and computed on the basis of the uplift force divided by the surface area of the pile from the soil surface to the depth of the 0°C isotherm.

An inherent problem with the reaction beam and force-balance methods is that they underestimate the uplift shear stresses by not taking into account the resistive shear stresses on piles. The heaving forces measured in these tests are used to estimate an average uplift shear stress which acts on the pile from the soil surface to the depth of the 0°C isotherm. No

Table 1. Maximum Average Uplift Shear Stresses Measured on Steel, Concrete and Wood Piles.

INVESTIGATORS	SOIL TYPE	YEAR OF TEST	PILE DIAMETER (mm)	SHEAR STRESS (kPa) STEEL	VINYL	CONCRETE	WOOD
Kinosita & Ono, 1983	Silty Clay	1961-62	72	207			
			76		162	114 (uncoated)	
	Loam	1961-62	94			51 (resin coated)	
Crory & Reed, 1965	Silty	1956-57	203	152			
		1957-58	203	159			
		1958-59	356				55
		1962-63	356				83
		1962-63	203	283			
Soviet data reported by Tsytovich, 1975	?	1958-63	?				97-165
Penner & Irwin, 1969	Clay	1966-67	89	83			
		1967-68	89	83			
Penner & Gold, 1971	Clay	1970	89	114		134	90
Penner, 1974	Clay	1970-71	76			114	116
		1970-71	156			150	177
		1970-71	305			119	139
		1971-72	76	255		192	131
		1971-72	152	203		249	226
		1971-72	305	172		141	243
Domaschuk, 1982	Silty		76 x 76 angle	345			
Penner & Goodrich, 1983	Clay with frozen gravel surface layer, Thompson, Manitoba	1972-73	169	379	(loads exceeded cell capacity)		
			323	179			
			458	124			
		1973-74	169	117			
			323	76			
			458	69			
		1974-75	169	69			
			323	55			
			458	48			
	Clay, Ottawa, Ontario	1971-72	169	93			
			323	70			

account is made for resistive shear stresses developed on the pile in the soil below the 0°C isotherm. Therefore, the reaction beam and force-balance methods actually measure a net uplift force which is the total uplift load less the total restraining load acting on the pile.

Johnson and Esch (1985) reported on the 1982-83 and 1983-84 winter seasons from this study using the initial calibration results. The magnitude and distribution of strains, forces and stresses differ slightly from the results of this report due to differences in the calibration results used for the reports. Figure 2 shows the maximum measured adfreeze shear stresses for the H pile as a function of temperature from October 1983 through March 1984 (Johnson and Esch, 1985). Their results indicated that the apparent relationship between adfreeze stress and temperature also depended on the rate and magnitude of soil heave and that it was not possible to completely separate the effects of soil heave and temperature on shear stresses.

The above investigators suggested a number of controlling influences for frost heaving forces acting on foundation piles. These included (1) soil type and temperature, (2) rate and magnitude of soil surface heave, (3) changes in soil temperature, (4) soil temperature gradients and (5) the availability of moisture in the soil. Maximum shear stresses generally occurred during the early freezing period when heaving rates were high. Maximum uplift forces often occurred near the time of maximum frost penetration.

METHODS AND MATERIALS

Soil Conditions

The test site was located at the USACRREL-Alaska, Farmers Loop Field Station, Fairbanks, Alaska (Figure 3). The soils (Fairbanks silt) are

primarily deep colluvial deposits of slightly organic silts with occasional wood fragments and peat layers (Crory and Reed, 1965; Linell, 1973; Esch, 1982). Moisture content was not measured in the fall preceding the 1982-83 measurement program; however, observation of the borehole cuttings and other evidence indicated that the soil deposits were saturated below a depth of about 0.5 m. A soil log taken prior to the 1983-84 winter indicated the moisture content of the soil was 40% near the surface and

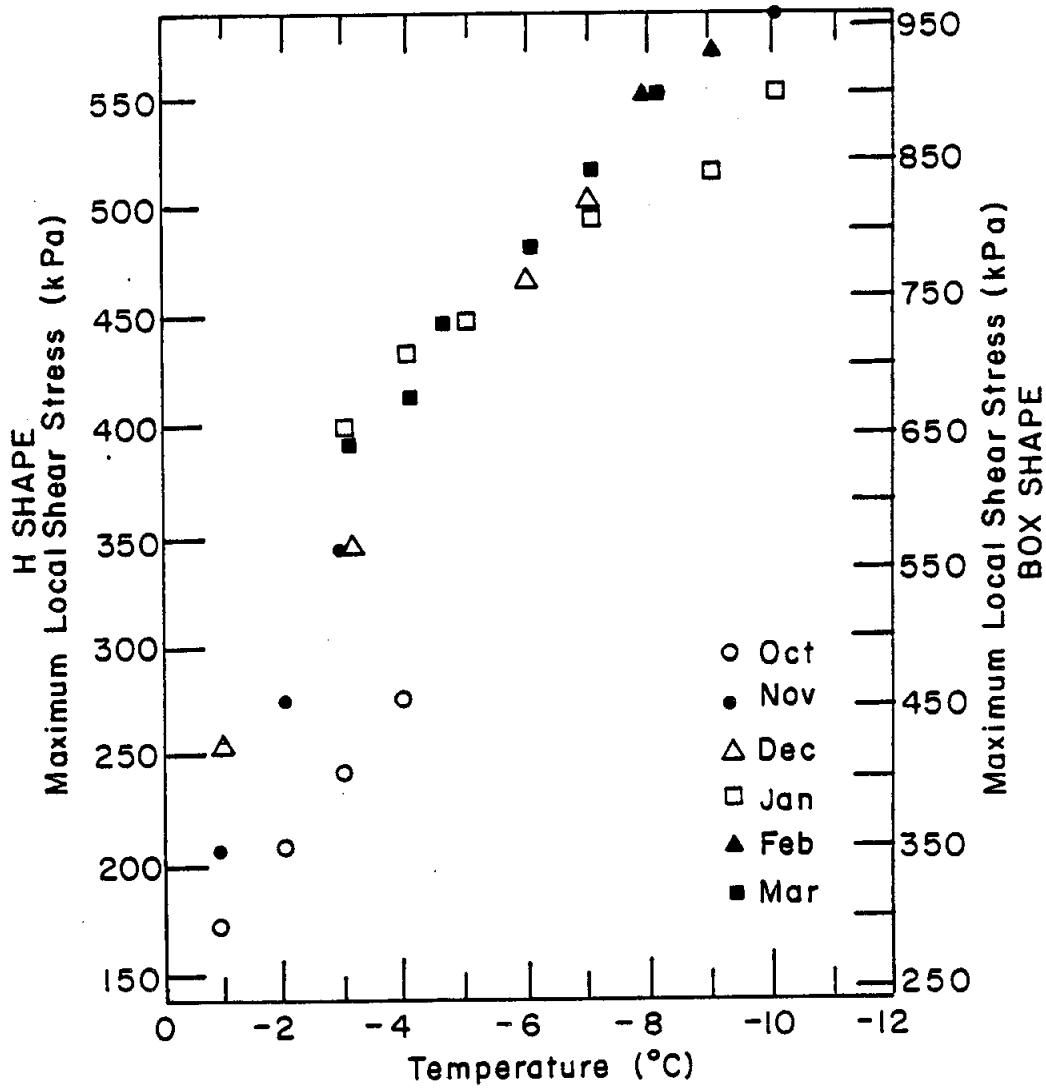

Figure 2. Shear stress as a function of temperature for the H pile from October 1983 through March 1984 (from Johnson and Esch, 1985).

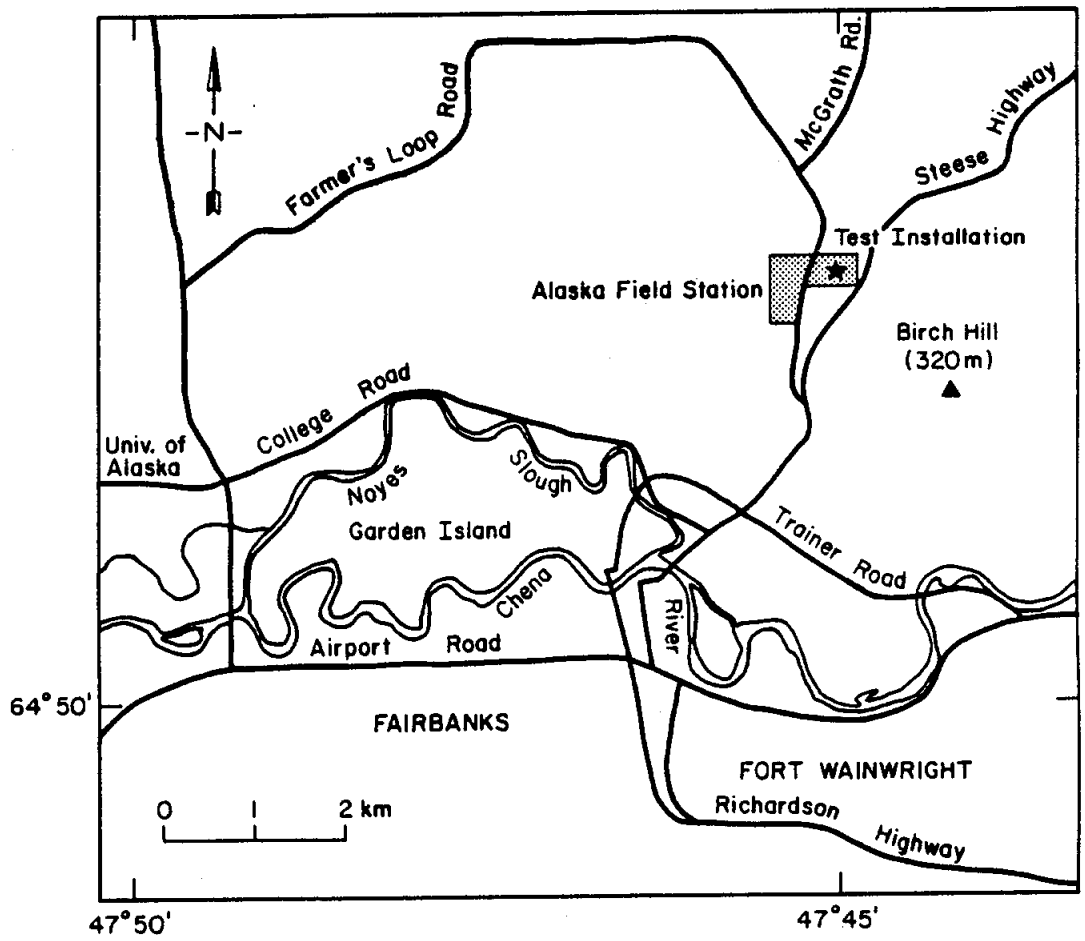

Figure 3. Experiment site location map.

varied from 25% to 29% between the surface and a depth of about 2.4 m. Prior to the beginning of the 1982-83 winter season, the soil was unfrozen to a depth of about 2.5 m with permafrost below. Measurements of the depth to permafrost in September 1984 indicated that the depth of unfrozen ground was approximately 2.5 m where the ground was snow-covered during the winter, 1.6 m between the piles, and 2 m immediately adjacent to the piles. This indicated that the top of the permafrost table had moved toward the surface of the experimental site as a result of maintaining a snow-free surface to intensify frost heaving. The thickness of the seasonally thawed or active layer between the piles at the beginning of the winter season was 2.3 m in 1982, 1.6 m in 1983 and 1.6 m in 1984. The soil in the active layer froze to the depth of the permafrost each winter during the study as illustrated in Figure 4. Frost heaving at the site ranges from 2 to 7 cm during a typical winter.

Site Preparation and Plan

The experimental site had been cleared of vegetation and covered with a 30-cm layer of gravel during an earlier study designed to investigate methods of pre-thawing permafrost. The location of the pile study site was previously designated as "Plot D," and the average thaw depth was measured at 2.5 m in the fall of 1982 (Esch, 1983). Most of the 30-cm layer of gravel was removed during site preparation, leaving a thin layer of gravel. Two instrumented piles, a pipe pile and an H pile, were installed at the test site for this study. A reference benchmark, temperature probes and an instrumentation hut were also installed (Fig. 5).

The ground around the piles was kept free of snow throughout the measurement program. A roof structure was installed over the piles for the

1983-84 and 1984-85 seasons to keep the snow off the site and thereby increase the frost penetration and intensify frost heave.

Two commonly encountered situations for pile installations in Alaska are aufeis buildup around piles near river crossings and the use of gravel backfill around the top of piles. The experimental configuration was designed to allow for surficial ice buildup and the use of gravel backfill. Ice collars 1.8 m in diameter were installed around the upper sections of the piles during the 1982-83 and 1984-85 seasons in an effort to measure the adfreeze effects of surface ice deposits on pilejacking. The

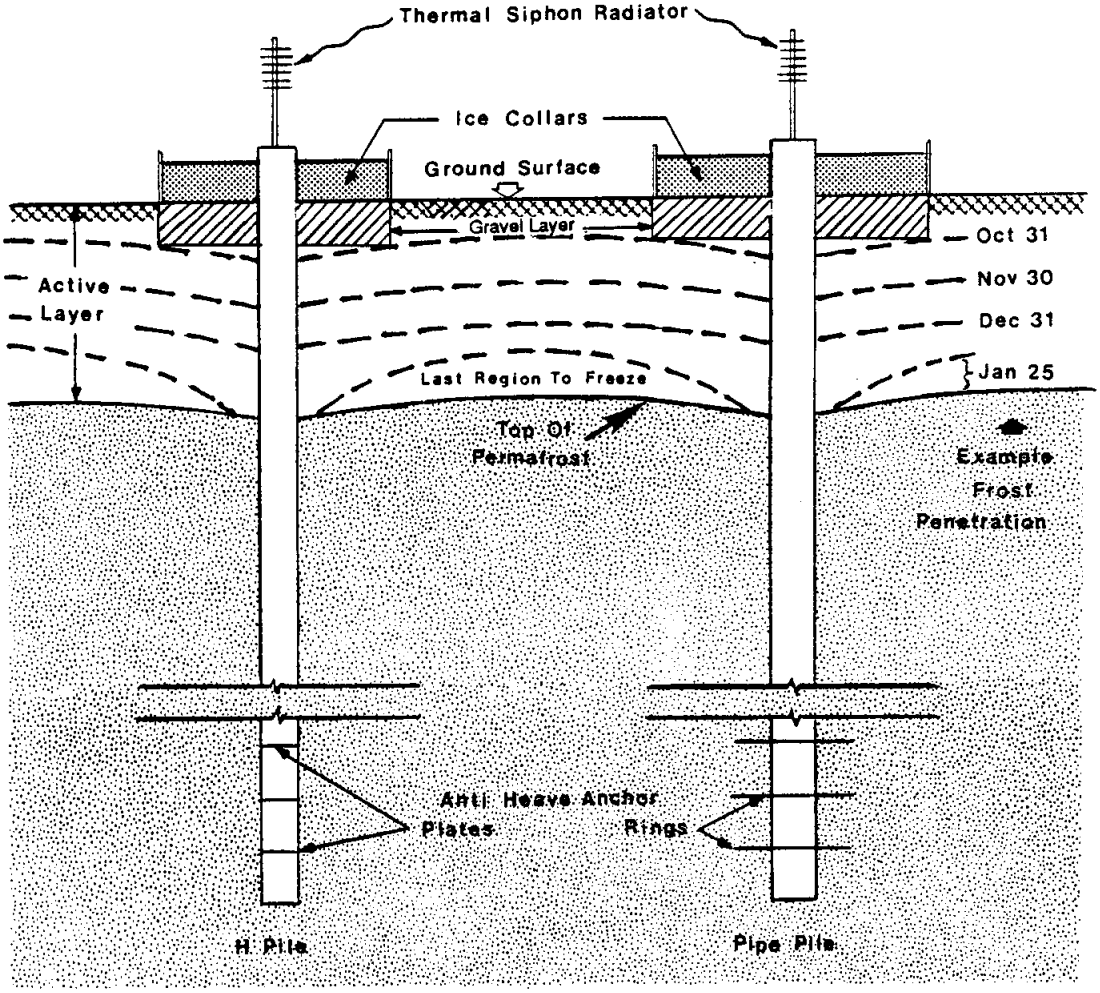

Figure 4. Illustration showing development of frost penetration at the experiment site.

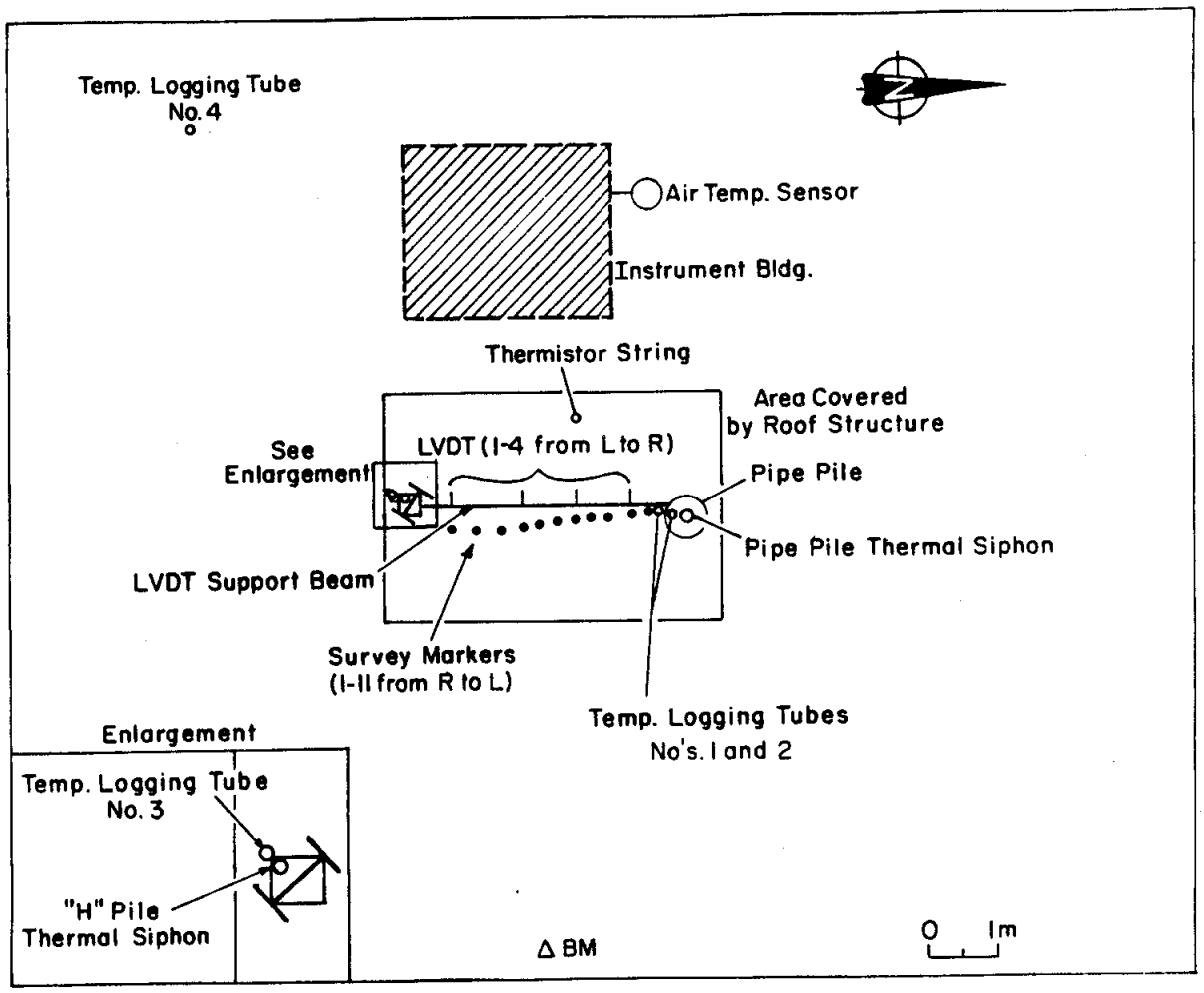

Figure 5. Plan view of the experimental site.

ice collars for the 1982-83 season were placed between 5 and 13 January 1983 to a thickness of 25 cm. The ice collars for the 1984-85 season were placed between 16 and 20 November 1984 to a thickness of 45 cm. Ice collars were not used during the 1983-84 season. A 0.6-m-thick by 1.8-m-diameter gravel layer was placed around the tops of the piles on 17-23 August 1983 prior to the 1983-84 winter season and left in place throughout the 1984-85 season. The gravel layer was placed by excavating the soil from around the tops of the piles and backfilling with gravel to the original ground surface.

Instrumentation and Installation of Piles

An H pile (HP10x57, 25.4 cm web, 85 kg/lineal meter) and a pipe pile (standard weight, 12 in. nominal diameter, 30.5 cm I.D., 0.95-cm wall thickness) were each instrumented with hermetically sealed weldable strain gauges (HITEC Corp., 350-ohm strain gauges) and copper-constantan thermocouples. These were placed every 15.2 cm along the upper 3 m of the 9.45-m length of both piles as shown in Figure 6. The gauges were mounted along the centerline on both sides of the web for the H pile and on diametrically opposite sides of the pipe pile. Strain gauges oriented at

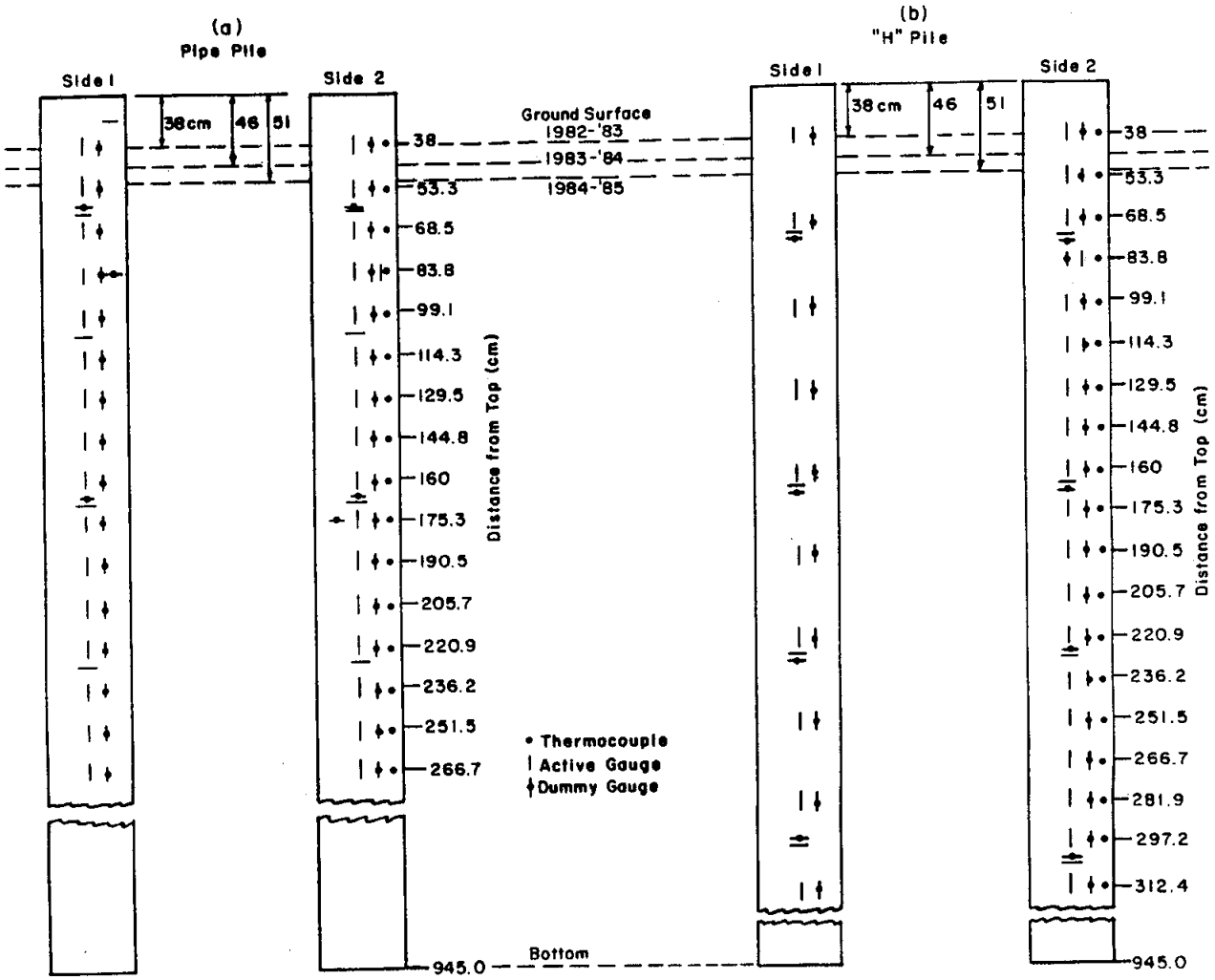

Figure 6. Strain and thermocouple installation layout for (a) the pipe pile and (b) the H pile.

90° to the axial direction were interspersed between the axially oriented gauges along the length of the instrumented sections. These were used to measure transverse strains in the piles and to estimate the magnitude of horizontal compressive stresses in the soil acting on the piles. Temperature-induced apparent strains were measured using strain gauges mounted on thin metal plates with the same thermal expansion properties as the piles, with one end fixed to the pile to ensure that the gauge-shim system was unstressed (shown as dummy gauges in Fig. 6). Dummy gauges were wired to active gauges to cancel temperature-induced apparent strain (shown as pairs of gauges in Figure 6). The gauges were coated with a waterproof coating and polyurethane foam to provide corrosion protection and insulation.

Angle sections (L5x5x3/8, 12.7-cm legs, 0.95 cm thick) were welded over the gauges on each side of the H pile web to provide mechanical protection. Figure 7 shows the installation scheme for two axially oriented and one transverse strain gauge with a thermocouple installed next to each of the axial gauges on the H pile. A 3.35 m-long tube was placed inside of the angle on one side of the pile and connected to a watertight box section (4x4x1/4, 10.2-cm sides, 0.64 cm thick) which extended the remaining length of the H pile. The tube and box section were used as a guide and housing for a thermal siphon. Polyurethane foam was used to fill the cavity inside the angle sections for the length of the instrumented pile section. Frost heave resistance was obtained through steel plates welded between the flanges of the H pile at 0.3-m intervals over the bottom 3.0 m of the pile (Fig. 8).

The upper 2.74 m of the pipe pile was cut into three 0.91-m sections to facilitate placement of instrumentation on the pile (Fig. 9). After

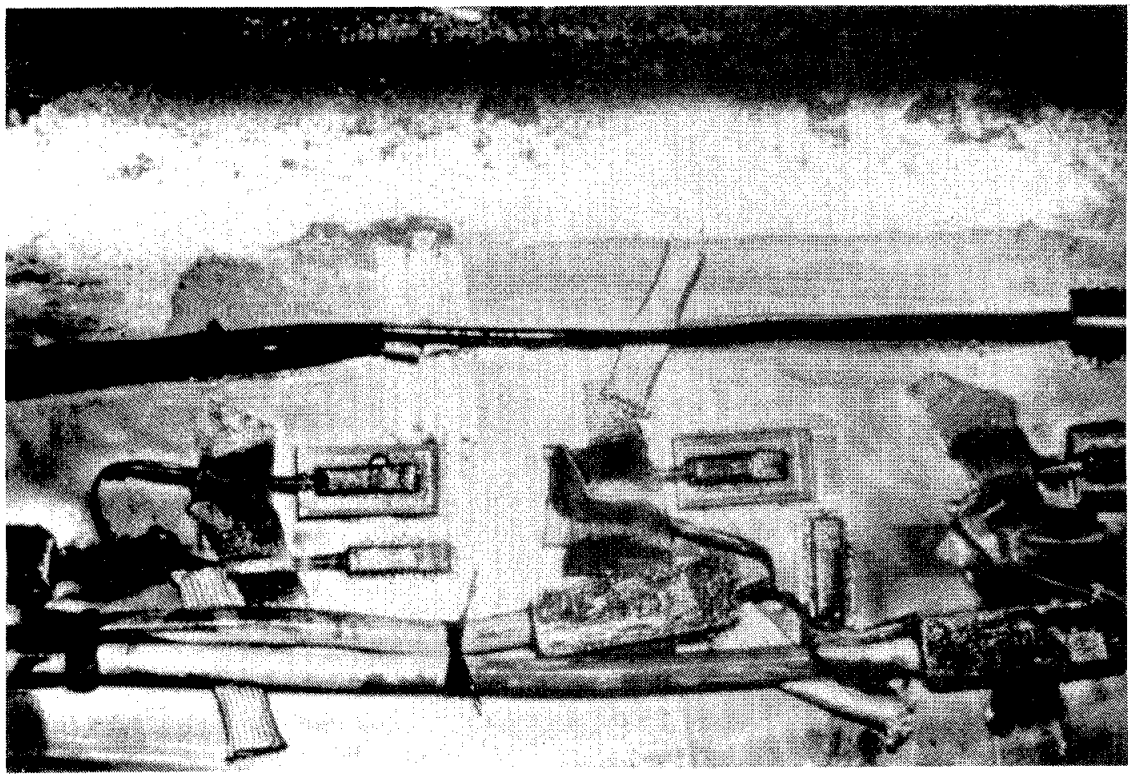

Figure 7. Close-up view of axial and transverse strain gauge and thermocouple installations on the H pile.

Figure 8. Instrumented H pile after installation of protective angles, guide tube and retention bars.

Figure 9. End view of a strain gauge and thermocouple-instrumented 0.91-m-long pipe pile section.

instrumentation placement, these pile sections were welded together, calibrated and then welded to the lower uninstrumented section of the pipe pile. The gauges were kept cool during welding by blowing a stream of air through the pile and running water over the outer skin. Concentric rings with a 40.6-cm outer diameter were welded to the lower 3.0-m section of the pipe pile at 0.3-m intervals to help prevent the pile from heaving throughout the winter period.

Two tubes were placed in the interior of the pipe pile. One tube was suspended in the center of the pile as a guide for a thermal siphon. The second tube was slightly offset from the center and was used to pour a slurry of water and sand in the uninstrumented portion of the pipe pile after installation to provide for better thermal conduction between the thermal siphon and the pipe walls. Once both tubes were in place, poly-

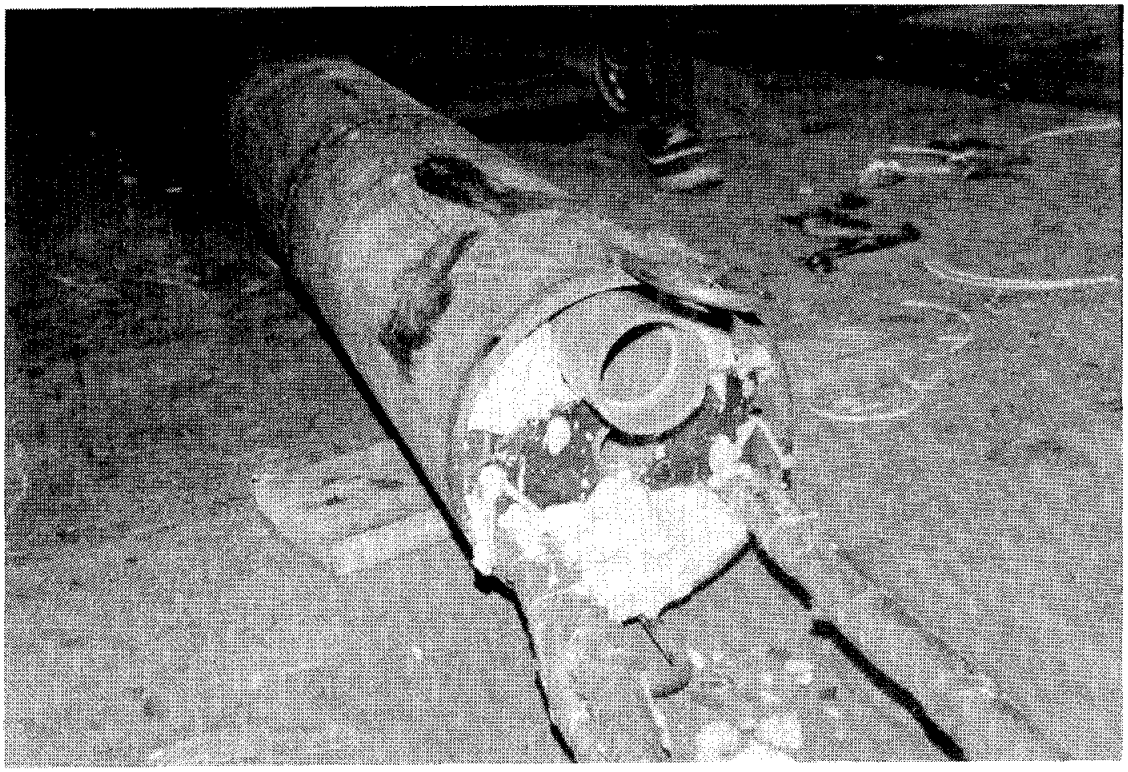

Figure 10. Instrumented pipe pile after welding of the three instrumented sections to the uninstrumented section and installation of the polyurethane foam.

urethane foam was used to fill the upper 2.75-m cavity of the pile and thereby minimize convective cooling (Fig. 10).

Both the H and pipe piles were calibrated in compression prior to installation and in tension at the end of the experiment. A description of the initial (compression) and field (tension) calibration procedures is given in Appendix B.

After the initial calibration the piles were installed in holes augered to a depth of approximately 9 m. The holes around the piles were backfilled during the week of 31 October 1982 with a saturated sand slurry mixture for the lower 6 m and with native silt at 40% water content by weight for the upper 3 m. Thermal siphon tubes with propane as the refrigerating fluid were installed in both piles to aid in freezing the backfill

slurry and cool the permafrost, thereby increasing the frost jacking resistance of the piles in combination with the rings and plates welded on for the same purpose. Insulation surrounded the upper third of the thermal cooling probes in the H and Pipe piles. This helped reduce air cooling of the piles and radial freezing of the soil, which might have altered soil temperatures and reduced heave stresses. Three temperature logging tubes consisting of 1-in. PVC tubing filled with diesel fuel were installed at the locations shown in Figure 5 to a depth of 9 m around the piles to monitor the effectiveness of the thermal siphons. Temperature readings were taken in the logging tubes near the piles and at an adjacent undisturbed soil site on two different occasions. Tube #1 was located inside the pipe pile about 6.4 cm from the thermal siphon and tube #2 was located 25.4 cm outside of the pipe pile. Tube #3 was located about 29 cm from the H pile thermal siphon and Tube #4 was located 3.1 m from the H pile (Fig. 5). Figure 11 shows that the soil at depth immediately surrounding the pipe pile was about 2° to 4°C cooler than the undisturbed soil on 7 December 1982 and continued to cool throughout the winter. Figure 12 shows that the soil around the H pile at depth was about 0.5° to 3°C cooler than the undisturbed soil. The effectiveness of the thermal siphon for the H pile was less than that used in the pipe pile. This may have been due to differences in thermal contact between the piles and their thermal siphons.

Temperature Measurements

Temperatures for the soil, piles and air were recorded throughout the study. Copper-constantan thermocouples were installed at 15.2-cm intervals on each pile. An air temperature sensor was mounted in a protective housing on the north side of the instrumentation hut. Soil temperatures were

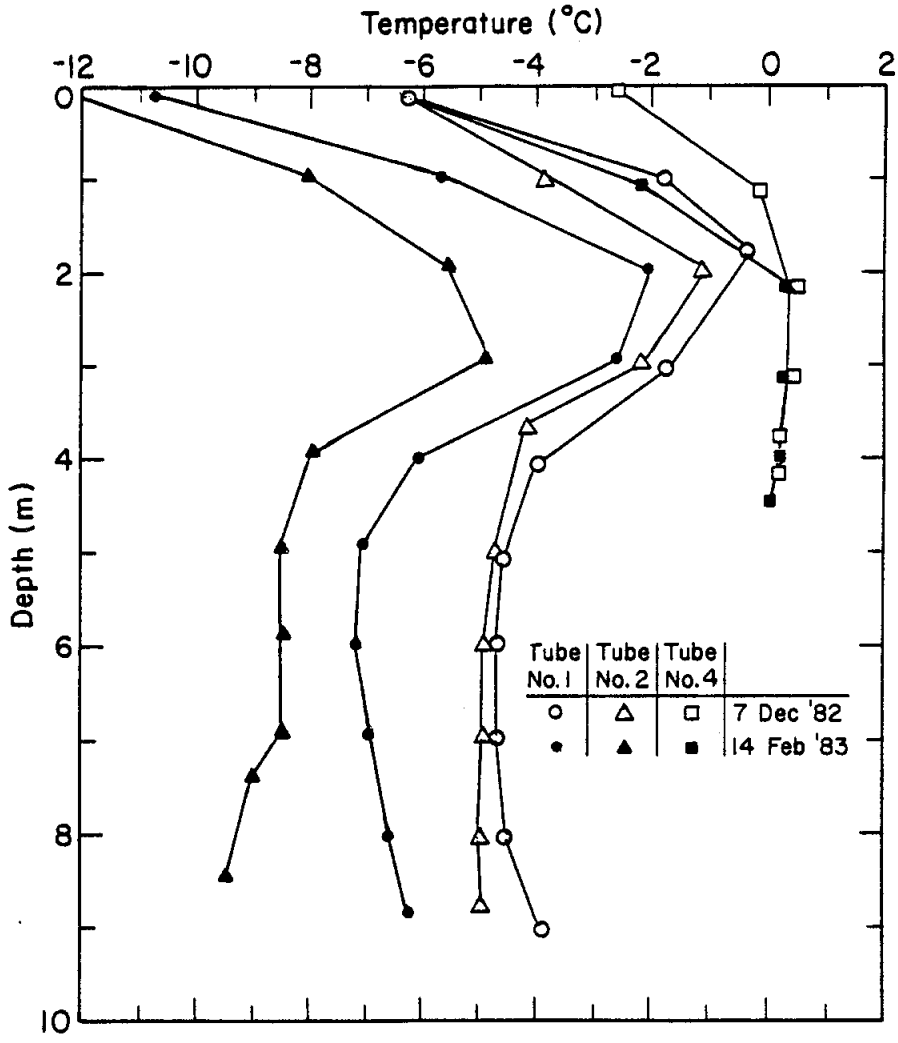

Figure 11. Temperature profiles in the vicinity of the pipe pile and in undisturbed soil. Tube #1 was located inside the pipe 6.4 cm from the thermal siphon, tube #2 was located about 25.4 cm from the thermal siphon, and tube #4 was located about 3.1 m from the experimental site.

measured at the location of the thermistor string in Figure 5 using thermistors spaced every 15.2 cm to a depth of 2.75 m.

Soil Surface Heave Measurements

Standard level survey practices were used during the 1982-83 season to determine changes in elevation of the piles and of several intermediate survey markers between the piles as shown in Figure 5. These observations were made monthly, with differences in elevation between surveys being

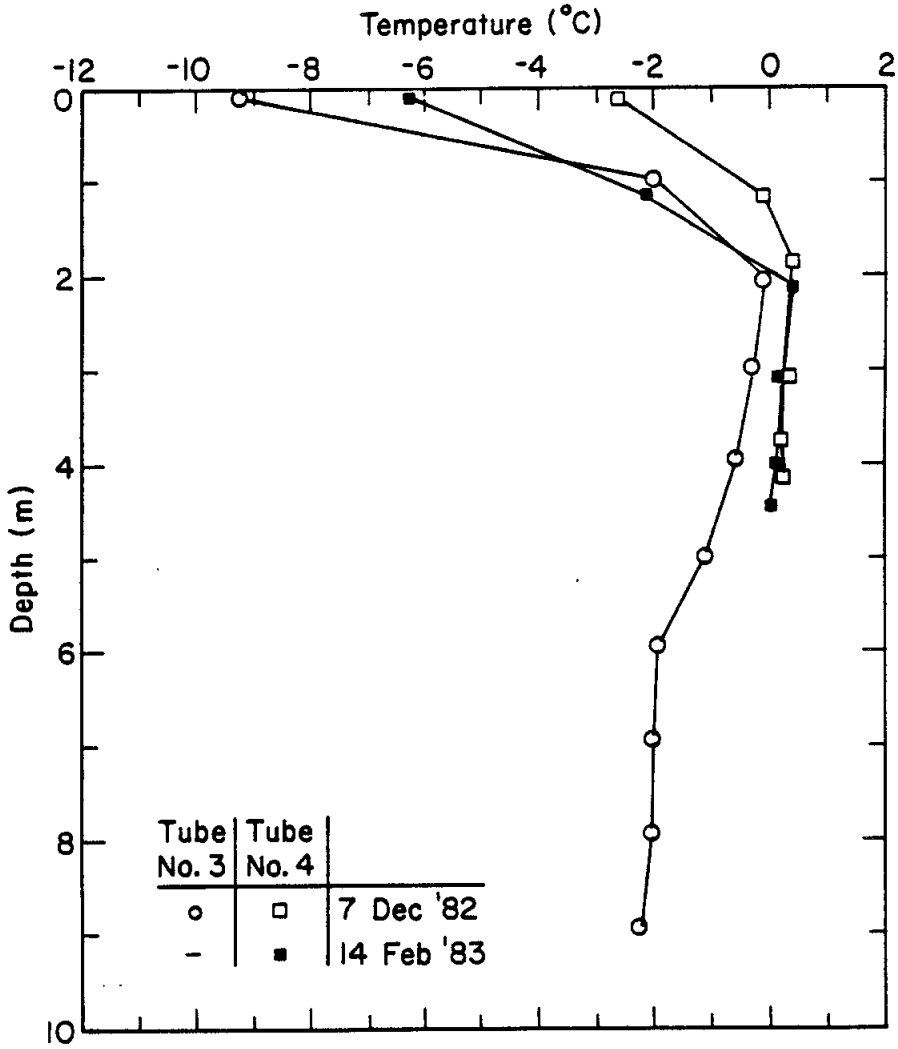

Figure 12. Soil temperature profile near the H pile. Tube #3 was about 29.2 cm from the thermal siphon and tube #4, undisturbed soil, was about 3.1 m from the experimental site.

determined to an accuracy of 1 mm. Survey markers 1, 2, 10 and 11 were covered with ice on 10 January 1983 to create an ice layer around the tops of the piles. The vertical displacements for markers 3 through 9 were used to determine the average incremental and accumulated vertical displacements for the soil surface for the 1982-83 season (Fig. 13). Figure 13 also shows the survey results for the H and pipe piles during the winter season. The survey measurements indicated that the piles did not change elevation during the 1982-83 season. Therefore, linear variable displacement

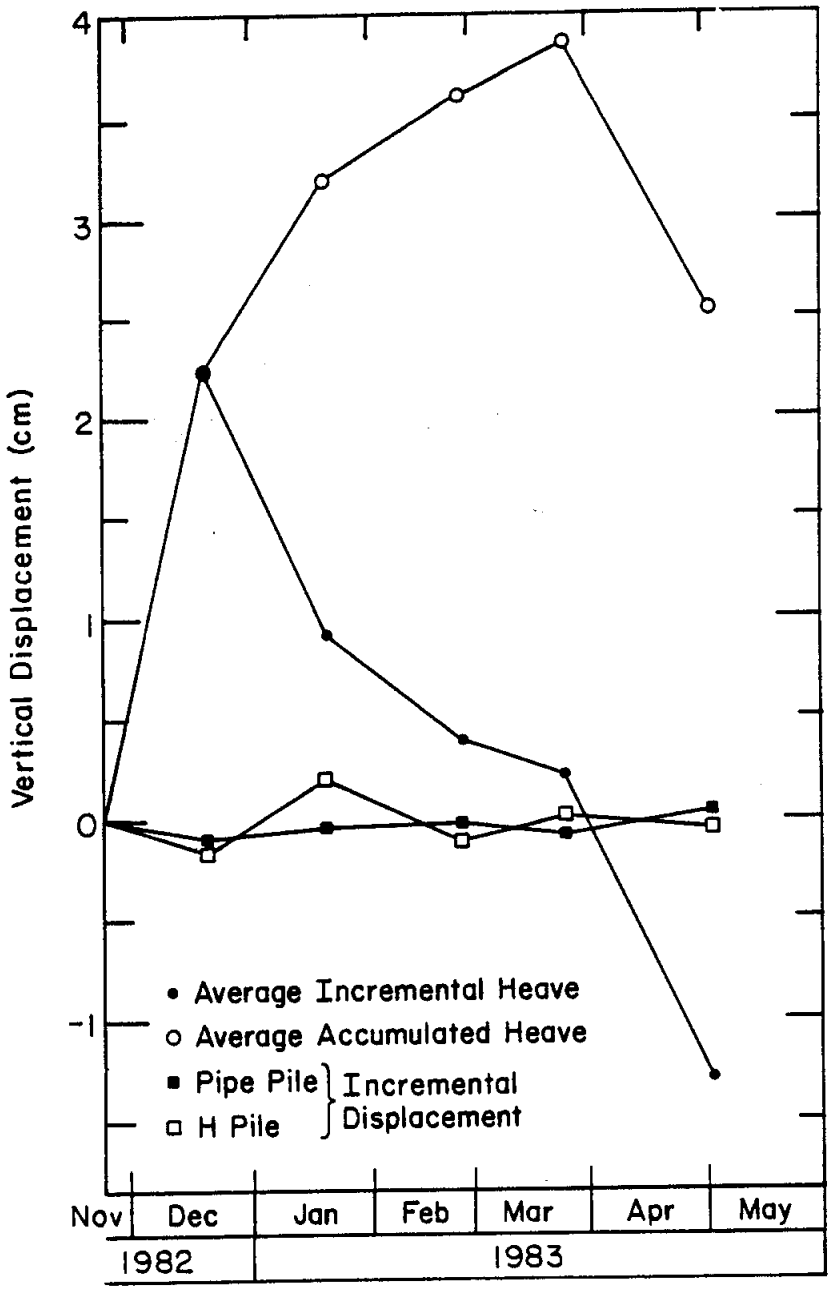

Figure 13. Average incremental and accumulated soil surface vertical heave and incremental vertical displacement for the H and pipe piles.

transformers (LVDT) mounted on a beam suspended between the piles were used to measure the ground surface heave during the 1983-84 and 1984-85 seasons. The LVDT's were located along the beam at distances of 0.3 and 1.2 m from the H pile and 0.4 and 1.2 m from the pipe pile for the 1983-84 season and at distances of 0.3 and 0.9 m from both the H pile and pipe pile

for the 1984-85 season (Fig. 5). A reference elevation was established at the top of the pipe pile and the ground level elevation determined from the reference elevation for each year of the study. The ground surface was 0.38, 0.46 and 0.51 m below the top of the pipe pile for the 1982-83, 1983-84 and 1984-85 winter seasons respectively as a result of thaw consolidation and the disturbances caused by placing a gravel layer and ice collars around the tops of the piles (Fig. 6). The onset of vertical displacement due to frost heave was missed for all three winter seasons, so the vertical displacements measured are relative to the time heave measurements started each season. Vertical displacements of the soil surface prior to the beginning of displacement measurements are considered to be minimal.

Force and Shear Stress Calculations

The magnitude of frost-heave-induced shear stress along the soil/pile interface was determined using resistance strain gauge measurements to calculate the internal axial stresses in the piles (Appendix A). These stresses were then used to calculate the internal axial forces in the piles at the gauge locations. The frost-heave-induced shear stresses along the soil/pile interface were then calculated by dividing the difference in force between two adjacent strain gauges by the corresponding pile surface area.

Internal axial stresses on both the H and pipe piles can be determined from

$$\sigma'_z = E\ \varepsilon'_z \qquad (1)$$

where

σ'_z = the internal axial stress in the pile

E = Young's modulus determined from the field calibration test results (Appendix B)

ε'_z = the internal axial strain in the pile.

Internal strains, stresses and forces in the piles are denoted by primed variables. External stresses and forces are denoted by unprimed variables. Equation 1 is valid only if the confining soil stresses acting on the pile are small. A comparison of the measured magnitude of transverse strain to axial strain indicated that for the H pile and the pipe pile the confining forces were small compared to the axial frost heaving forces (Appendix A).

The internal axial forces acting in the piles were calculated using the results from equation 1 and

$$F'_{z_i} = \sigma'_{z_i} A \qquad (2)$$

where

F'_{z_i} = the internal axial force at depth i

σ'_{z_i} = the internal axial stress at depth i

A = the cross-sectional area of the pile ($A = 94.2$ cm^2 for the pipe pile and $A = 155.0$ cm^2 for the H pile).

The frost-heave-induced shear stresses along the soil/pile interface were calculated from

$$\begin{matrix}\sigma_{xz} \\ \sigma_{rz}\end{matrix} = (F'_{z_i} - F'_{z_j}) / (S \Delta z) \qquad (3)$$

where

σ_{xz} = shear stress at the soil/pile interface from depth i to depth j for the H pile

σ_{z_i} = shear stress at the soil/pile interface from depth i to depth j for the pipe pile

F'_{z_i} = internal axial force acting at a depth greater than the internal axial force F'_{z_j} in the pile

S = surface area of the pile in meter^2 per lineal meter

Δz = pile length in meters from depth i to depth j.

Average maximum shear stresses were calculated by dividing the peak uplift force by the surface area of the pile from the soil surface to the depth of the peak uplift force.

The strain, stresses and forces due to the ice collars and gravel layer could not be determined from the resistance strain gauge measurements since the field calibration results had determined that the upper strain gauges were not reliable (Appendix B). Consequently the effects of the ice and gravel layers on the piles had to be addressed indirectly.

Experiments on polycrystalline freshwater ice have shown that for long-term creep the deformation can be described by

$$\dot{\varepsilon} = A (\tau_c)^n \qquad (4)$$

where

$\dot{\varepsilon}$ = strain rate in the ice

A = constant that depends on the ice temperature, ice crystal fabric and other variations in ice properties

τ_c = shear stress over the thickness of the ice collar at the ice/pile interface

n = constant determined from experiments (Patterson, 1981).

The magnitude of $\dot{\varepsilon}$ can be estimated by using the measured rates of soil surface heave near the piles and the assumption that soil displacement is constrained only in a narrow region around the piles. Experimental results by Penner and Irwin (1969) and Saltykov (1944) indicate that soil surface heave is constrained only within 1 cm of a pile.

The strain rate in the ice was calculated from

$$\dot{\varepsilon} = 1/2 (\Delta \dot{\mu} / \Delta y) \qquad (5)$$

where

$\dot{\varepsilon}$ = strain rate in the ice

$\Delta\dot{\mu} = \dot{\mu}_n - \dot{\mu}_o$

where

$\dot{\mu}_n$ = soil surface displacement rate as measured near the pile

$\dot{\mu}_o$ = soil surface displacement rate at the pile

Δy = narrow region in which soil displacement is constrained (1 cm).

The soil surface displacement rate at the pile was assumed to be zero, a conservative assumption that will result in peak ice strain rates. The shear stress at the ice/pile interface over the thickness of the ice collar is found by combining equations 4 and 5 and solving for τ_c to obtain

$$\tau_c = (\dot{\varepsilon}/A)^{1/n} \qquad (6)$$

Table 2 gives values of A for n=3 and several different temperatures from the experimental results reported by Patterson (1981). Representative values of A were determined for the ice temperatures measured in the study at or near the soil surface.

Table 2. Values of Flow Law Parameter (A) for Different Temperatures and n=3 (from Patterson, 1981).

T (°C)	$A(s^{-1}\ kPa^{-3})$
0	5.3×10^{-15}
-5	1.7×10^{-15}
-10	5.2×10^{-16}
-15	3.1×10^{-16}
-20	1.8×10^{-16}
-25	1.0×10^{-16}
-30	5.4×10^{-17}
-35	2.9×10^{-17}
-40	1.5×10^{-17}
-45	7.7×10^{-18}
-50	3.8×10^{-18}

The uplift force on the piles at the ground surface due to an overlying ice collar was calculated from

$$F_c = \tau_c S_c t_c \tag{7}$$

where

F_c = uplift force on the pile at the ground surface due to an overlying ice collar,

τ_c = shear stress at the ice/pile interface over the thickness of the ice collar

S_c = surface area of the pile in meter^2 per lineal meter

t_c = thickness of the ice collar in meters.

Shear stresses at the soil/pile interface from the ground surface to the depth of the first functioning strain gauge were determined from

$$\begin{matrix}\sigma_{xz_1} \\ \sigma_{rz_1}\end{matrix} = (F'_{z_1} - F_c) / (S \Delta z) \tag{8}$$

where

σ_{xz_1} = shear stress at the soil/pile interface for the H pile from the ground surface to the depth of the first functioning strain gauge

σ_{rz_1} = shear stress at the soil/pile interface for the pipe pile from the ground surface to the depth of the first functioning strain gauge

F'_{z_1} = internal axial force on the pile at the depth of the first functioning strain gauge

F_c = uplift force on the pile at the ground surface due to an overlying ice collar (F_c = 0 when there is no ice collar)

S = surface area of the pile in meter^2 per lineal meter

Δz = pile length in meters from the ground surface to the depth of the first functioning strain gauge.

The depths to the first functioning strain gauge on the H pile are nearly the same as the thickness of the gravel layer placed around the pile.

Therefore, the heaving force on the H pile due to the gravel layer for the last two winter seasons was calculated from

$$F_G = F'_{z_1} - F_c \tag{9}$$

where

F_G = heaving force on the H pile due to the gravel layer

F'_{z_1} = interval axial force on the H pile at the depth of the first functioning strain gauge, near the bottom of the gravel layer for the last two winter seasons

F_c = uplift force on the H pile at the ground surface due to an overlying ice collar (F_c = 0 when there is no ice collar).

The depths of the first functioning strain gauge on the pipe pile are greater than the thickness of the gravel layer. Consequently, the heaving force on the pipe pile due to the gravel layer was not determined.

Data Aquisition Periods

The H and pipe piles were installed on 29 October 1982, and routine data acquisition began on 19 November after the installation of the instrument hut, electrical power, and connection of all strain and temperature sensors to an HP 3497A datalogger. Soil surface heave had already begun and freezeback of the soil adjacent to the piles was complete by the time the datalogging was started. Strain and temperature measurements were automatically recorded at intervals varying between two and twelve hours throughout the study. Data acquisition for the 1982-83 season ended on 13 April 1983 before thaw consolidation occurred in the soil surrounding the piles. Data were obtained continuously (except for a few data gaps) for the 1983-84 and 1984-85 seasons, from 9 September 1983 to 6 May 1985. Unfortunately one of the data gaps (28 September to 20 October 1983) occurred at the beginning of the 1983-84 frost heave season so the onset of frost-heave-induced effects were missed. Consequently, the

initiation of soil surface heave and the associated forces were not measured until the beginning of the 1984-85 season.

EXPERIMENTAL RESULTS

A common period of interest was selected for graphical presentation of the results of this study from 1 September 1982, 1983 or 1984 to 1 June 1983, 1984 or 1985. The frost heave season generally begins by mid-October and ends by late April or early May. This common period covers the initiation, occurrence and end of the frost heave season and allows direct comparison between the three winter seasons of data.

Air, Ground, Pile and Ice Collar Temperatures

The air and ground temperatures for the 1982-83, 1983-84 and 1984-85 seasons are shown in Figures 14 and 15. There were five major low-temperature periods during each season when the air temperature dropped below -25°C for several days or more. Ground temperatures throughout the active layer above the permafrost measured at the thermistor string location in Figure 5 were at or below 0°C by early April for the first winter season and by early January for the last two winter seasons.

H and pipe pile temperatures for the 1982-83, 1983-84 and 1984-85 seasons are shown in Figures 16 and 17. The soil around both piles was thawed to a depth of 0.5 m on 23-24 November 1982 by covering and heating the tops of the piles in an unsuccessful effort to establish an unstrained (thawed soil) reference for the strain gauges. The effect of this heating shows up as a temperature spike in the 1982-83 pile temperatures (Figures 16 and 17). The temperatures along the H and pipe piles were slightly lower than in the adjacent undisturbed ground. The pipe pile temperature was generally lower than the H pile temperature during the winter, due to better thermal contact with the thermal siphon at depth.

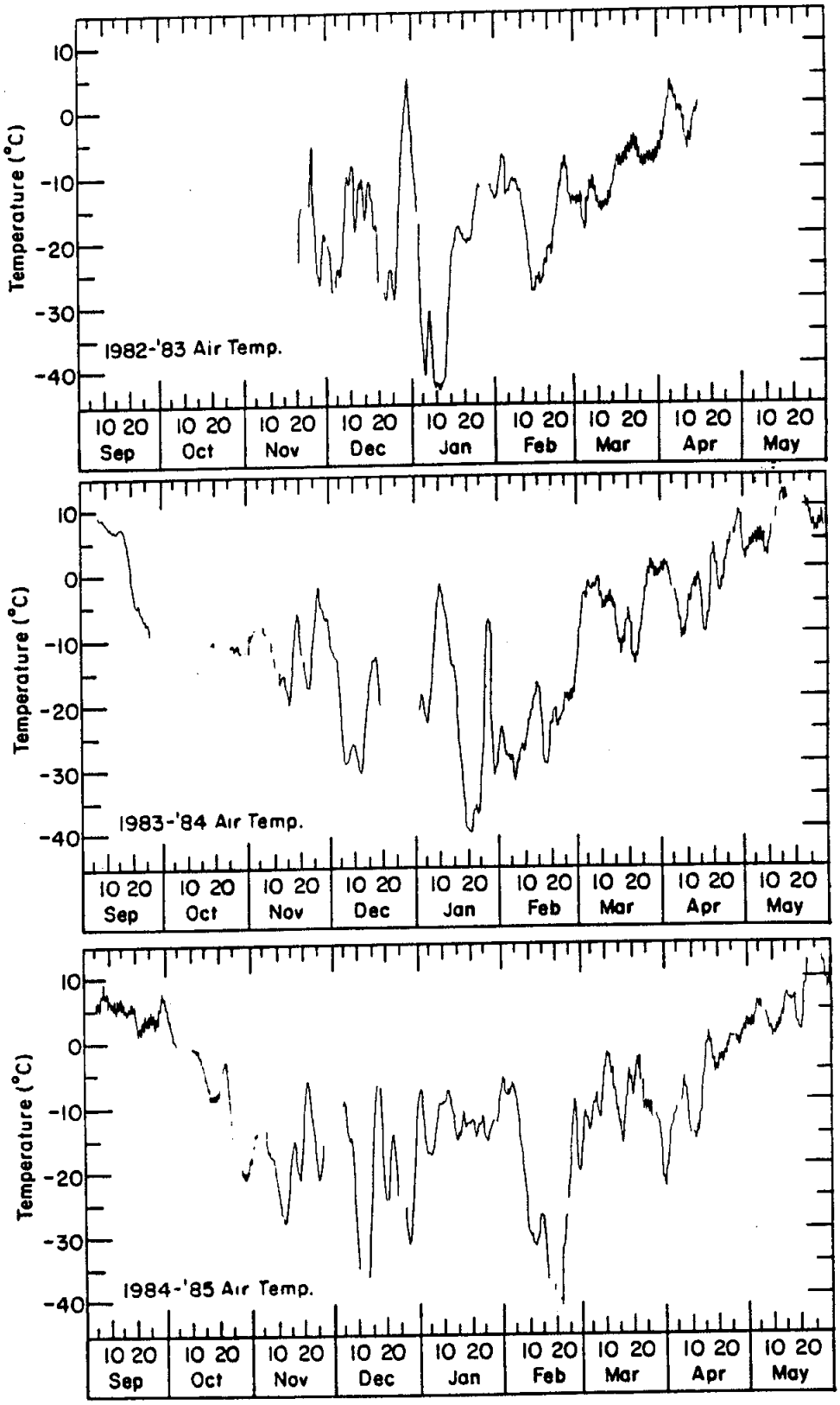

Figure 14. Air temperature for the 1982-83, 1983-84 and 1984-85 seasons.

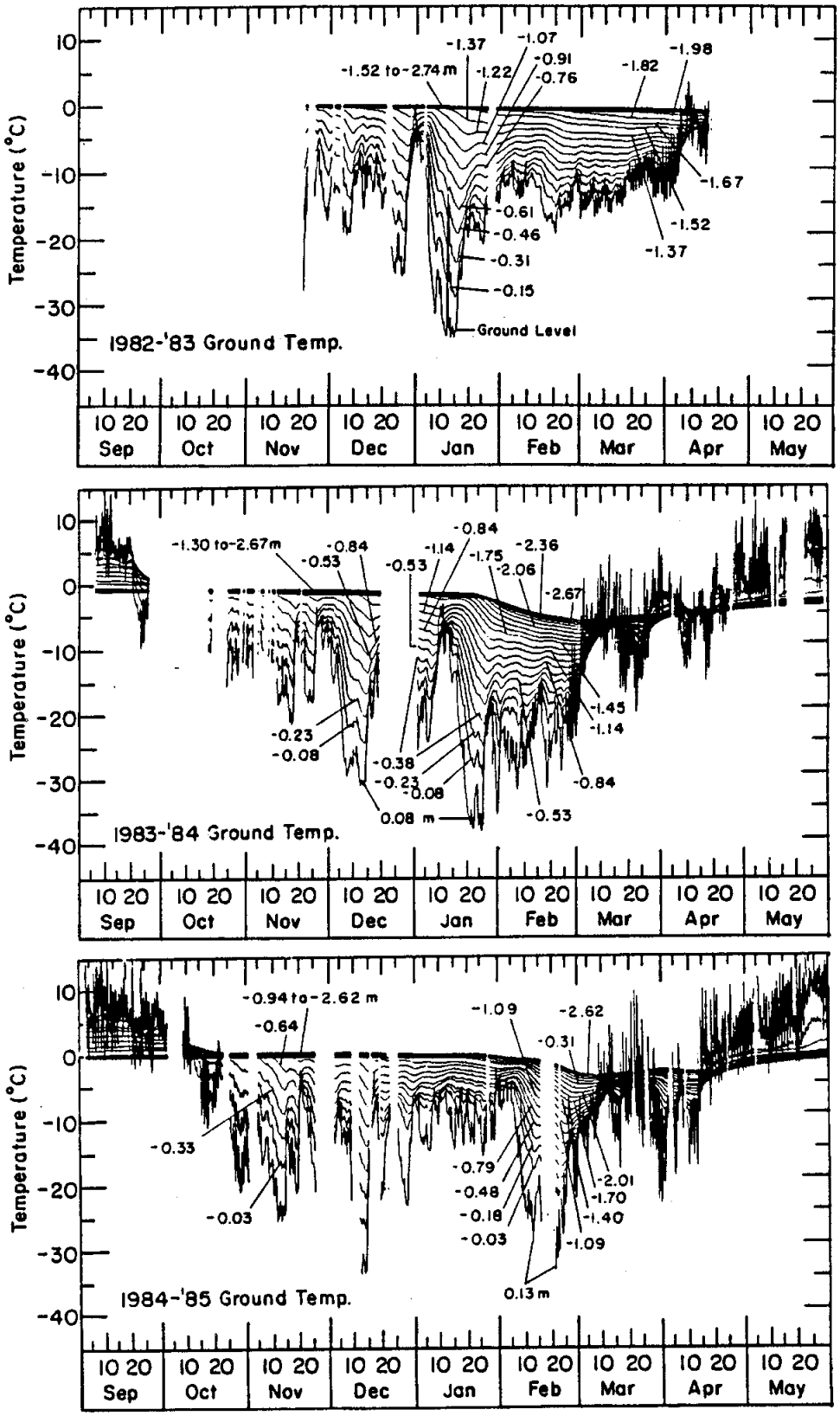

Figure 15. Ground temperature at different depths for the 1982-83, 1983-84 and 1984-85 seasons.

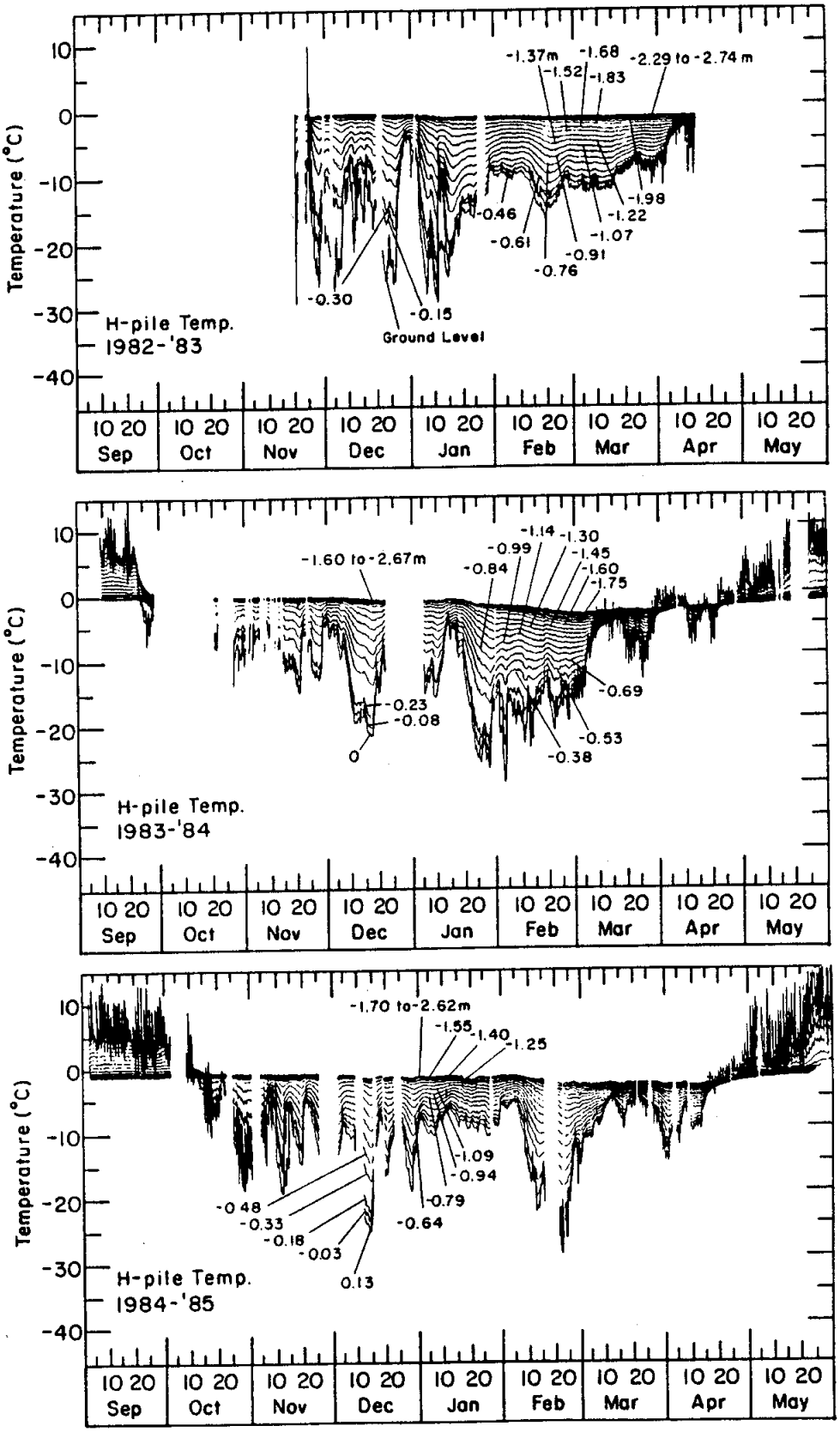

Figure 16. H pile temperature at different depths for the 1982-83, 1983-84 and 1984-85 seasons.

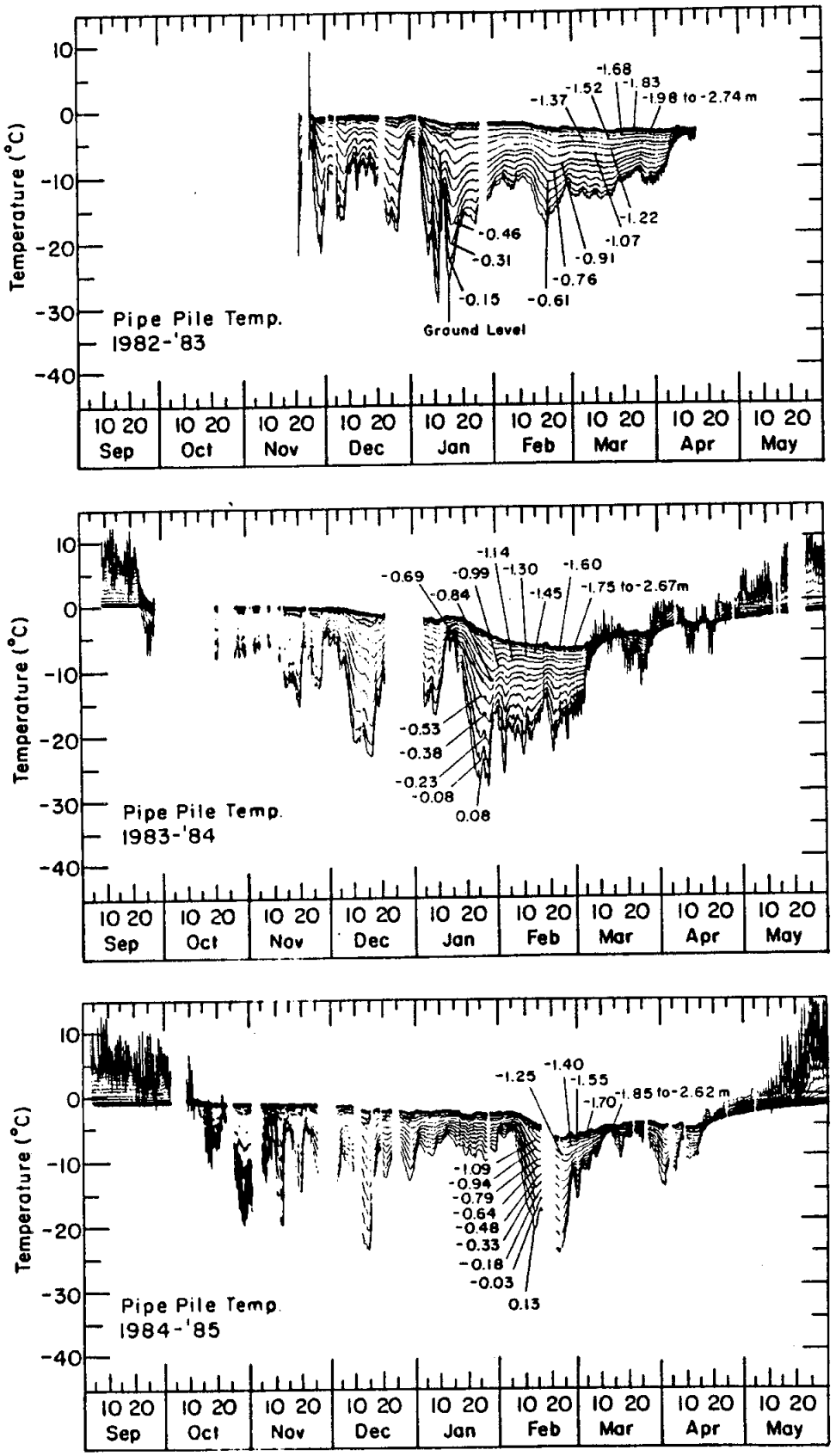

Figure 17. Pipe pile temperature at different depths for the 1982-83, 1983-84 and 1984-85 seasons.

Soil and pile temperatures were lower during the second and third winter seasons as a result of the roof structure sheltering the site (Figs. 15, 16 and 17).

The ice collars were formed by periodically pouring water into a 1.8-m-diameter confining ring surrounding the tops of the piles and allowing it to freeze in layers. This resulted in the sudden temperature rises during the periods of 5 to 13 January 1983 and 16 to 20 November 1984 in Figures 16 and 17. Ice collars were not used on the piles during the 1983-84 winter season.

The ground surface surrounding the piles and thermistor string was lower during the last two years of the study due to thaw consolidation of the soil around the piles and the disturbances caused by placing the gravel layer and ice collars (Fig. 6). As a result, the upper temperature sensor on both piles and the thermistor string were no longer below ground. Consequently, the soil and pile temperature records for the last two seasons show the effect of the upper temperature sensor recording air or ice collar temperatures at or near the ground surface (Fig. 15, 16 and 17). The temperature data from the upper sensor on both piles were used to represent the ice temperature when computing the ice/pile shear stresses over the thickness of the ice collar.

Pile Stability and Soil Surface Heave

The H pile and the pipe pile did not heave during the first year of the study as shown in Figure 13, at least within the resolution of the survey methods (± 1.0 mm). Subsequent surveys also showed that the piles were stable. The effectiveness of the thermal siphons and anchor rings/plates in refrigerating and anchoring the lower ends of the test piles in the permafrost was demonstrated by the stability of the test

piles. Figure 18 shows the soil surface heave for the 1982-83, 1983-84 and 1984-85 seasons. The ground surface displacements shown in Figure 18 may not represent the absolute or maximum accumulated displacements due to frost heave since the measurements were not initiated at the onset of frost heave. Soil surface displacements prior to the onset of frost heave were considered to be minimal. The large displacement of the soil indicated by the LVDT located 0.4 m from the pipe pile in 1983-84 relative to the displacements indicated by the other three LVDT's is probably the result of more frost heave in the vicinity of the pipe pile. Unfortunately, the LVDT's were reset during a data gap on 2 to 5 November 1984 (as shown by the obvious break in the 1984-85 soil displacements) and an ice collar was used around the piles, making it impossible to verify whether larger soil surface displacements again occurred in the vicinity of the pipe pile during the 1984-85 season. Soil surface displacements of 2 to 7 cm are indicated on Figure 18.

Forces and Shear Stresses

A true unstrained reference used to determine strains was obtained for both piles during the field calibration tests on 20-21 June 1985, when the piles were completely free of the surrounding soil by excavation and truly unloaded (Appendix B). These unstrained references were called common references since they were applied to all three seasons of data to determine the total strains, stresses, and forces on the piles. Figure 19 shows the total forces on the H pile for all three seasons of the study. Both positive tensile (uplift) and negative compressive (resistive) forces are shown on the H pile in Figure 19. The initial tensile load on the H pile after installation is believed to be the loading on the pile caused by freezeback of the backfill slurry. The remnant compressive and tensile

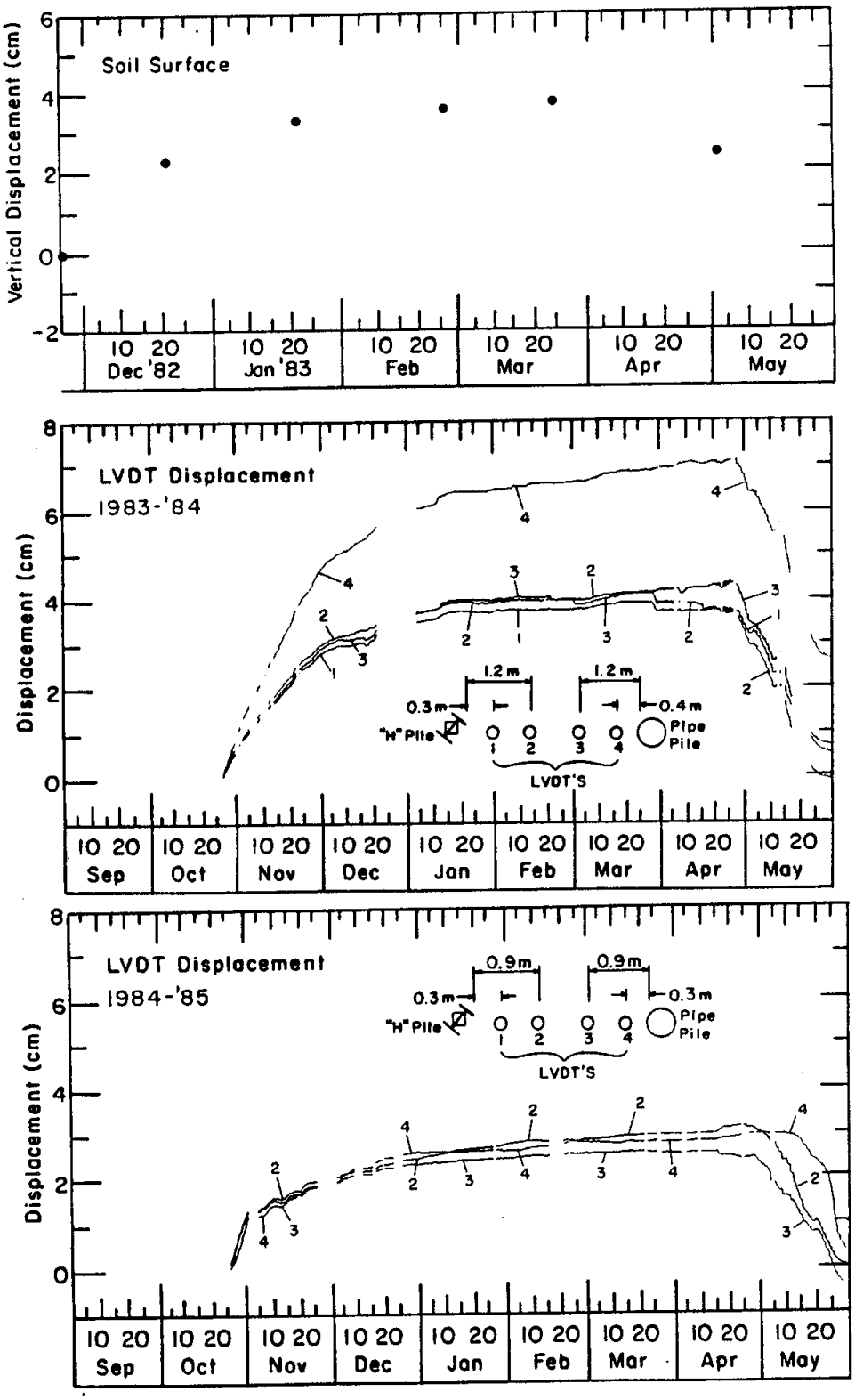

Figure 18. Soil surface heave for the 1982-83, 1983-84 and 1984-85 seasons. LVDT displacements for points 1, 2, 3 and 4 indicate soil surface displacements taken at the locations indicated.

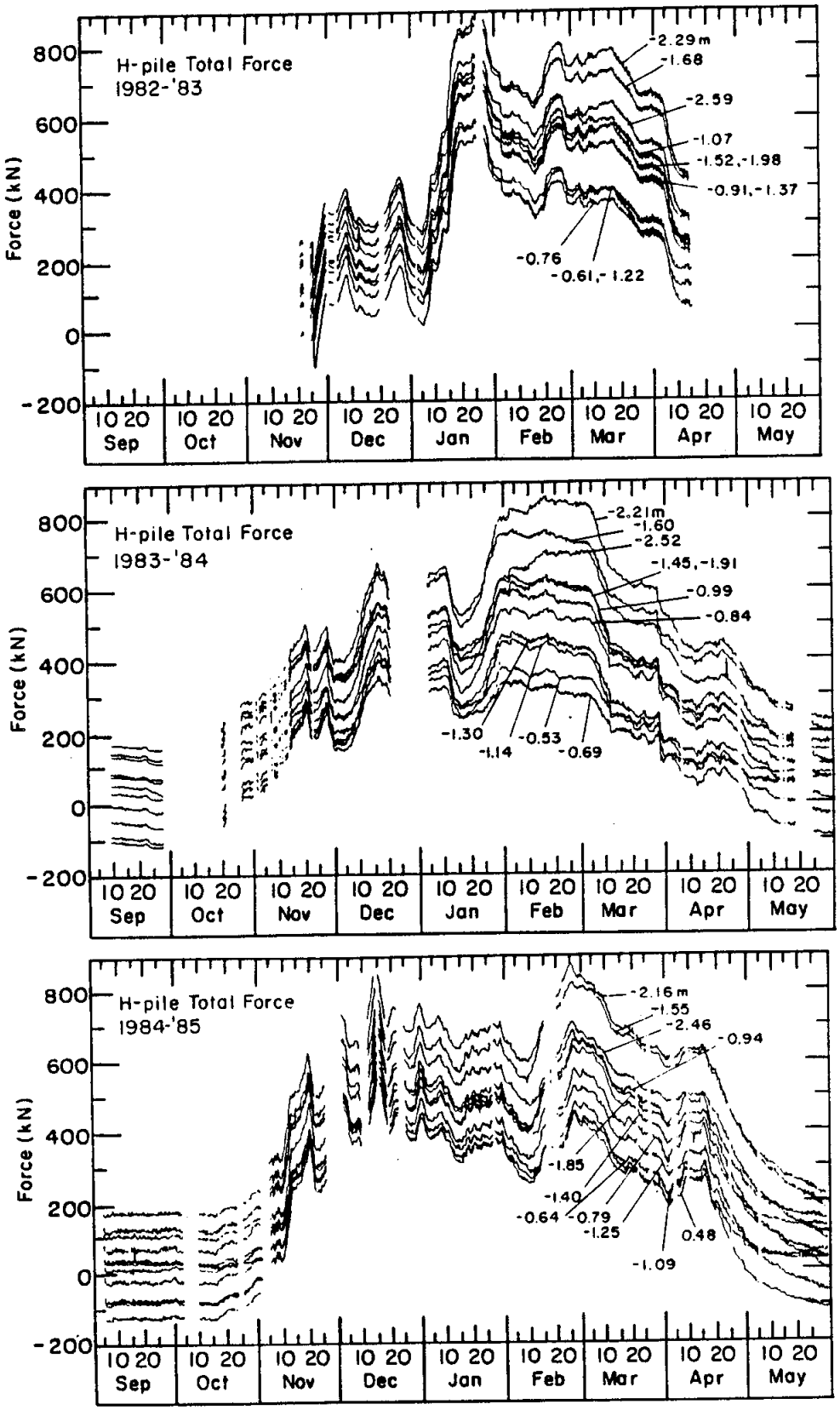

Figure 19. Total force on the H pile at different depths for the 1982-83, 1983-84 and 1984-85 seasons.

forces on the H pile at the beginning and end of the 1983-84 and 1984-85 frost heave seasons are considered to be the result of the redistribution of forces due to thaw consolidation of the adjacent soils (Fig. 19). The total forces shown in Figure 19 give the complete loading history including the effects of soil thaw consolidation and frost-heave-induced uplift on the H pile during the periods of interest.

Three local references (one for each data season) were used to take in-situ strains into account and to determine frost heave strains, stresses and forces relative to the time of the local reference. The total forces relative to the common reference began to increase on the H pile on 15 October 1984, the beginning of the 1984-85 frost heave season (Fig. 19). The first set of strain measurements taken on 15 October 1984 were selected as the local reference for the 1984-85 season. The selection of the local references for the 1982-83 and 1983-84 data sets was not as clear cut since the onset of the total force increase was missed for both years (Fig. 19). The local references were selected as near as possible to the onset of the total force increase for the 1982-83 and 1983-84 seasons (24 November 1982 and 28 September 1983 respectively). Consequently, the frost heave force and shear stress values for the first two seasons do not represent the absolute or maximum values. The local references selected for the pipe pile were taken at the same times as those for the H pile.

Frost heave forces for the three seasons covered in the study are shown in Figure 20 for the H pile and Figure 21 for the pipe pile. Table 3 is a summary of the magnitude, times and depths of occurrence of the forces and shear stresses on both piles during the study.

Strains, stresses and forces could not be determined for the 1982-83 data set on the pipe pile since the field calibration results do not apply

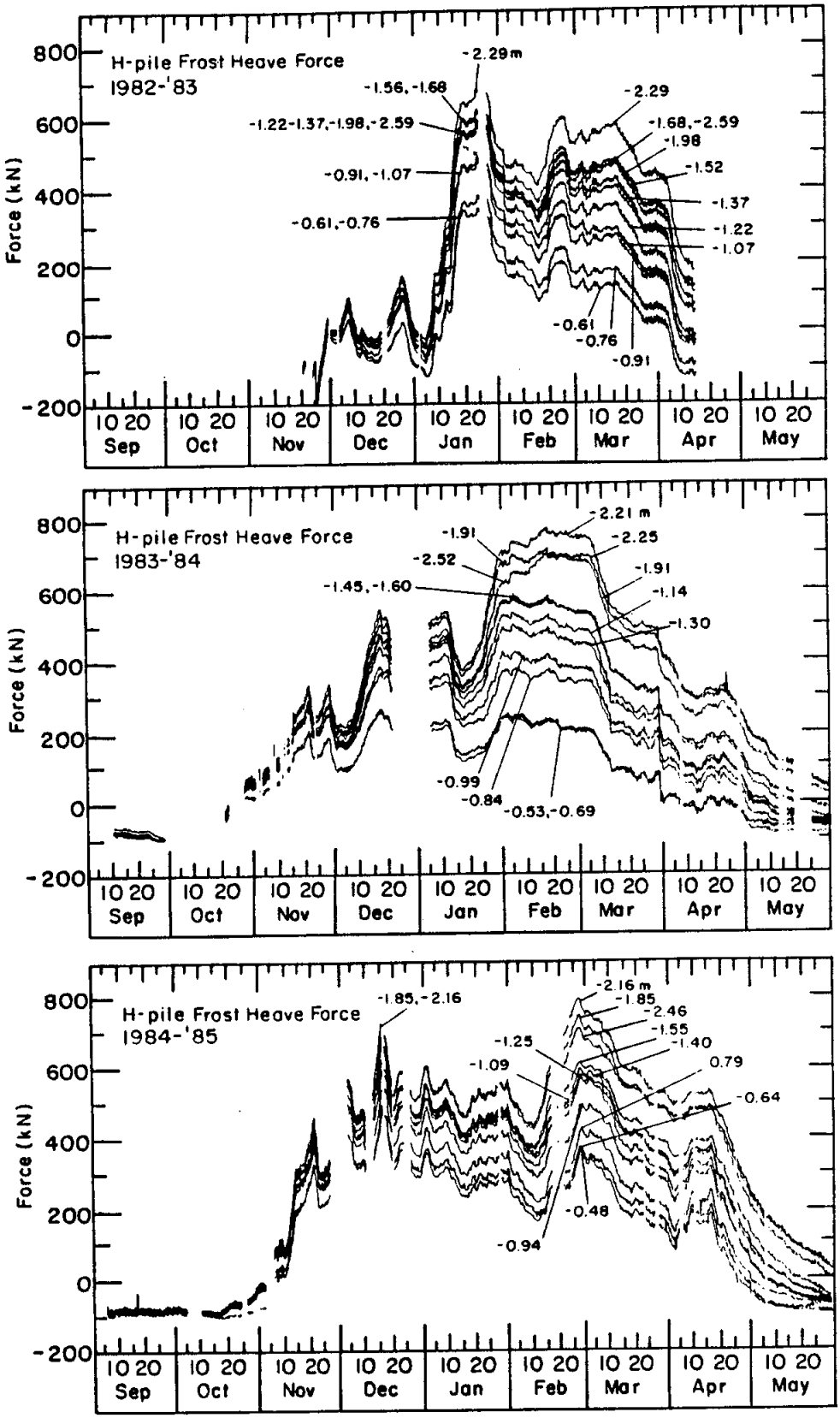

Figure 20. Frost heave force on the H pile at different depths for the 1982-83, 1983-84 and 1984-85 seasons.

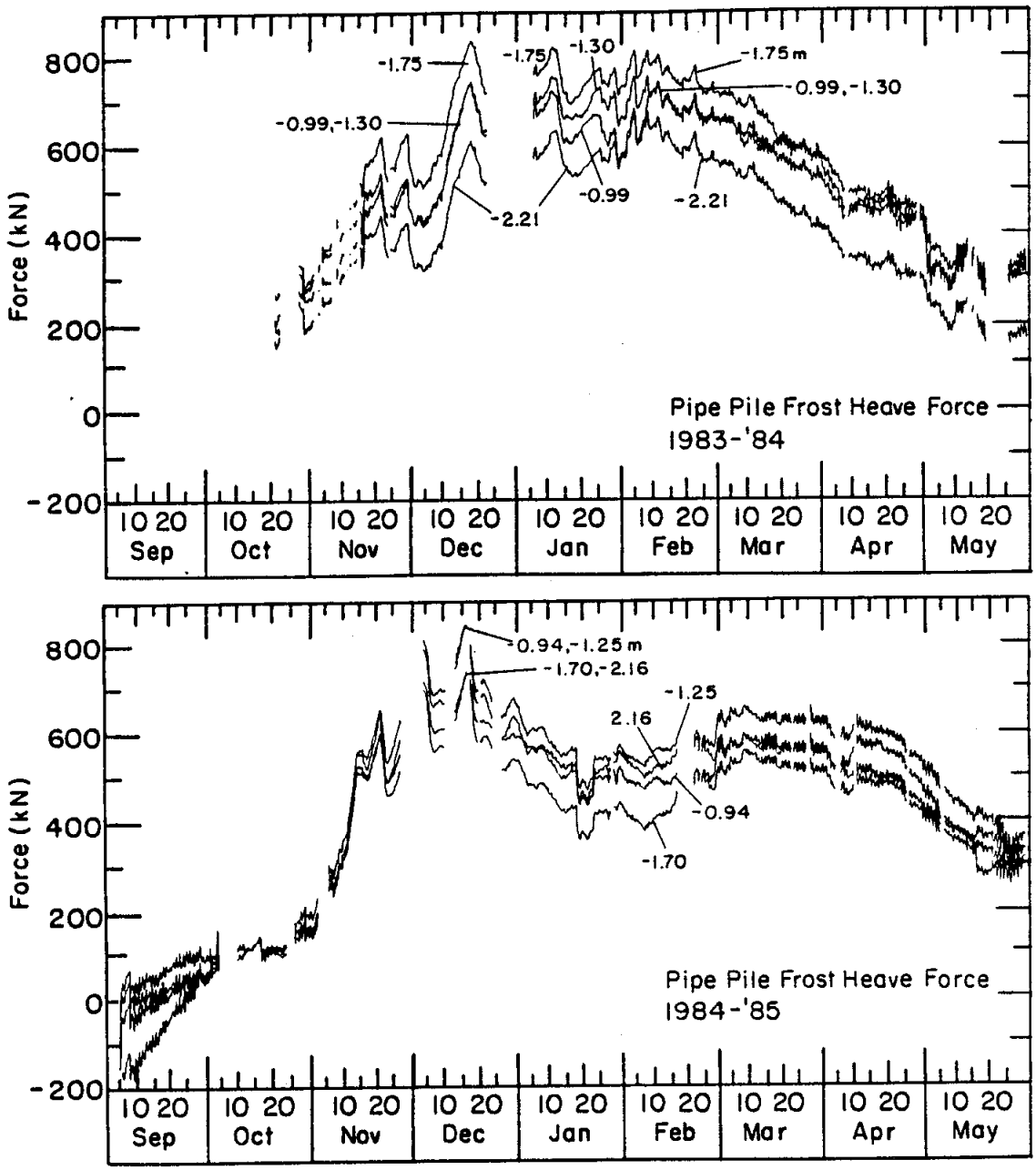

Figure 21. Frost heave force on the pipe pile at different depths for the 1983-84 and 1984-85 seasons.

Table 3. Summary of Maximum Forces and Average Shear Stresses on the H and Pipe Piles.

	H pile			Pipe Pile *	
	1982-83	1983-84	1984-85	1983-84	1984-85
Date Peak Frost Heaving Force Occurred	24 Jan 1983	17 Feb 1984	26 Feb 1985	17 Dec 1983	15 Dec 1984
Depth Below Ground Surface Where Peak Force Occurred (m)	2.29	2.21	2.16	1.75	0.94
Peak Frost Heaving Force (kN)	752	790	802	1118	1115
Thickness of the Active Layer Between the Piles at the Beginning of the Season (m)	2.3	1.6	1.6	1.6	1.6
Thickness of Ice Collar (m)	0.25	---	0.45	---	0.45
Heaving Force Due to Ice Collar (kN)**	151	---	118	---	185
Ice/Pile Shear Stress Due to Ice Collar (kPa)**	588	---	255	---	401
Maximum Average Soil/Pile Shear Stress Using "Boxed in" (H) Surface Area of the H Pile (kPa)***	256	348	308	---	---
Maximum Average Soil/Pile Shear Stress Using Actual Surface Area of the Pipe Pile (kPa)***	157	214	190	627	972
Maximum Internal Stress in Pile (MPa)	48.5	51.0	51.7	118.7	118.4
Heaving Force Due to Gravel Layer (kN)**	---	280	292	---	---

* The pipe pile results should be considered suspect until verified by further research (see comments in text).

** The force and shear stresses for the ice and gravel layers had to be calculated indirectly (see text) and may be too high for the ice layer and consequently too low for the gravel layer.

*** Computed using the pile surface areas from the soil surface to the depth of the peak frost heaving force on the pile.

to the full bridge completion circuits used on the pipe pile during the 1982-83 season (Appendix B). During the study the pipe pile suffered the loss of 86% of the strain gauges on the pile. The few remaining good gauges appear to be giving reliable results, which are given in Table 3 for the 1983-84 and 1984-85 seasons. The peak frost heave forces on the pipe pile were 43% higher and occurred earlier in the season and at a shallower depth than those for the H pile. The magnitudes of frost heave forces and average soil/pile shear stresses for the pipe pile appear too high in comparison with the H pile results and values reported by others. The pipe pile results should be considered suspect until verified by further research.

The peak forces on the H pile were essentially the same for all three winter seasons, varying by only ± 29 kN from the average peak force. The peak forces on the H pile occurred late in the season and at an average depth of 2.2 m, which was 0.6 m below the top of the permafrost table during the last two winter seasons of the study (Table 3).

The calculated heaving force and ice/pile shear stress due to the ice collars are given in Table 3. The ice collars may have contributed 15 to 20% of the peak forces. These results were obtained using the indirect methods described in the "methods and materials" section, since all of the upper strain gauge sensors were unreliable (Appendix B). The ice/pile shear stresses given in Table 3 can vary considerably with changes in ice temperature and/or strain rate. Consequently, the calculated ice collar forces may be too high and should be used with caution. The average maximum soil/pile shear stresses given in Table 3 are computed on the basis of the "boxed in" (for the H pile) and actual surface areas of the H and

pipe piles from the soil surface to the depth of the peak frost heave force on the piles. The 0.6-m-thick gravel backfill layer around the H pile may have contributed about 35% of the peak forces measured on the pile during the second and third winter seasons (Table 3). The gravel backfill replaced the native soil around the tops of both piles. The higher peak forces measured on the pipe pile may be due to a larger contribution from the gravel layer; however, the force due to the gravel layer on the pipe pile could not be determined because of the lack of a reliable strain gauge on the upper portion of the pile.

Figures 22 and 23 show the pile temperature, shear stress distribution and frost heave force on the H pile during the 1984-85 season on the 15th of each month from October through May. The shaded area shows the shear stress distribution between good strain gauge sensor levels on the H pile. The ice/pile shear stress and the uplift force due to the ice collar are shown above the ground surface or zero depth value. Soil/pile shear stresses are not uniform along the length of the pile, but vary considerably in sign and magnitude over time and depth. Generally the uplift shear stresses due to frost heaving act from the ground surface to the depth of the maximum force on the pile, and the restraining shear stresses act from the depth of the maximum force on the pile downward until the uplift force is balanced. However, there are zones of resistive soil/pile shear stresses which reduce the frost heave force on the pile between the soil surface and the depth of the peak force. These resistive soil/pile shear stresses and the corresponding reduction in frost heave force are larger than those values which could be attributed to the

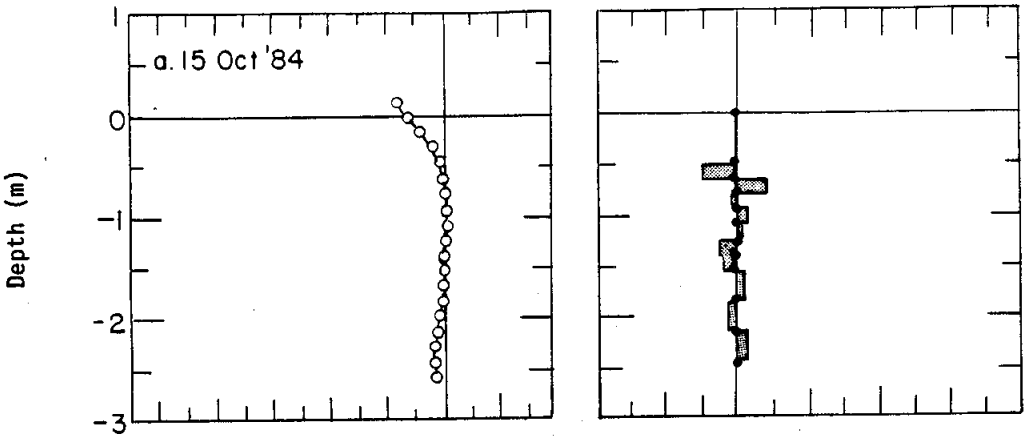

a. 15 October 1984.

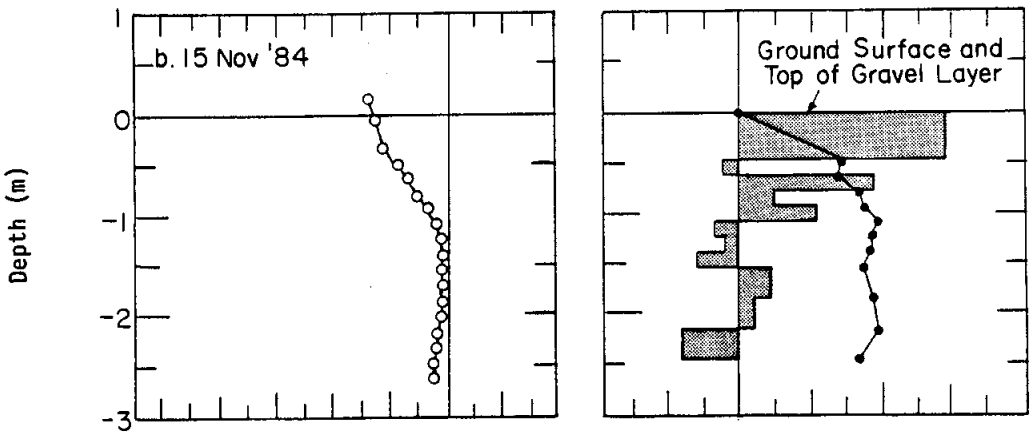

b. 15 November 1984.

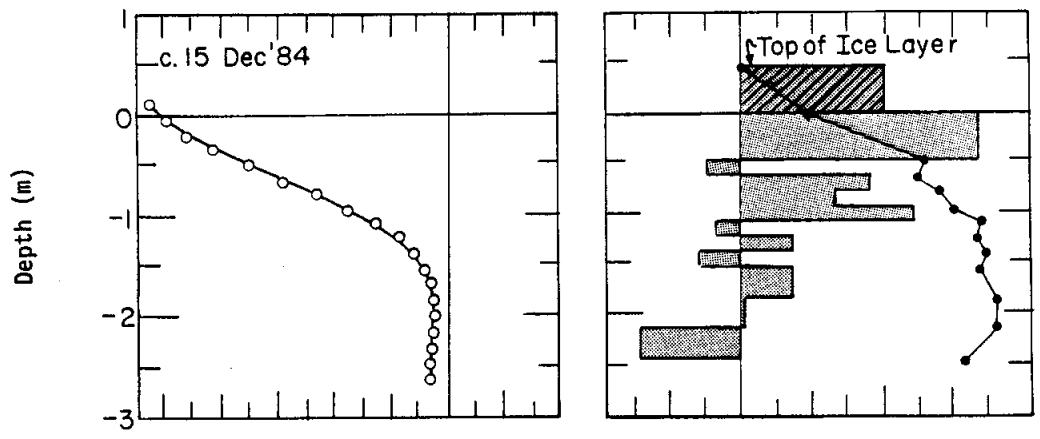

c. 15 December 1984.

Figure 22. Pile temperature, shear stress distribution (shaded area), and force as a function of depth for the H pile during the 1984-85 season.

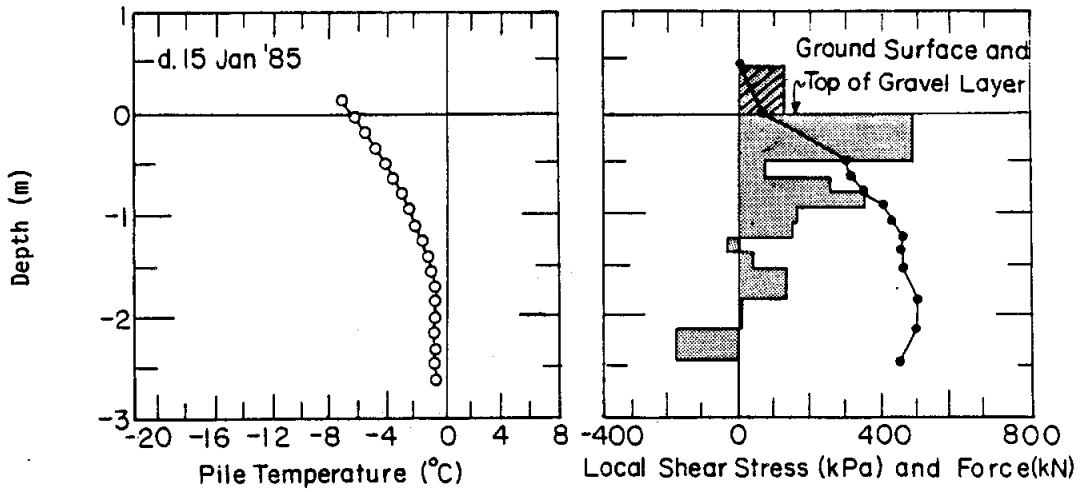

d. 15 January 1985.

Figure 22 (cont'd). Pile temperature, shear stress distribution (shaded area), and force as a function of depth for the H pile during the 1984-85 season.

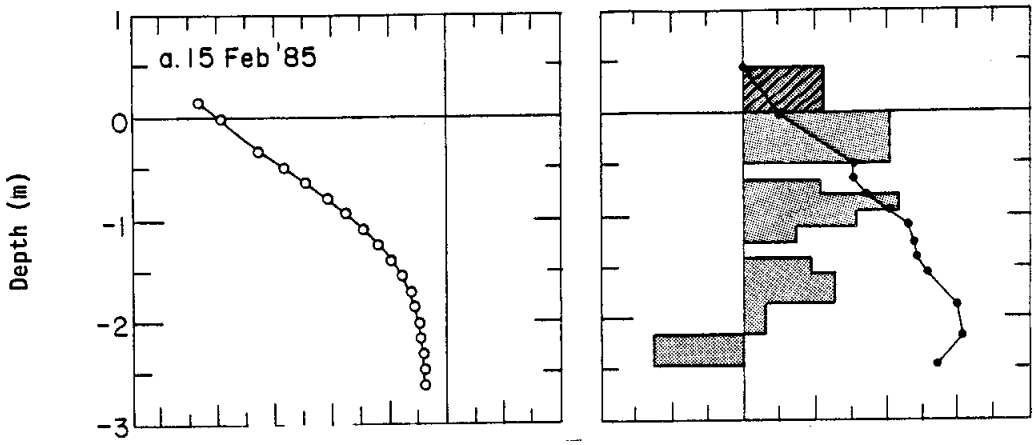

a. 15 February 1985.

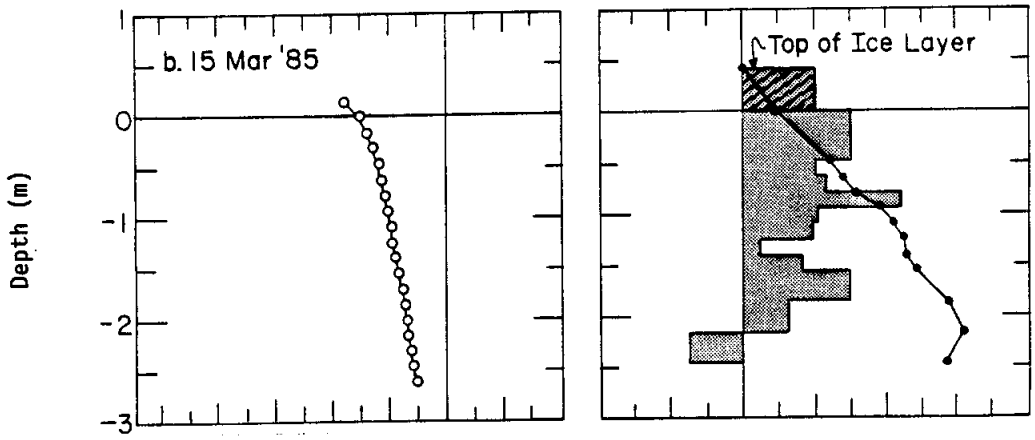

b. 15 March 1985.

Figure 23. Pile temperature, shear stress distribution (shaded area), and force as a function of depth for the H pile during the 1984-85 season.

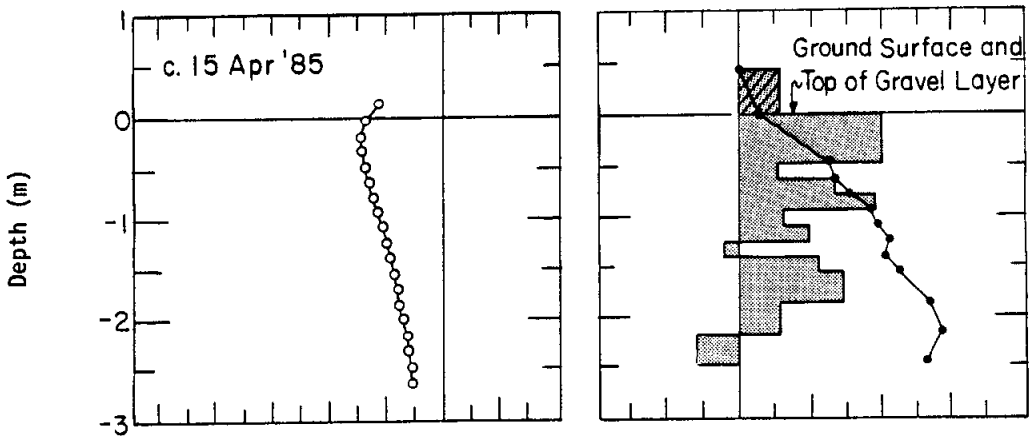

c. 15 April 1985.

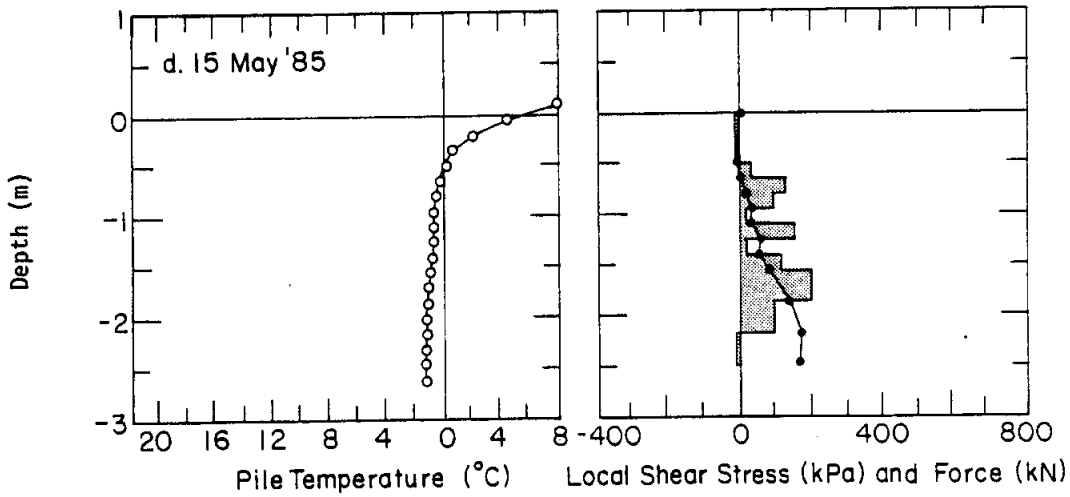

d. 15 May 1985.

Figure 23 (cont'd). Pile temperature, shear stress distribution (shaded area), and force as a function of depth for the H pile during the 1984-85 season.

variability associated with the estimate of Young's modulus for the gauges. The zones of resistive soil/pile shear stress may be due to bands of slightly different soil type or moisture/ice content. A detailed investigation of soil type and moisture/ice content with depth and time is needed to adequately investigate the zones of resistive shear stress between the soil surface and the depth of the peak force. The top of the permafrost table was at a depth of 1.6 m at the beginning of the 1984-85 winter season. The depth of the maximum force on the H pile was 0.6 m

below the top of the permafrost table during the 1984-85 season. Uplift soil/pile shear stresses are present in the permafrost throughout the winter season.

The majority of experiments to measure frost heaving forces acting on piles have been conducted on piles embedded in non-permafrost soil. In analyzing the results of those experiments it has been implicitly assumed that once the soil temperature is lower than 0°C (i.e. when the soil is frozen) that soil heave and frost heaving forces are negligible. The results of our experiments and those of Crory and Reed (1965) indicate that soil heave and frost heave forces continue to be generated throughout the winter even in frozen ground (Fig. 18, 19 and 20). Ground temperatures throughout the active layer above the permafrost were at or below 0°C by early April for the first winter season and by early January for the last two winter seasons (Fig. 15). Peak frost heave forces occurred on the piles when the soil temperatures were below 0°C at depths below the top of the permafrost table. Significant soil heaving occurred after all ground temperatures fell below 0°C (Fig. 18). A comparison of Figures 18, 19 and 20 shows that the soil heave rate is very small during the period of maximum uplift forces.

The fact that soil heave and increases in pile uplift forces are occurring even when soil temperatures are below 0°C leads us to hypothesize an explanation that incorporates the existence and migration of unfrozen water within the frozen soil. Experiments have shown that a mixture of ice and unfrozen water is present in soils at temperatures below 0°C. Experiments have also shown that a frozen soil containing both ice and unfrozen water that is subjected to a temperature gradient causes water to move towards the colder soil (Dirkson and Miller, 1966; Oliphant et. al.,

1983). The resulting migration of water toward the colder soil tends to enhance ice lens formation and consequently soil heaving. The water migration continues until the unfrozen water and ice content in the source zone is reduced to insignificant levels (Tice et al., 1982). Measurements of unfrozen water content as a function of temperature for soils show that the percentage of unfrozen water decreases exponentially with decreasing temperature (Fig. 24). Experiments on Fairbanks silt indicate that frost heaving may be insignificant for soil temperatures in Fairbanks silt below -2°C (Anderson and Morgenstern, 1973).

The unfrozen water content-temperature relationship may explain why the heave forces acting on piles embedded in permafrost respond so rapidly to temperature changes. On cooling, the unfrozen water will migrate toward the colder soil, causing an increase in ice lens growth, and the percent of unfrozen water will decrease exponentially as a function of temperature.

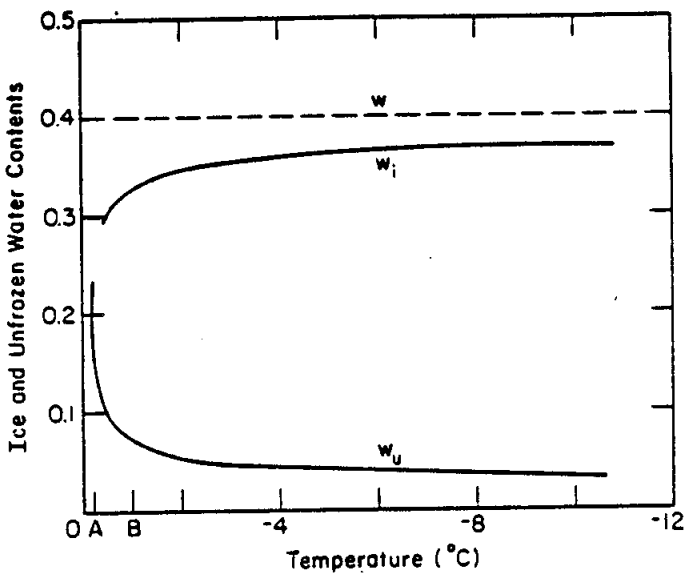

Figure 24. Unfrozen water and ice contents in Fairbanks silt (after A. Tice). Rate of maximum freezing occurs at A for unfrozen soil and at B for soils that are cooling, and the highest temperature is -1°C.

This may contribute to increased heave forces. On warming, the percent of unfrozen water will increase exponentially as a function of temperature, resulting in a decrease in heave forces. The rapid change in unfrozen water content will also result in a significant change in the mechanical properties of the soil. An increase in unfrozen water content will reduce soil shear strength, resulting in increased creep and lower shear stresses and forces on the piles.

The ice and unfrozen water content versus temperature relationship for in-situ soils may be useful in developing a method for designing pile installations in both permafrost and unfrozen soils. During soil cooling, soil temperature measurements and the percent unfrozen water-temperature relationship for the soil could be used to determine the depth of maximum freezing rate (i.e. the depth at which unfrozen water is being most rapidly converted to ice) in the soil, which ultimately is related to the depth over which shear stresses and uplift forces act on a pile. This depth may possibly be determined from the slope of the ice and unfrozen water content versus temperature curve (Fig. 24). The depth of maximum heave force might be expected to coincide with the depth of most rapid freezing. This depth depends on the soil temperature and will vary with soil type. For non-permafrost soils the depth of most rapid freezing is near the 0°C isotherm (it usually occurs at temperatures somewhat lower than 0°C; Fig. 24). For permafrost soils the depth to the maximum rate of freezing may still be useful in establishing pile installation designs. This can be accomplished by monitoring the soil temperature as a function of depth and time throughout a winter. The soil temperatures are used with the ice and unfrozen water content curves to estimate the depths of maximum freezing rate over time. The depth of maximum freezing rate is then used when calculating the depth of action for frost heaving stresses over time.

Presently few ice and unfrozen water content versus temperature relationships have been determined, and their dependence on initial soil water content have been poorly investigated. A large number of ice and unfrozen water content relationships for different soils would have to be determined before the proposed pile installation design method could be routinely used.

Spatial and Temporal Location of Peak Forces

Figures 25, 26 and 27 give comparisons of air temperature, ground temperature as a function of depth and time, and H pile frost heave force and temperature as functions of depth and time for the 1982-83, 1983-84 and 1984-84 seasons, respectively. Figures 28 and 29 give similar comparisons for the 1983-84 and 1984-85 seasons for the pipe pile. The spatial and temporal location of the maximum force on the piles for each season is indicated on Figures 25-29. The highest uplift forces acting on the piles occurred during the coldest periods of the winter (Fig. 25-29). The forces for both piles generally increased after a decrease in air temperature and decreased after an increase in air temperature. Changes in the forces acting on the piles usually lagged behind corresponding air temperatures from 1 to 8 days, with the longer lag times occurring later in the winter season. This was caused by the time required for an air temperature wave to propagate into the soil. Soil temperature changes at depth may affect the forces acting on the piles by changing the rate of soil heaving, the amount of unfrozen water in the soil, the adfreeze strength of the soil adjacent to the piles, or the creep properties of the soil, or by causing differential thermal expansion between the piles and the soil. The maximum forces (Fig. 25-29) do not necessarily coincide with the 0°C isotherm as

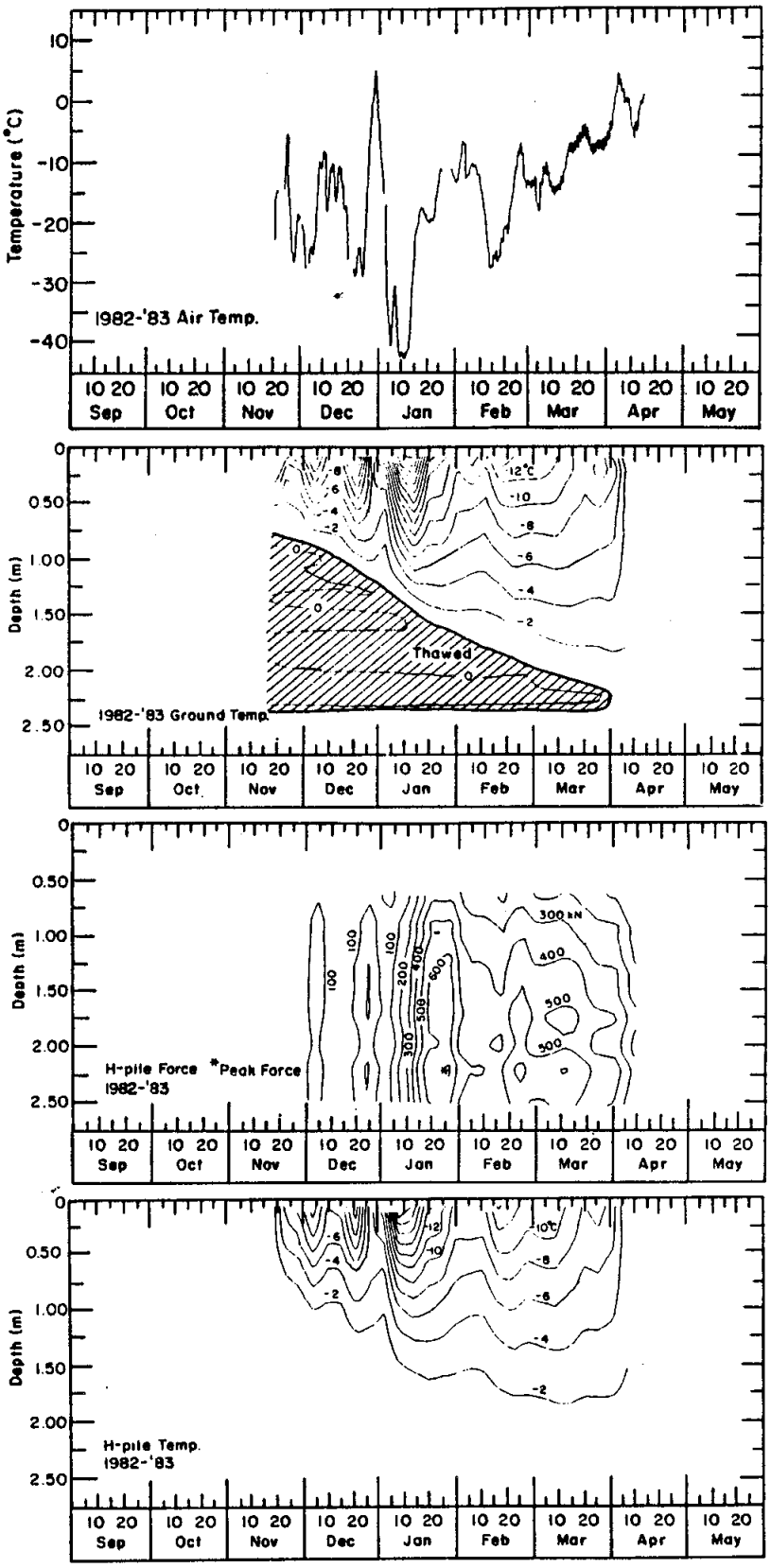

Figure 25. Comparison of air temperature, ground temperature as a function of depth and time, and H pile frost heave force and temperature as a function of depth and time for the 1982-83 season.

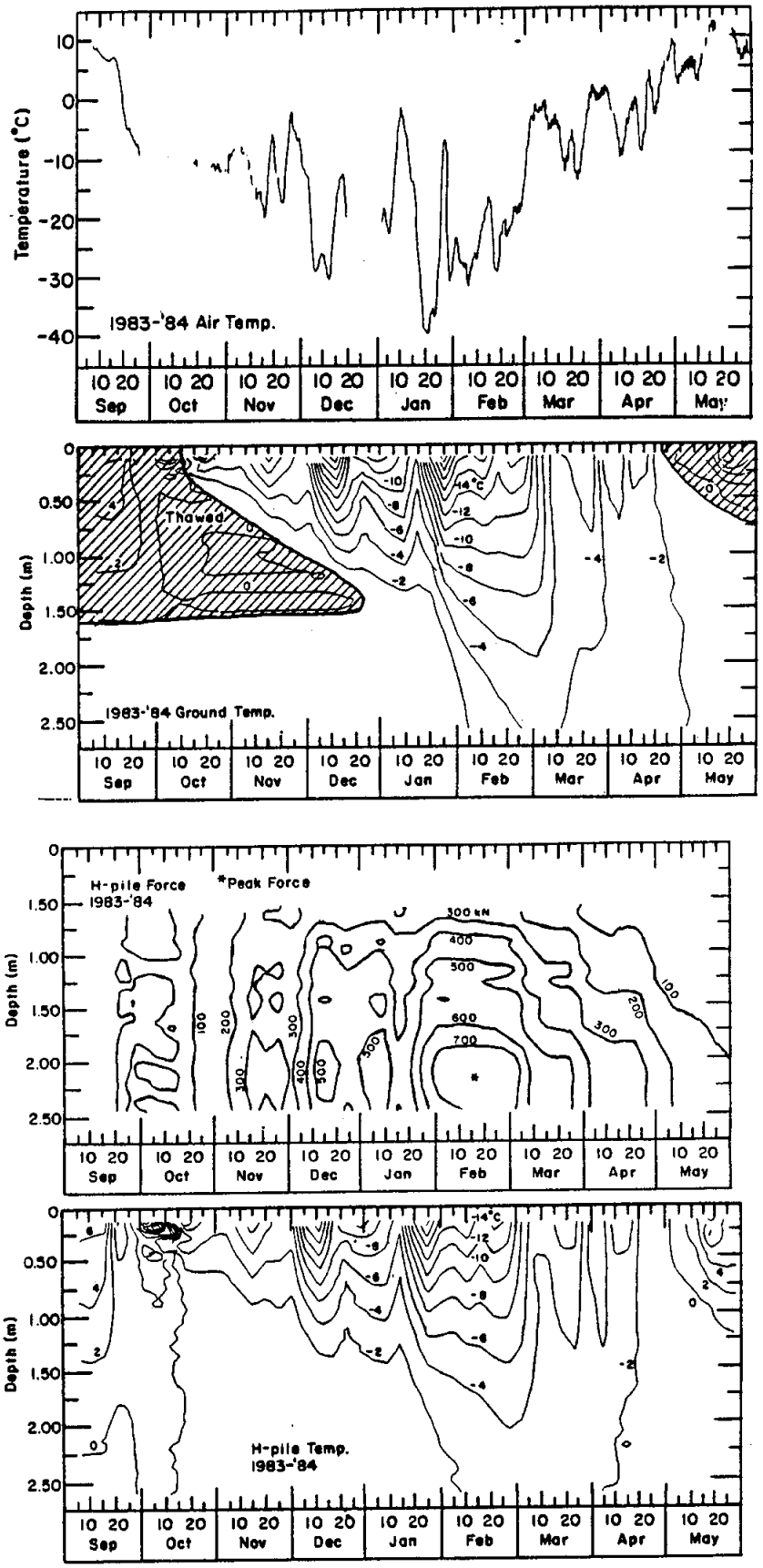

Figure 26. Comparison of air temperature, ground temperature as a function of depth and time, and H pile frost heave force and temperature as a function of depth and time for the 1983-84 season.

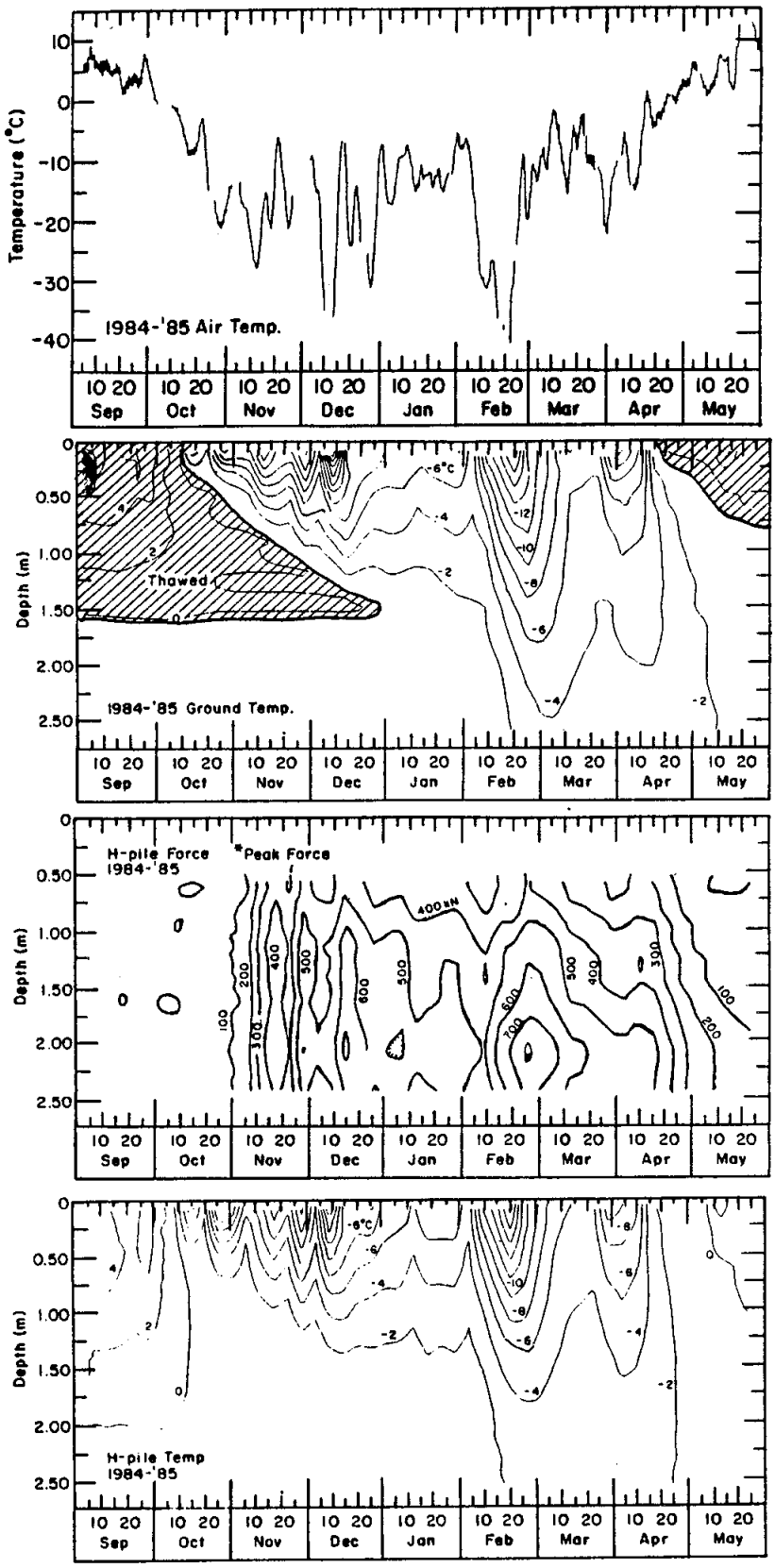

Figure 27. Comparison of air temperature, ground temperature as a function of depth and time, and H pile frost heave force and temperature as a function of depth and time for the 1984-85 season.

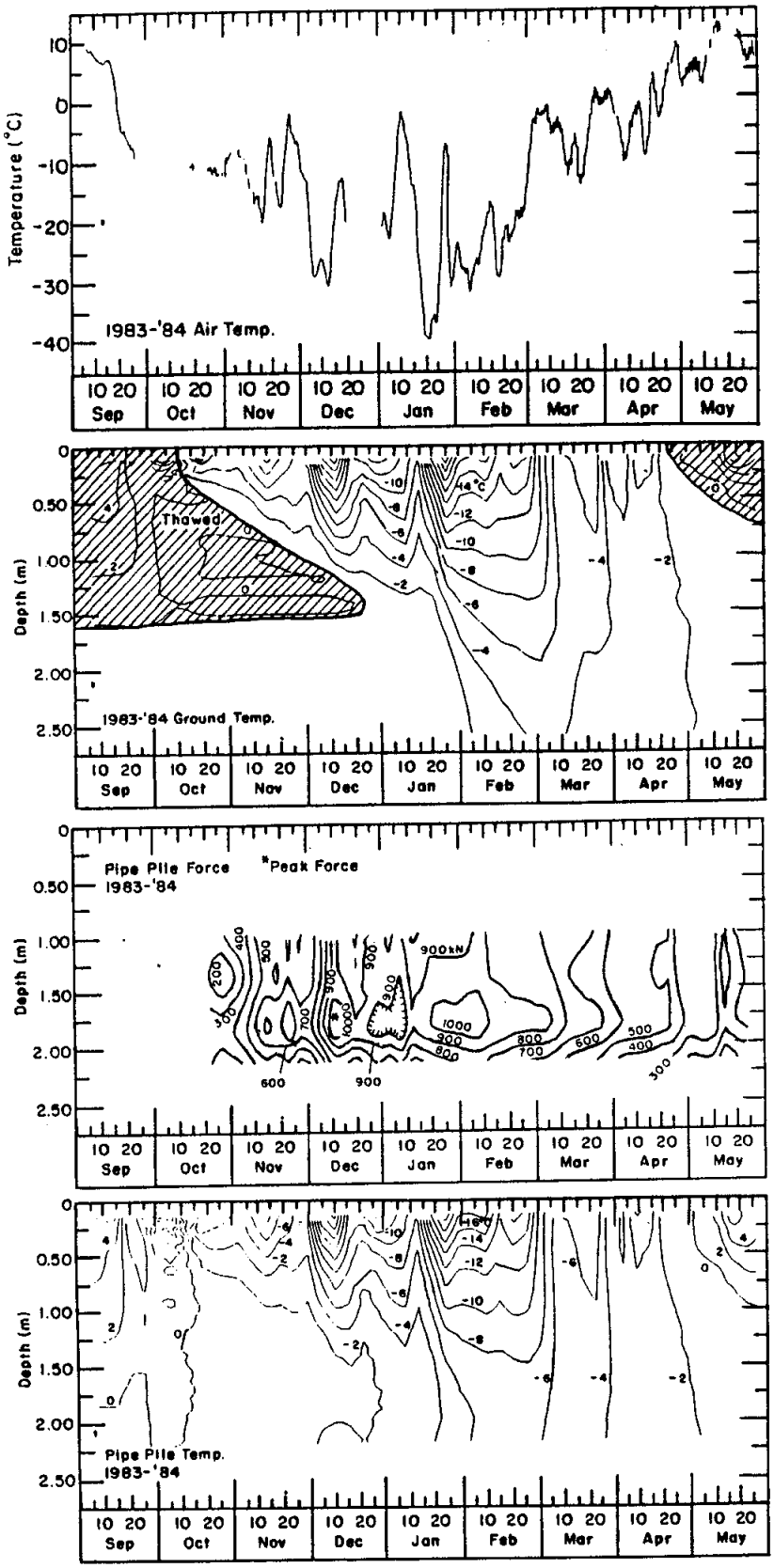

Figure 28. Comparison of air temperature, ground temperature as a function of depth and time, and pipe pile frost heave force and temperature as a function of depth and time for the 1983-84 season.

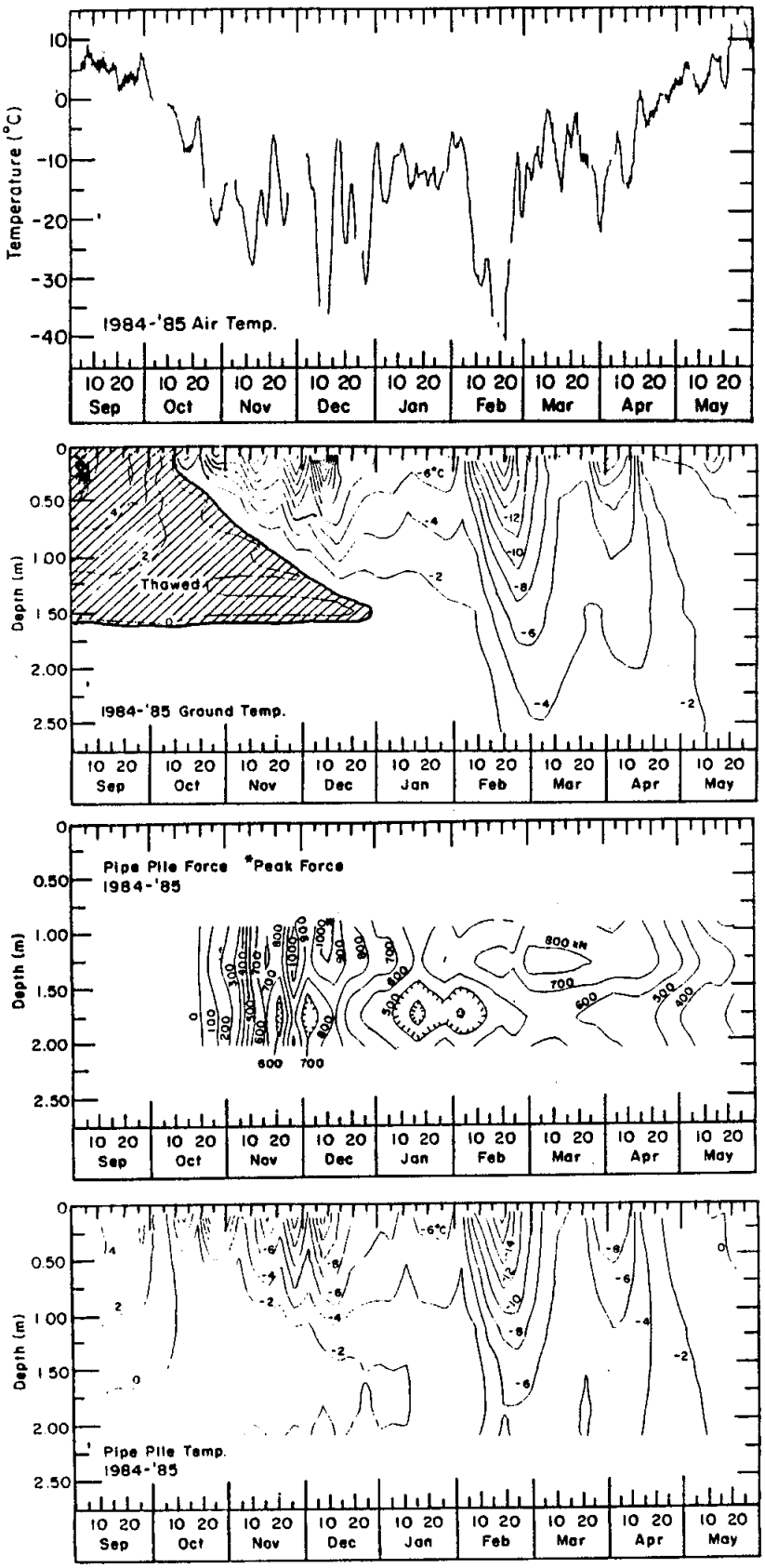

Figure 29. Comparison of air temperature, ground temperature as a function of depth and time, and pipe pile frost heave force and temperature as a function of depth and time for the 1984-85 season.

has been assumed in past studies. During the last two years of the study the peak frost heave forces on the H pile occurred at an average depth of 2.2 m, which is within the permafrost zone (Fig. 25-27). The shallower average depth of 1.4 m for the peak uplift forces on the pipe pile (Fig. 28 and 29) may be the result of the pipe pile-soil interface being colder due to better thermal contact with the thermal siphon at depth. In the spring, uplift forces are relieved from the surface down as the ground warms. A general reduction in force values also occurs over the full length of the piles (Fig. 25-29).

CONCLUSIONS

Calculated forces, as determined from the instrumented piles, indicate that the magnitude of frost-heaving uplift forces acting on a pile increase from the soil surface to a maximum value at depth, then decrease due to the restraining action of the soil or permafrost on the pile (Fig. 22 and 23). The depth of maximum forces does not necessarily coincide with the 0°C isotherm, as has been assumed in past studies. Therefore, average soil/pile shear stresses should be calculated on the basis of the pile surface area from the soil surface to the depth of the peak frost heave force when calculating shear stress from measured uplift forces. The average depths of the maximum frost heave forces were 2.2 m on the H pile and 1.4 m on the pipe pile. The peak frost heave forces on the H pile during the three winters of the study were 752, 790 and 802 kN. The peak frost heave forces on the pipe pile during the second and third winter seasons of the study were 1118 and 1115 kN. Maximum internal tensile stresses on the H pile were 48.5, 51.0 and 51.7 MPa during the three winters. Maximum internal tensile stresses on the pipe pile were 118.7 and

118.4 MPa for the second and third winter seasons. The heave forces that may have been contributed by the ice collars at the top of the piles during the 1982-83 and 1984-85 seasons were 151 and 118 kN, respectively, for the H pile and 185 kN during the third winter season on the pipe pile. The heave forces that may have been contributed by the gravel layer around the top of the H pile during the 1983-84 and 1984-85 seasons were about 280 and 292 kN, respectively.

Maximum average soil/pile shear stresses computed on the basis of the "boxed in" surface area of the H pile from the soil surface to the depth of peak frost heave force were 256, 348 and 308 kPa during the three winters on the H pile. Maximum average soil/pile shear stresses computed using the actual surface areas of the piles from the soil surface to the depth of the peak frost heave force were 157, 214 and 190 kPa during the three winters on the H pile, and 627 and 972 kPa during the second and third winter seasons on the pipe pile. Calculated ice/pile shear stresses due to the ice collars at the tops of the piles were 588 and 255 kPa for the H pile and 401 kPa for the pipe pile during the winters that ice collars were in place.

The forces and stresses resulting from the ice and gravel layers could not be determined directly because of strain gauge malfunctions. The forces and stresses were calculated indirectly and may be too high for the ice layer and consequently too low for the gravel layer.

Maximum heaving forces and shear stresses occurred during periods of maximum cold and soil surface heave magnitude. These forces were not related to the depth of frost for most of the winter since the soil adjacent to the piles was frozen to the permafrost table. The forces for both piles

generally increased after a decrease in air temperature and decreased after an increase in air temperature. Changes in forces acting on the piles usually lagged behind corresponding air temperature changes by several days.

The highest rates of soil surface heave occurred from the onset of heave in October to the end of December, and then the heave rates decreased through the rest of the winter. Soil surface displacements of 2 to 7 cm were measured at the experiment site.

The important mechanisms that determine the magnitude of uplift heave forces are: 1) soil heaving as the driving force, and 2) soil temperature, which controls the unfrozen water content, the mechanical properties of the soil and the area of influence of heaving pressures.

The higher forces and shear stresses on the pipe pile in this study may be the result of the soil/pile interface being colder than the soil/pile interface of the H pile due to better thermal contact with the thermal siphon at depth. The pipe pile results are considered suspect until verified by further research.

It is beyond the scope of this study to develop a method for designing pile installations in permafrost. However, an outline of how the results of this study might be used to design pile installations is presented below.

Past design methods for pile installations in soils subjected to frost heaving have utilized the 0°C isotherm as the reference to determine average expected shear stresses and uplift forces. This method may not be useful when permafrost is present and a unique 0°C isotherm does not exist. We suggest an alternate method of designing pile installations using the unfrozen water content-temperature relationship for the in-situ

soil type. During soil cooling, soil temperature measurements and the percent unfrozen water-temperature relationship for the soil could be used to determine the depth of maximum freezing rate (i.e. the depth at which unfrozen water is being most rapidly converted to ice) in soil, which ultimately is related to the depth over which shear stresses and uplift forces act on a pile. This depth can be determined from the slope of the ice and unfrozen water content versus temperature curve (Fig. 24). The depth of maximum heave force might be expected to coincide with the depth of most rapid freezing. This depth depends on the soil temperature and will vary with soil type. For non-permafrost soils the depth of most rapid freezing is near the 0°C isotherm (it usually occurs at temperatures somewhat lower than 0°C; Figure 24). For permafrost soils the depth to the maximum rate of freezing may still be useful in establishing pile installation designs. This can be accomplished by monitoring soil temperature as a function of depth and time throughout a winter. The soil temperatures are used with the ice and unfrozen water content curves to estimate the depths of maximum freezing rate over time. The depth of maximum freezing rate is then used when calculating the depth of action for frost heaving stresses.

RECOMMENDATIONS

The following recommendations are offered at the conclusion of this study:

1. The use of electric strain gauges as a method of measuring and determining frost heave forces on piles is recommended, since they take uplift and resistive shear stresses into account to determine the magnitude of peak forces on a pile and provide information concerning the spatial and temporal location of the forces. Soil/pile shear stress distributions along the pile can be determined from the results provided by this method.

Quarter bridge gauge configurations and the use of redundant strain gauges are recommended to provide better reliability, allow for easier data interpretation and accommodate the relatively high failure rate of strain gauges. Gauge calibration is required at the beginning and end of the experiment to verify the applicability of the initial calibration.

2. Further evaluation should be made of the H pile data set, as this may lead to a method of estimating the depth and timing of the peak force that would take into account the effect of unfrozen water on the frost heave forces.

3. Continued research on the unfrozen water-temperature relationship for frost-susceptible soils is recommended, as it may contribute to a better method of designing pile installations in permafrost and non-permafrost regions. Present design methods for pile installations in soils subjected to frost heaving utilize the 0°C isotherm as the reference to determine expected shear stresses and uplift forces. This method may not be useful in permafrost where a unique 0°C isotherm does not exist.

4. The pipe pile results need verification and the effects of the thermal siphon should be studied further. A comparative approach is recommended that uses a pipe pile without a thermal siphon and one with a thermal siphon. The adfreeze effects of an ice layer and gravel backfill should also be investigated using a similar comparative approach.

5. The influence of ice layers and different fill materials should be investigated further. Strain gauge malfunctions during this study prevented us from determining the force contributions resulting from the ice and gravel layers in a direct manner.

LITERATURE CITED

Anderson, D.M. and N.R. Morgenstern, 1973. Physics, chemistry, and mechanics of frozen ground. In: Proc. 2nd Int. Conf. Permafrost, North Amer. Contrib., pp.257-288.

Crory, F.E. and R.E. Reed, 1965. Measurement of frost heaving forces on piles. U.S. Army Cold Regions Res. and Eng. Lab., Technical Report 145.

Dirksen, C. and P.J. Miller, 1966. Closed-system freezing of unsaturated soils. Soil Science Society of America Proceedings, Vol. 30, pp. 168-173.

Domaschuk, L., 1982. Frost heave forces on embedded structural units. In: Proc. 4th Canadian Permafrost Conference, pp. 487-496.

Esch, D.C., 1982. Thawing of permafrost by passive solar means. Proc. 4th Canadian Permafrost Conference, pp. 560-569.

Esch, D.C., 1983. Permafrost prethawing by surface modification. Alaska Department of Transportation report AK-RD-83-23.

Johnson, J.B. and D.C. Esch, 1985. Frostjacking forces on H and pipe piles embedded in Fairbanks silt. In: Proc. 4th Int. Sym. Ground Freezing, Sapporo, Japan, Vol. 2, pp.125-133.

Johnston, G.H. and B. Ladanyi, 1972. Field studies of grouted rod anchors in permafrost. Can. Geotech. J., 9(2), pp 176-194.

Kinosita, S., 1967. Heaving force of frozen soils. In: Proc. Int. Conf. Low Temp. Sci. 11, pp. 1345-1360.

Kinosita, S., and T. Ono, 1963. Heaving forces of frozen ground. Mainly on the Results of Field Research. Low Temp. Sci. Lab. Teron Kagaku Ser. A-21, pp. 117-139 (N.R.C. Tech. Transl. 1246, 1966).

Kinosita, S., Y. Suzuki, K. Horiguchi and M. Fukuda, 1978. Observations of frost heaving action in the experimental site, Tomakamai, Japan. In: Proc. 3rd Int. Conf. Permafrost, Vol. 1, pp. 676-678.

Linell, K.A., 1973. Long-term effects of vegetation cover on permafrost stability in an area of discontinuous permafrost. In: North American Contribution, 2nd Int. Permafrost Conference (13-28 July 1973 Yakutsk, USSR), pp. 688-693.

Oliphant, J.L., A.R. Tice and Y. Nakano, 1983. Water migration due to a temperature gradient in frozen soil. In: Proc. 4th Int. Conf. Permafrost, Fairbanks, Alaska, pp. 951-956.

Paterson, W.S.B.,1981. The physics of glaciers. Pergamon Press, pp. 20-41.

Penner, E., 1970. Frost heaving forces in Leda Clay. Can. Geotech.J. 7(1), pp. 8-16.

Penner, E., 1972. Influence of freezing rate on frost heaving. Hwy. Res. Bd. Record No. 393, pp. 56-64.

Penner, E., 1974. Uplift forces on foundations in frost heaving soils. Can. Geotech. J., 11(3), pp. 323-338.

Penner, E. and L.W. Gold, 1971. Transfer of heaving forces by adfreezing to columns and foundation walls in frost susceptible soils. Can. Geotech. J., 8(4), pp. 514-526.

Penner, E. and L.E. Goodrich, 1983. Adfreezing stresses on steel piles, Thompson, Manitoba. In: Proc. 4th Int. Conf. Permafrost, Fairbanks, Alaska, pp. 979-983.

Penner, E. and W.W. Irwin, 1969. Adfreezing of Leda Clay to anchored footings columns. Can. Geotech. J., 6(3), pp. 327-337.

Pewe, T.L., Geologic hazards in the Fairbanks area, Alaska, Special Report 15, Alaska Geological and Geophysical Surveys, 109 p.

Saltykov, N.I., 1944. Calculating frost heaving forces on foundations. Izvestiia Akademia Nauk SSSR, Otdelenie Tekhnickeskikh Nauk, No. 6, pp. 305-412 (Translation 46 by Jaroslov J. Peel, Sipre Bibliography Project, Library of Congress, Washington).

Sohlberg, E.T., 1965. Strain gage instrumentation of steel piles in snow, USACRREL TR 152, 30 p.

Sutherland, H.B. and P.N. Gaskin, 1973. Porewater and heaving pressures developed in partially frozen soils. In: Proc. 2nd Int. Conf. Permafrost, North Amer. Contrib., pp. 409-419.

Tice, A.R., J.L. Oliphant, Y. Nakano and T.F. Jenkins, 1982. Relationship between the ice and unfrozen water phases in frozen soil as determined by phased nuclear magnetic reasonance and physical desorption data. USACRREL Report 82-15.

Trow, W.A., 1955. Frost action on small footings. Hwy. Res. Board Bull. No. 100, pp. 22-27.

Tsytovich, N.A., 1975. The mechanics of frozen ground. McGraw-Hill Book Co., pp. 157-162.

Yong, R.N., 1967. On the relationship between partial soil freezing and surface forces. In: Proc. Int. Conf. Low Temp. Sci. II, pp. 1376-1385.

Yong, R.N. and J.C. Osler, 1971. Heaving and heaving pressures in frozen soils. Can. Geotech. J., 8(2), pp. 272-282.

APPENDIX A. Instrumentation and Data Reduction

Strain Measurements

A Hewlett Packard (HP) 3497A data acquisition/control unit and an HP 85F computer were used to measure the static strains in both the pipe and H piles. The strain gauges were connected into Wheatstone bridges where one or more of the resistors were active strain gauges (Figure Ala). The

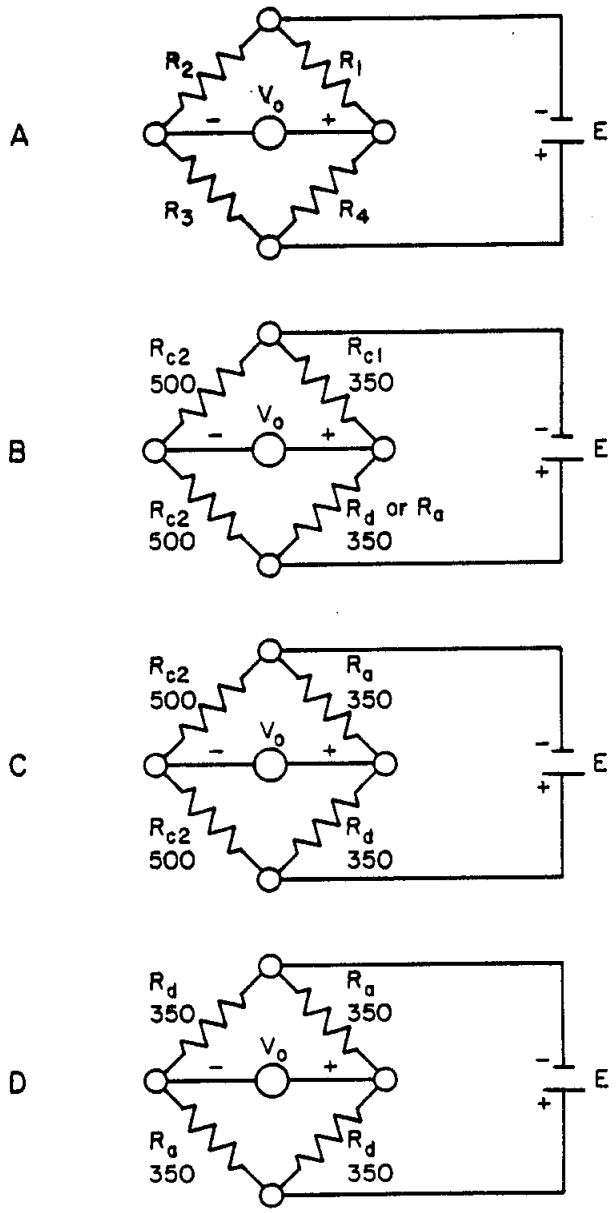

Figure A1. Wheatstone bridge circuits used to measure strain gauge resistance changes. (A) general wheatstone bridge; circuits B, C and D were used to measure one active strain gauge, uniaxial strain with temperature compensation using one active gauge, and uniaxial strain with temperature compensation using two active gauges.

unstrained voltage ratio for a Wheatstone bridge where all the resistors have a fixed value is given by

(A1) $$(V_o/V_i)_u = [R_1/(R_1 + R_4) - R_2/(R_2 + R_3)]$$

where V_i is the excitation voltage to the bridge (5 volts nominally for this experiment), V_o is the output voltage and R_1, R_2, R_3, and R_4 are the resistances of the bridge arms. If the resistance of one of the bridge arms changed due to straining, for example, the arm $(R_4 + \Delta R_4)$, then the strained voltage ratio would be

(A2) $$(V_o/V_i)_s = [R_1/(R_1 + R_4 + \Delta R_4) - R_2/(R_2 + R_3)].$$

The change in the voltage ratio between the strained and unstrained condition is given by

(A3) $$V_r = [(V_o/V_i)_s - (V_o/V_i)_u] = [R_1/(R_1 + R_4 + \Delta R_4) - R_4/(R_1 + R_4)].$$

If $R_1 = R_4$ then

(A4) $$(-4V_r)/(1 + 2V_r) = (\Delta R_4)/(R_4).$$

The relationship between strain and changes in resistance for resistance strain gauges is

(A5) $$GF \times \varepsilon = (\Delta R)/(R),$$

where ε is the strain and GF is the gauge factor determined by manufacturing processes. Strain is positive for positive resistance changes, which occur when the gauge is extended, and can be calculated from

(A6) $$\varepsilon_4 = (-4V_r)/(GF \times (1 + 2V_r)).$$

Equation A6 describes the situation of a Wheatstone bridge where one of the arms is an active strain gauge and the remaining arms of the bridge consist of resistors with fixed values.

In this study three different Wheatstone bridge setups were used with the strain gauges. The setup with a single active or dummy strain gauge as

shown in Figure A1b was called a quarter bridge setup since three completion resistors were required to complete the Wheatstone bridge circuit. The strain for the quarter bridge setup is given by

(A7) $\varepsilon_a = (-4V_r)/(GF \times (1 + 2V_r))$.

Fixed-value precision resistors R_{C1} and R_{C2} shown in Figure A1b were used to complete the bridge. The precision resistors were accessed on the strain gauge multiplexer card that plugs into the backplane of the HP 3497A. All bridge setups were determined with reference to the bridge completion circuit in the HP 3497A.

One active strain gauge and one dummy gauge were used in a bridge setup to provide temperature compensation to the strain gauge circuit and to measure uniaxial strain (Figure A1c). The dummy strain gauge, R_d, responds only to thermally induced apparent strains. The active strain gauge, R_a, responds to both thermally and stress induced strains. Thus, the temperature compensated strain for one active gauge connected to a temperature compensating gauge is given by

(A8) $\varepsilon_a = (4V_r)/(GF \times (1 - 2V_r))$.

This bridge setup required two completion resistors to complete the circuit and was called a half bridge setup.

The final Wheatstone bridge setup consisted of two active gauges and two dummy gauges (Figure A1d). Two of the gauges were for temperature compensation and two gauges were mounted on surfaces that were diametrically opposite from each other in the pipe pile and on opposite sides of the web for the H pile (transverse gauges only). The resulting measurement was an average uniaxial strain given by

(A9) $\varepsilon_a = (-2V_r)/(GF \times (1 + V_r))$.

Since this bridge setup did not require any completion resistors in the circuit it was called a full bridge setup.

The strain at a gauge depends on the unstrained voltage ratio used in equation A3 as the reference for the strain calculations. During the field calibration tests a true unstrained common reference was determined for each strain gauge which is used to compute total strain at the gauge (Appendix B). The unstrained common references were determined when the upper portion of the piles were free of the surrounding soil by excavation and the piles were experiencing no load. Three local unstrained references (one for each winter data set) were also determined by inspection of the strain data and used in equation A3 to compute frost-heave-induced strains in the piles relative to the time of the local reference.

The strain gauges used to measure longitudinal strain were connected so as to reduce errors associated with temperature changes. The gauges did not exhibit any significant temperature sensitivity.

Force and Stress Calculations

After the strain measurements were obtained, the tangential forces and shear stresses acting on the piles were calculated. Several basic assumptions were used in developing the calculation scheme for forces and stresses:

1. Forces acting on the piles were due primarily to vertical shear stresses acting on the surface skin of the pile,
2. Shear stresses along the H and pipe pile surfaces were the result of frost heaving forces or soil friction and were symmetrical in the horizontal plane,
3. The stresses acting on the piles in a horizontal plane at any given depth in the soil had azimuthal symmetry.

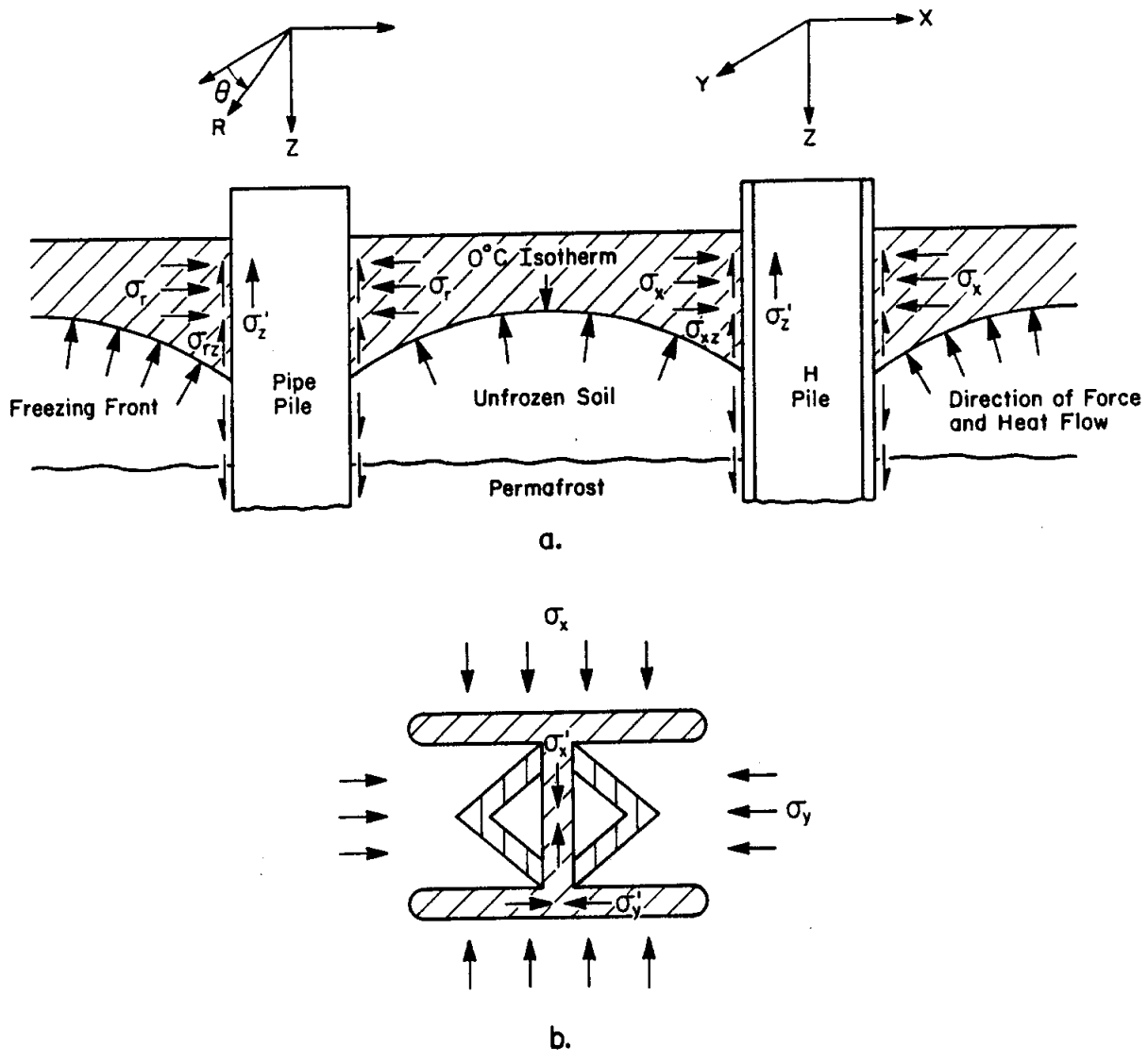

Figure A2. Diagram showing (A) the direction of force and heat flow and (B) the forces acting on the H pile in the horizontal plane using two active gauges.

Figure A2 shows the force diagram for both the pipe and H piles. A cylindrical coordinate system was used to describe the pipe pile, and a Cartesian coordinate system was used for the H pile. Internal strains, stresses and forces in the piles are denoted by primed variables. External stresses and forces are denoted by unprimed variables.

The above assumptions imply that the stress conditions in the soil acting on the H pile are given by

(A10) $\sigma_x = \sigma_y$, $\sigma_{xz} = \sigma_{yz}$.

The stress-strain relationship for the pile is given by

$$\varepsilon'_z = (\sigma'_z)/(E) - (\nu)/(E)\ (\sigma'_x + \sigma'_y) \quad \text{and}$$

(A11)

$$\varepsilon'_x = (\sigma'_x)/(E) - (\nu)/(E)\ (\sigma'_y + \sigma'_z)$$

where ε'_z and ε'_x can be determined from strain gauges mounted on the pile, Young's modulus is E, ν is Poisson's ratio for the pile and σ'_x, σ'_y, σ'_z are the stresses in the pile acting along the x, y and z coordinate axes. The system of equations (A11) are not solvable in their present form since there are only two equations and three unknowns. If, however, it is assumed that σ'_y in the vicinity of the ε'_x and ε'_z strain gauges is zero, due to the protective angle iron, then the equations become

$$\varepsilon'_z = (\sigma'_z)/(E) - (\nu\sigma'_x)/(E) \quad \text{and}$$

(A12)

$$\varepsilon'_x = (\sigma'_x)/(E) - (\nu\sigma'_z)/(E)\ .$$

Futhermore, the magnitude of transverse stresses, σ'_x, is determined by soil confining forces acting against the pile. If these forces are small compared to σ'_z, then equation A12 can be simplified. One method of estimating the magnitude of σ_x is to compare ε'_x to ε'_z. If $\varepsilon'_x \approx -\nu\varepsilon'_z$ then the transverse strain is primarily a Poisson's ratio effect caused by σ'_z, and $\sigma'_x << \sigma'_z$. This result would also imply that $\sigma'_y << \sigma'_z$, and the longitudinal stress in the pile can then be given by

(A13) $\quad \sigma'_z = E\varepsilon'_z.$

If, however, $\varepsilon'_x > -\nu\varepsilon'_z$ then the longitudinal stress must be calculated using

(A14) $\quad \sigma'_z = E(\sigma'_z + \nu\varepsilon'_x)/(1-\nu^2).$

The strain data for the 1983-84 season indicated that $\varepsilon'_x \approx -\nu\varepsilon'_z$, so equation A13 was used to calculate stress in the H pile (Fig. A3).

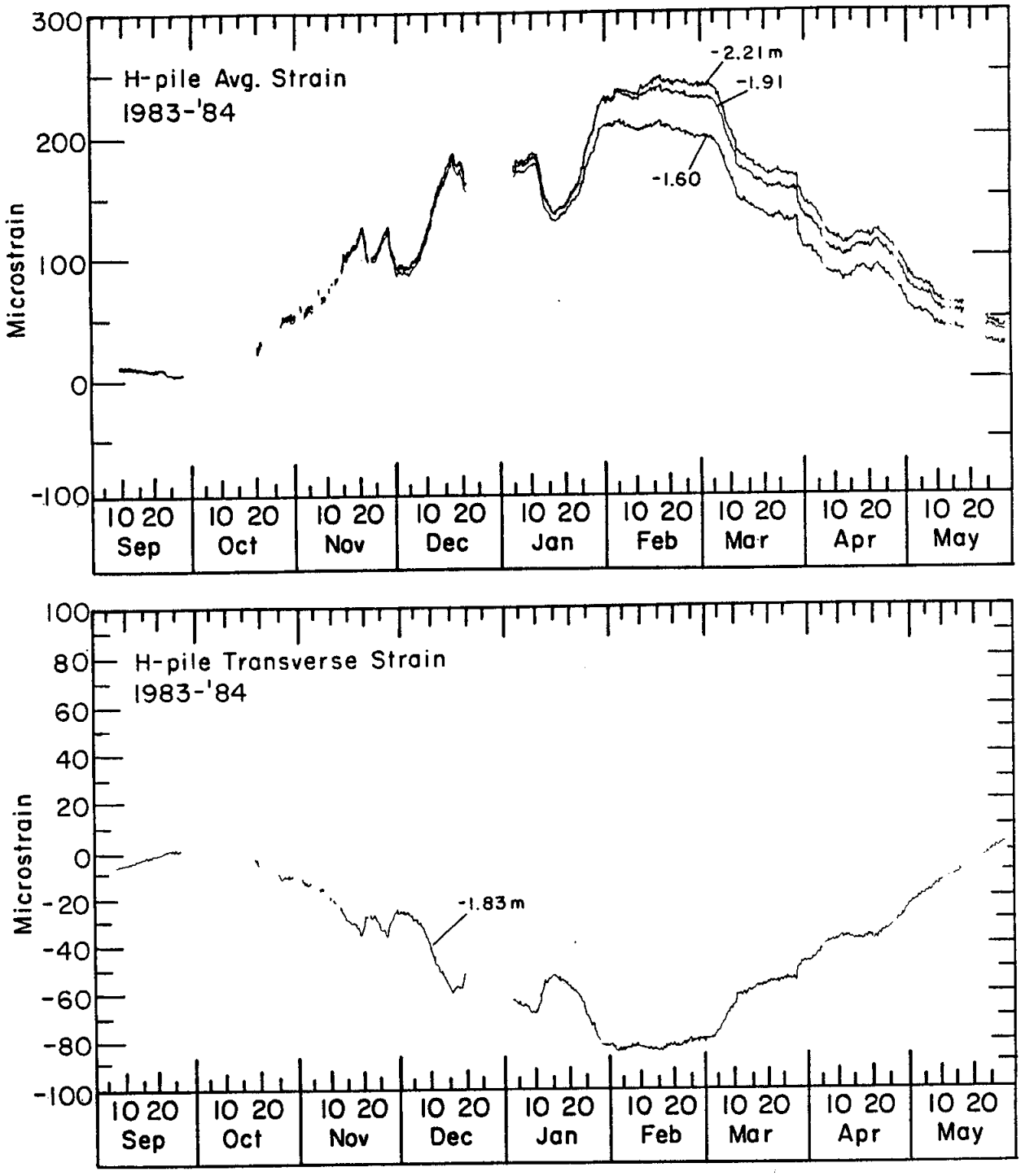

Figure A3. Average longitudinal strain for the H pile at depths of 1.60, 1.91 and 2.21 m for the period of 1 Sep 1983 to 1 June 1984, and average transverse strain for the H pile at a depth of 1.83 m for the period 1 Sep 1983 to 1 June 1984.

The internal axial force acting in the pile was determined from equation A13 by first calculating the axial force in the pile at each strain gauge depth using

(A15) $F'_z = \sigma'_z \times CA_H = E\ \varepsilon'_z \times CA_H$

where CA_H is the cross-sectional area of the H pile ($CA_H = 0.01550\ m^2$). The shear stress acting on the pile was then determined from

(A16) $\sigma_{xz} = ((F'_z)_i - (F'_z)_{i-1})/(SA_H \times \Delta z)$

where $SA_H = 1.67102\ m^2$, the actual surface area of the H pile per lineal meter, and Δz is the distance in meters between two adjacent strain gauge locations. Shear stresses computed on the basis of the "boxed in" surface area of the H pile used $SA_H = 1.02789\ m^2$ per lineal meter of pile ("boxed-in" surface area = 2 (flange width + pile depth)). The force difference between two adjacent strain gauge depths is given by $((F'_z)_i - (F'_z)_{i-1})$, where the ith strain gauge location is deeper in the soil than the ith-1 location. This means that s_{xz} is positive for an upwardly directed local shear stress.

Calculating the shear stresses for the pipe pile was done in a similar manner as for the H pile. The stress conditions along the pipe-soil interface are given, due to the assumptions of the problem, by

(A17) $\sigma_r = \sigma_\theta$, and $\sigma_{zr} = \sigma_{z\theta}$.

The strains for the pipe pile are given by

(A18)
$$\varepsilon'_\theta = (\sigma'_\theta - \nu\sigma'_z)/E \quad \text{and}$$
$$\varepsilon'_z = (\sigma'_z - \nu\sigma'_\theta)/E.$$

The radial component of stress, σ'_r, is zero since the strain gauges are mounted on a free surface.

Analysis of the 1982-83 winter's records indicated that, for large magnitude changes in ε'_z, $\varepsilon'_\theta \approx -\nu\varepsilon'_z$. Therefore $\sigma'_\theta \ll \sigma'_z$ and the stress in the pipe pile was determined from

(A19) $\sigma'_z = E\varepsilon'_z$.

The tangential force and shear stresses on the pile were then calculated from

(A20) $F'_x = \sigma'_z \times CA_p$

(A21) $\sigma_{rz} = ((F'_z)_i - (F'_z)_{i-1})/(SA_p \times \Delta z)$

where $CA_p = 0.00942\ m^2$ is the cross-sectional area of the pipe pile, $SA_p = 1.01740\ m^2$ is the surface area per lineal meter of the pile and Δz is the distance in meters between adjacent strain gauges.

Temperature Measurements

Both thermocouples and thermistors were used to measure temperatures. Thermocouple voltages were referenced against a thermocouple compensation unit built into the HP 3497A multiplexer card. The compensated voltages were converted to degrees celsius using the HP85A computer/controller and outputted to a storage tape. The resistance of the thermistors was measured using a 10-micro-amp constant current source provided by the HP 3497A, which was activated only during the measurement period. The calibration of each thermistor was checked at the freezing point prior to their installation. The 0°C thermistor resistance data were then used to adjust the manufacturer's calibration curve for the thermistors. The temperature in kelvins was calculated from

(A22) $1/T = A + B(\ln R) + C(\ln R)^3$

where T is the temperature in kelvins and R is the thermistor resistance.

A, B and C are coefficients that are calculated from the corrected calibration curve for each thermistor:

(A23) $A = y_1 - Bx_1 - Cx_1^3$

(A24) $$B = \frac{(x_1^3 - x_3^3)(y_1 - y_2) - (y_1 - y_3)(x_1^3 - x_2^3)}{(x_1 - x_2)(x_1^3 - x_3^3) - (x_1 - x_3)(x_1^3 - x_2^3)}$$

(A25) $$C = \frac{(x_1 - x_3)(y_1 - y_2) - (x_1 - x_2)(y_1 - y_3)}{(x_1 - x_3)(x_1^3 - x_2^3) - (x_1^3 - x_3^3)(x_1 - x_2)}$$

where $y_1 = 1/T$, $y_2 = 1/T_2$, $y_3 = 1/T_3$, $x_1 = \ln R_1$, $x_2 = \ln R_2$ and $x_3 = \ln R_3$. For this study the corrected resistances R_1, R_2 and R_3 for three temperatures 273.15K, 268.15K and 263.15K were used to calculate the A, B and C coefficients for each thermistor. Equation A22 was then used to calculate soil temperatures from the thermistor data.

APPENDIX B. Calibration Test Results for the H and Pipe Piles

Both the H and pipe piles were initially calibrated in compression from 0 to 44.5 kN. The initial calibration tests were conducted prior to installing the piles at the test site in order to determine an effective Young's modulus and Poisson's ratio for each strain gauge. A reaction beam loading device consisting of a 44.5-kN hydraulic cylinder, 44.5-kN calibrated load cell and loading platens constrained by four 1.9-cm steel rods was used to load both the pipe and H piles. The instrumented section of the pipe pile was continuously supported along its 2.7-m length and the 9.0-m-long H pile was supported every 0.3 m during the loading tests. Figure B1 shows the loading frame and data acquisition system used in the initial calibration test on the pipe pile. The initial calibration results were used until the field calibration was done in order to analyze the data during the 1982-83 and 1983-84 data collection seasons.

A concern throughout the study was the continued applicability of the initial calibration results to the analysis of the data. Several gauges were known to have been damaged during a lightning storm in the summer of 1983, and the concern was that this may have caused a calibration change in some of the undamaged gauges. Field calibration tests were conducted on 20-21 June 1985 to determine if there had been any change in the response characteristics of the gauges. The frozen ground surrounding the upper 3.7 meters of the piles was thawed with steam thaw points (Figure B2) and excavated away from the piles. The piles at depth were still frozen and anchored into the permafrost but now completely free of the surrounding soil throughout the upper instrumented section. During the soil thawing period and throughout the calibration tests the ground and pile temperatures were carefully monitored to maintain the frozen condition of

the piles at depth. A tensile load was applied to the piles with a crane pulling vertically against the restraining forces holding the pile in the permafrost at depth. Both piles were carefully monitored to insure that no vertical displacement occurred during the test loading and that the loading was truly vertical with no induced bending on the piles. The maximum tensile loads applied during the field calibration were 113 and 81 kN,

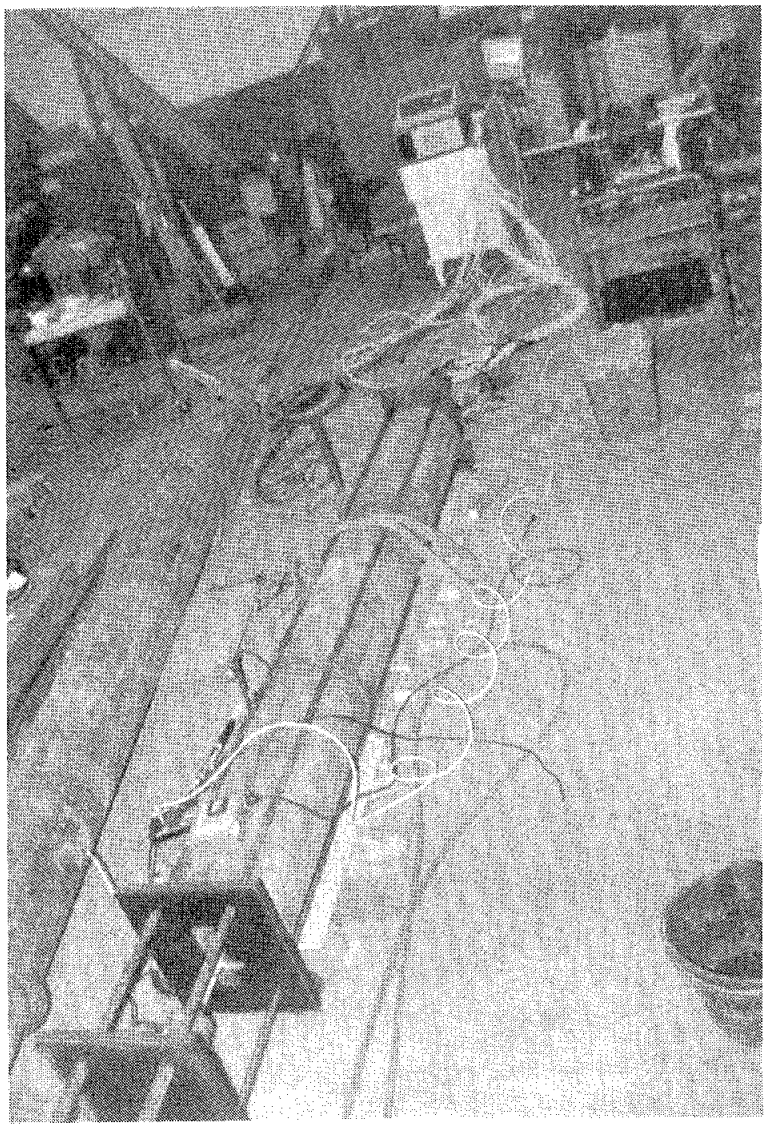

Figure B1. Load frame and data acquisition system used in the initial compression calibration tests (pipe pile calibration).

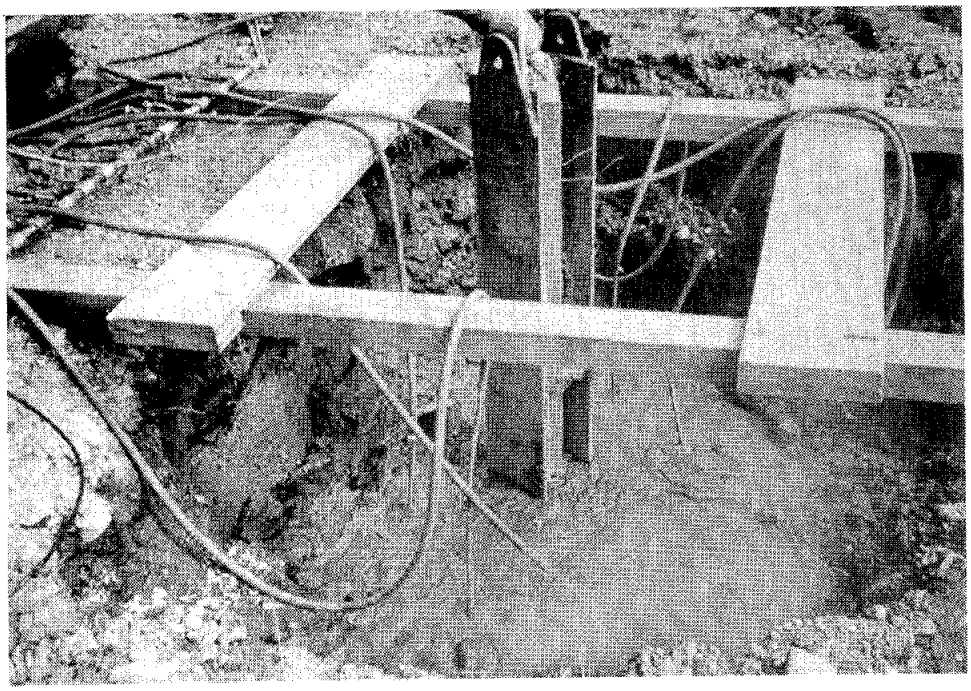

Figure B2. Thawing of frozen ground around the upper 3.7 meters of the H pile using steam thaw points prior to field calibration.

respectively, on the H and pipe piles. The limiting factor affecting the maximum load that could be applied to the piles was the ground support beneath the crane. As the load increased, the crane's outriggers and supports were forced deeper into the ground. Both piles where incrementally loaded in tension from zero to the maximum load that could be maintained and then incrementally unloaded. A 444.8-kN calibrated load cell was used to measure the load applied by the crane. Each test load was carefully monitored and the data rejected if the load varied by 0.5 kN or more. Strain measurements were made using the existing instrumentation and datalogging system, which recorded outputs from both piles throughout the calibration tests. The sensor outputs from the pile not being loaded in tension represented a true no-load, unconfined and unstrained condition. The unstrained observations were averaged, tested for outliers (none found)

and used as a common unstrained reference to compute total forces for comparison of all three data sets (1982-83, 1983-84 and 1984-85).

The data from both the initial compression calibration tests and from the field tension calibration tests were analyzed for comparison. Linear least-squares curve fits were used to determine the relationship between strain and stress from the strain-load measurements for each longitudinal strain gauge sensor. Figures B3 and B4 show representative plots of the strain-stress data and the best-fit line with a slope of 1/E, where E is Young's modulus. Figure B3 shows the results from a strain gauge that responded quite linearly, while Figure B4 shows the results from a malfunctioning gauge. The correlation coefficient for the least-squares curve fit to the data from the malfunctioning gauge was fairly high. It is apparent,

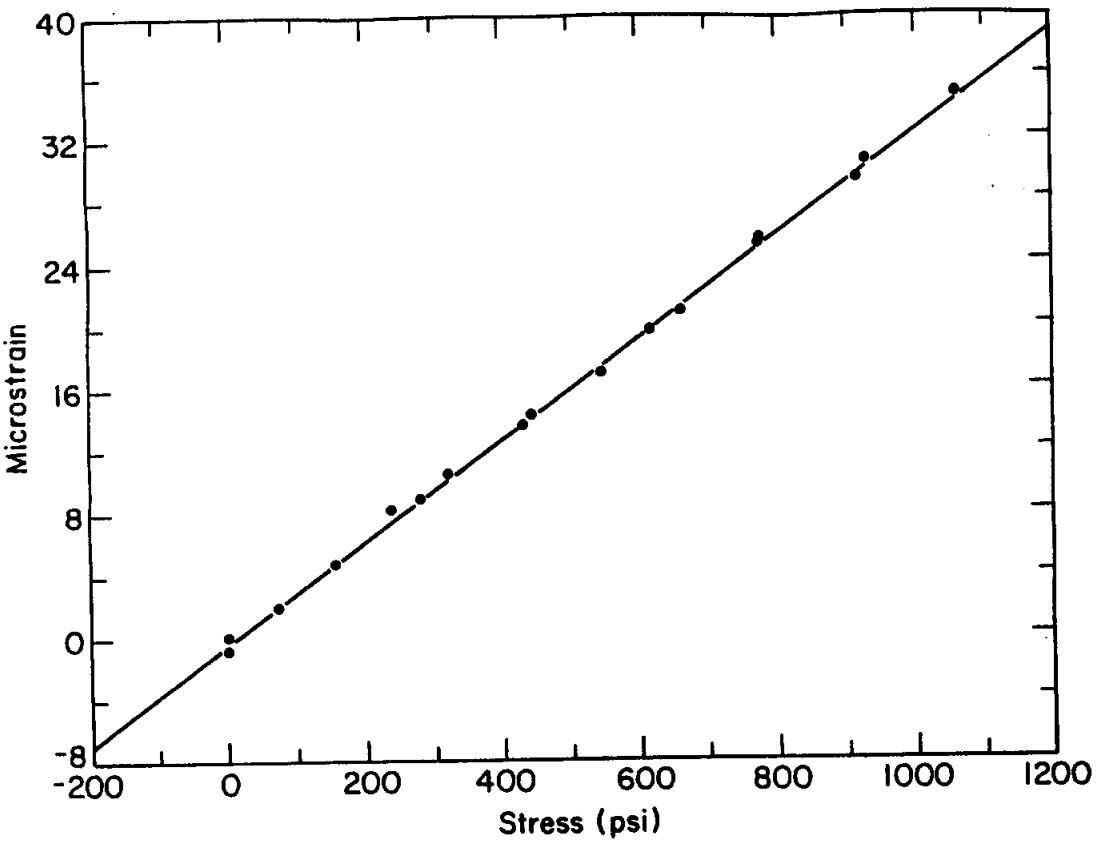

Figure B3. Strain-stress curve for strain gauge 21 on the H pile with correlation coefficient R = 1.00.

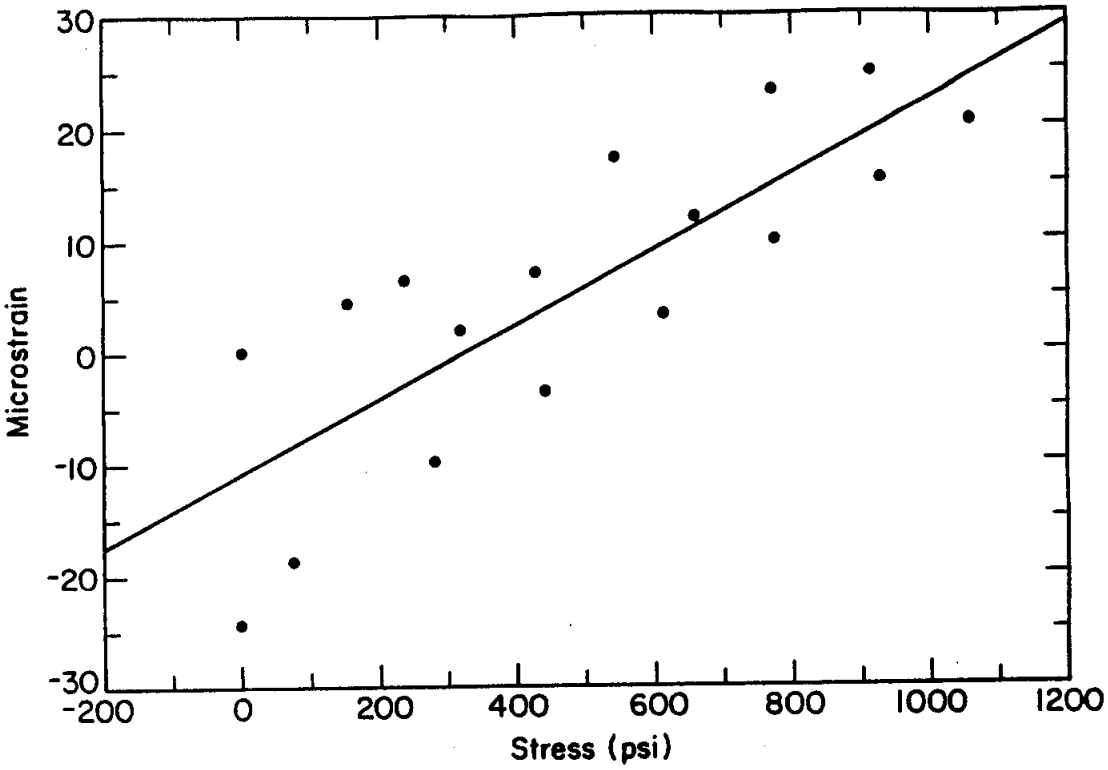

Figure B4. Strain-stress curve for malfunctioning strain gauge 11 on the H pile with correlation coefficient R = 0.81.

however, from the data point distribution that the gauge response was not reliable. Therefore, only data sets with correlation coefficients greater than r = 0.95 were accepted as functioning. The strain-stress response was also checked by examining the data plots for each gauge and through residual analyses of the data for each gauge.

A comparison was made between the averaged longitudinal gauge responses for both the initial and field calibration tests on the H pile. Figure B5 shows the results from the initial (compression) calibration test and Figure B6 shows the results from the field (tension) calibration test. Only the good longitudinal gauges (with correlation coefficients greater than 0.95) were used to determine the averaged longitudinal gauge responses. The initial calibration test showed a loading sequence effect (Fig. B5b) that was determined to be due to frictional losses between the pile

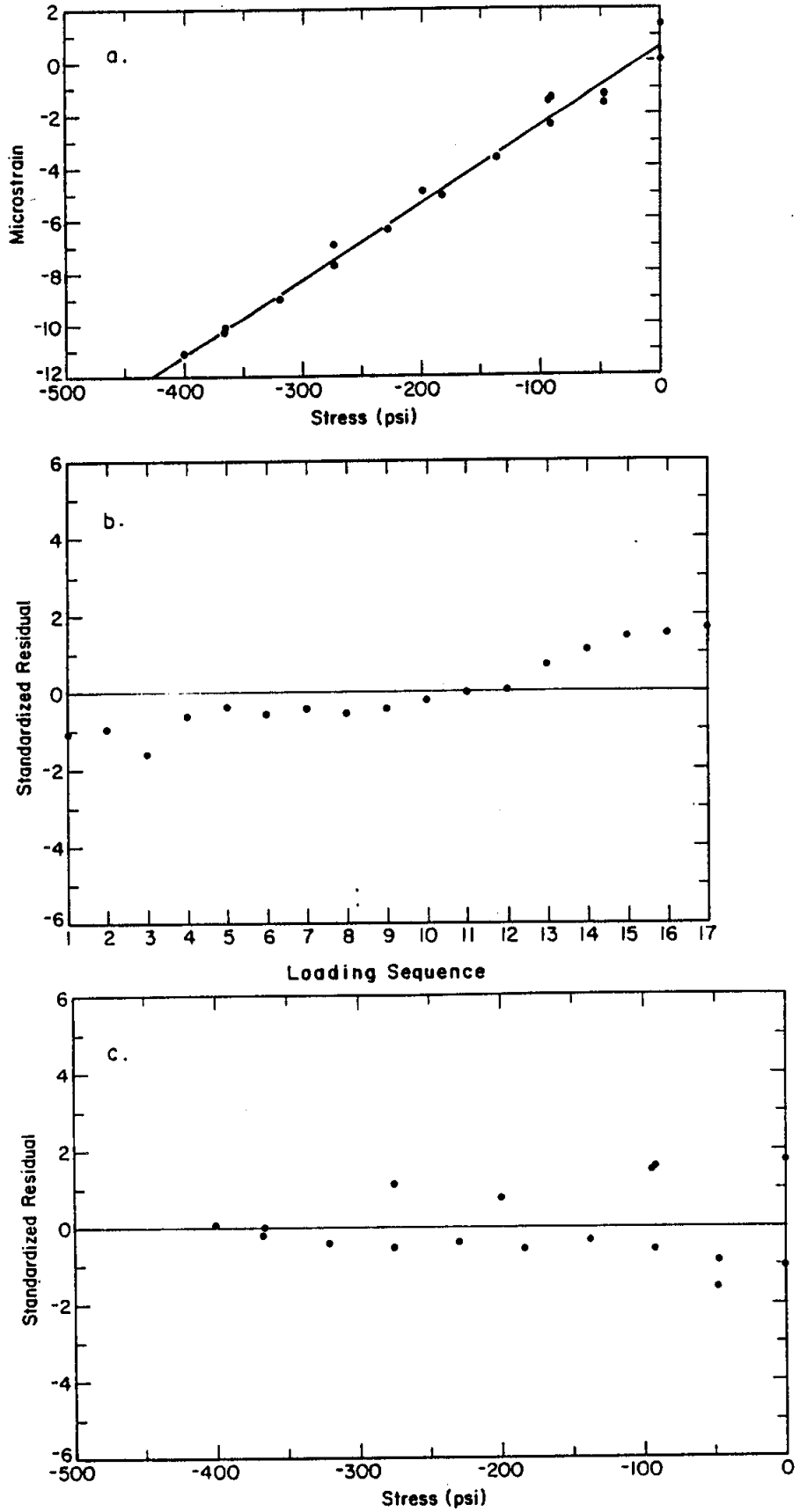

Figure B5. Averaged longitudinal gauge response for H pile from the initial (compression) calibration test. (a) strain-stress curve; (b) standardized residual vs loading sequence; (c) standardized residual vs averaged longitudinal stress.

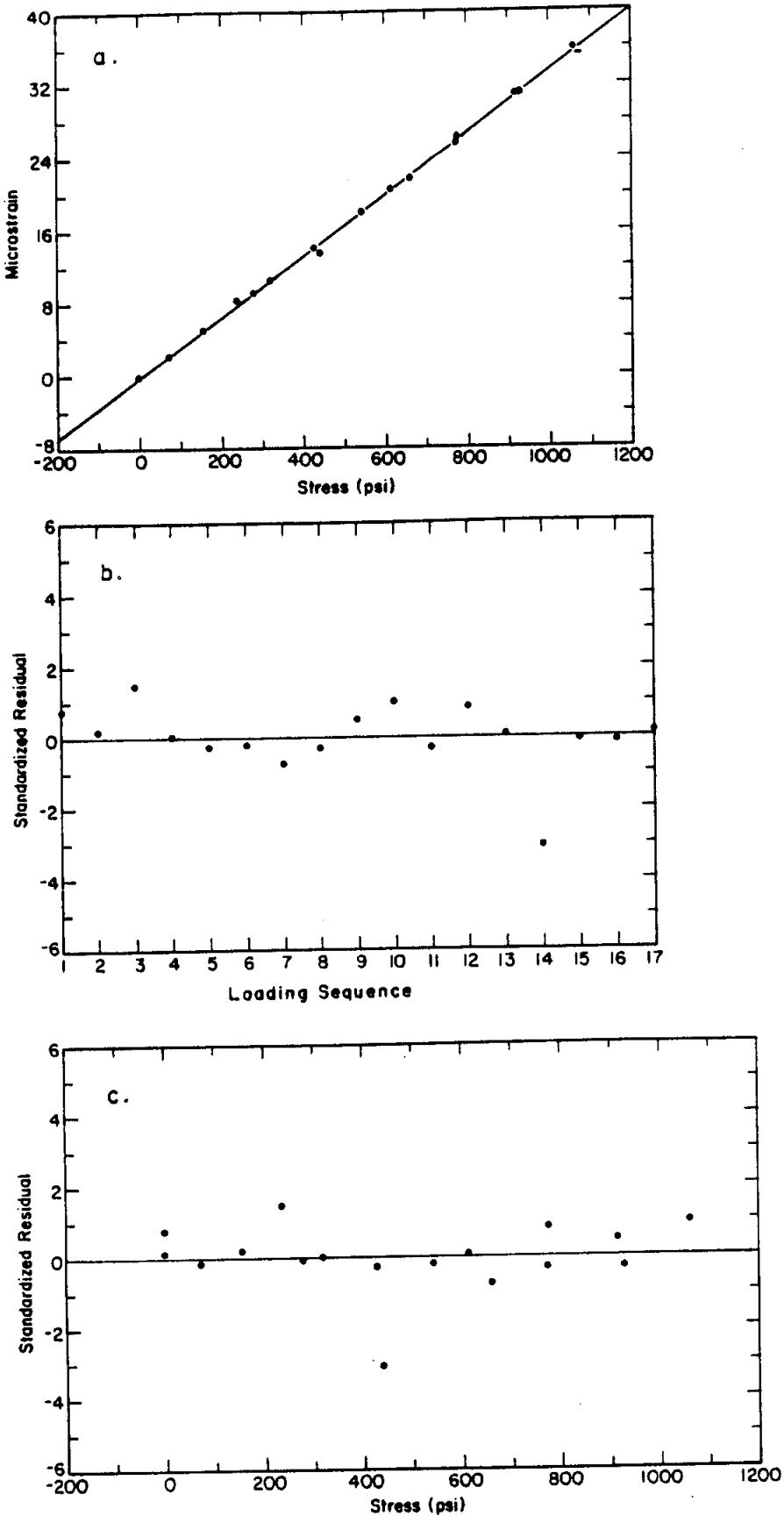

Figure B6. Averaged longitudinal gauge response for H pile from the field (tension) calibration test. (a) strain-stress curve; (b) standardized residual vs loading sequence; (c) standardized residual vs averaged longitudinal stress.

and the supports required when the pile was tested on its side during the compression test. The initial calibration also showed a non-constancy of error variance (Fig. B5c) indicating that the error variance is larger at the lower loads. The non-constancy of error variance problem is due to errors in determining the lower loads for measurements made at the low end of the load cells range. The results from the field (tension) calibration test show no sequence of loading (Fig. B6b) or non-constancy of error problem (Fig. B6c). The results from both the initial and field calibration were also tested to determine if the two regression lines (Figs. B5a and B6a) were the same and could be pooled. The test indicated that the results from the initial and field calibration where different and could not be pooled. Consequently, the results of the field calibration tests were determined to be better suited to the analysis of the data and were used for all three data sets (1982-83, 1983-84 and 1984-85).

Several gauges on both piles had acceptable gauge responses during the field calibration, but their response was found to deviate relative to comparable gauges over the period of record. The gauges that exhibited responses inconsistent with those of comparable gauges were considered bad.

Linear least-squares curve fits were used to determine the relationship between transverse strain and the average longitudinal strain of the "good" longitudinal gauges. Transverse gauge data sets with correlation coefficients less than -0.95 were accepted as functioning.

The field calibration results for the H pile are summarized in Table B1. Malfunctioning gauges are indicated by notes (#1 and #2). Only 15 of the 29 longitudinal gauges on the H pile were considered usable for the final data analysis. The effective Young's modulus averaged 203.67 GPa for the 15 good longitudinal gauges. This value is only slightly lower than the

Table B1. Field Calibration Results for the H Pile

LONGITUDINAL GAUGES

Distance from top of pile (meters)	SIDE ONE GAUGES Gauge Number Completion Circuit Type and Notes	Youngs Modulus (GPa)	Corr. Coeff.	SIDE TWO GAUGES Gauge Number Completion Circuit Type and Notes	Youngs Modulus (GPa)	Corr. Coeff.
0.38	1 (HB) #2	218.65	+1.00	15 (HB) #2	200.77	+0.97
0.53	NO GAUGE			16 (HB) #2	221.40	+0.99
0.69	2 (HB) #2	221.79	+1.00	17 (HB) #2	226.21	+0.97
0.84	NO GAUGE			19 (HB) #2	207.86	+0.99
0.99	4 (HB)	212.60	+0.99	20 (HB)	191.28	+1.00
1.14	NO GAUGE			21 (HB)	209.95	+1.00
1.30	5 (HB)	212.86	+0.99	22 (HB)	195.34	+1.00
1.45	NO GAUGE			23 (HB)	219.10	+0.99
1.60	6 (HB)	211.61	+0.99	24 (HB)	208.88	+0.96
1.75	NO GAUGE			26 (HB)	197.49	+1.00
1.91	8 (HB)	211.55	+1.00	27 (HB)	205.29	+1.00
2.06	NO GAUGE			28 (HB)	188.43	+0.99
2.21	9 (HB) #2	219.83	+1.00	29 (HB) #2	201.64	+1.00
2.36	NO GAUGE			31 (HB)	200.41	+1.00
2.52	11 (HB) #1	208.04	+0.81	32 (HB) #2	200.29	+1.00
2.67	NO GAUGE			33 (HB)	208.40	+0.97
2.82	12 (HB) #1	0.37	+0.64	34 (HB) #2	196.48	+1.00
2.97	NO GAUGE			35 (HB)	181.88	+0.96
3.12	14 (HB) #1	-12.89	-0.60	37 (HB) #2	188.57	+1.00

TRANSVERSE GAUGES

Distance from top of pile (meters)	SIDE ONE GAUGES Gauge Number Completion Circuit Type and Notes	Poisson's Ratio	Corr. Coeff.	SIDE TWO GAUGES Gauge Number Completion Circuit Type and Notes	Poisson's Ratio	Corr. Coeff.
0.76	3 (FB) #1	-0.28	+0.96	18 (FB) #1		
1.68	7 (FB) #1	10.39	-0.73	25 (FB) #1		
2.29	10 (FB)	0.35	-1.00	30 (FB)		
3.05	13 (FB) #1	-212.85	+0.39	36 (FB) #1		

NOTES: #1 Gauge considered bad if correlation coefficient of curve fit was less than +0.95 for Young's modulus or greater than -0.95 for Poisson's ratio.

#2 Gauge is considered bad since output from this gauge drifts relative to the other gauges over the period of record.

Completion circuit types: (FB) - Full Bridge (HB) - Half Bridge

published Young's modulus for steel of 206.84 GPa (30,000,000 psi). Only one out of four gauge pairs was considered usable for the transverse gauges on the H pile. The effective Poisson's ratio of 0.35 for gauge pair 10 and 30 is only slightly higher than the 0.33 value generally accepted as the Poisson's ratio of steel. Unfortunately the upper four gauge levels on the H pile were unusable as shown in Table B1.

The field calibration results for the pipe pile are summarized in Table B2. Malfunctioning gauges are indicated by notes (#1, #2 and #3). Several full bridge completion circuits (gauge pairs) were damaged and reconnected as half bridge circuits in July 1982 (Note #3). Only 5 of the 33 longitudinal gauges on the pipe pile were considered usable for the final data analysis. The effective Young's modulus averaged 229.08 GPa for the 5 good longitudinal gauges. This value is 11% higher than the published Young's modulus of 206.84 GPa for steel. Only 1 out of 11 transverse gauges was considered usable for the final data analysis on the pipe pile. The effective Poisson's ratio of 0.32 for gauge number 38 is only slightly lower than the 0.33 value generally accepted as the Poisson's ratio for steel.

The importance of field calibration for the strain gauges used to determine frost heave forces is apparent from the results shown in Tables B1 and B2. The final analysis for this study used only 45.9 and 13.6 percent of the total gauges installed on the H and pipe piles, respectively.

Table B2. Field Calibration Results for the Pipe Pile

LONGITUDINAL GAUGES

Distance from top of pile (meters)	SIDE ONE GAUGES Gauge Number Completion Circuit Type and Notes	Youngs Modulus (GPa)	Corr. Coeff.	SIDE TWO GAUGES Gauge Number Completion Circuit Type and Notes	Youngs Modulus (GPa)	Corr. Coeff.
0.38	1 (FB) #1	-1007.03	-0.94	21 (FB) #1		
0.53	2 (FB) #3			22 (HB) #2	405.26	+0.97
0.69	3 (HB) #1	364.61	+0.55	24 (FB) #3		
0.84	5 (FB) #3			25 (HB) #2	278.07	+0.99
0.84				26 (QB)	260.40	+1.00
0.99	6 (FB) #3			27 (HB) #1	261.60	+0.45
1.14	8 (FB) #3			29 (HB) #1	320.96	+0.80
1.30	9 (FB) #2	-338.02	-0.99	30 (FB) #2		
1.45	10 (FB) #3			31 (HB)	235.24	+0.99
1.60	11 (FB) #1	-0.72	-0.53	32 (FB) #1		
1.75	13 (FB) #3			34 (HB)	211.08	+0.99
1.91	14 (FB) #2	-342.20	-1.00	35 (FB) #2		
2.06	15 (FB) #3			36 (HB) #1	214.37	+0.83
2.21	16 (FB) #3			37 (HB)	232.33	+0.99
2.36	18 (FB) #2	-377.98	-0.97	39 (FB) #2		
2.52	19 (FB) #2	-318.87	-1.00	40 (FB) #2		
2.67	20 (FB) #3			41 (HB)	206.35	+0.98

TRANSVERSE GAUGES

Distance from top of pile (meters)	SIDE ONE GAUGES Gauge Number Completion Circuit Type and Notes	Poisson's Ratio	Corr. Coeff.	SIDE TWO GAUGES Gauge Number Completion Circuit Type and Notes	Poisson's Ratio	Corr. Coeff.
0.05	44 (QB) #1	-2403.56	+0.41			
0.61	4 (FB) #1	-0.03	+0.05	23 (FB) #1		
0.84	43 (QB) #1	0.00	-0.06			
1.07	7 (QB) #1	0.09	-0.85	28 (QB) #1	-0.04	+0.86
1.68	12 (FB) #1	-0.18	+0.96	33 (FB) #1		
1.75				42 (QB) #1	0.02	-0.32
2.29	17 (QB) #1	0.33	-0.95	38 (QB)	0.32	-0.96

NOTES: #1 Gauge considered bad if correlation coefficient of curve fit was less than +0.95 for Young's modulus or greater than -0.95 for Poisson's ratio.

#2 Gauge is considered bad since output from this gauge drifts relative to the other gauges over the period of record.

#3 This side of the original full bridge setup was damaged so gauge is bad. Other side reconnected as half bridge setup in July 1982.

Completion circuit types: (FB) - Full Bridge (HB) - Half Bridge
(QB) - Quarter Bridge